Aalto University
School of Engineering

Valtteri Mikkola

Impact of concentration, particle size and thermal conductivity on effective convective heat transfer of nanofluids

Thesis of diploma given in for the degree of Master of Science in Technology
Espoo 5.8.2015
Advisors: D.Sc Ari Seppälä, M.Sc Salla Puupponen

Aalto-yliopisto
Insinööritieteiden korkeakoulu

Aalto-yliopisto, PL 11000, 00076 AALTO
www.aalto.fi

Diplomityön tiivistelmä

Tekijä Valtteri Mikkola

Työn nimi Konsentraation, partikkelikoon ja lämmönjohtavuuden vaikutus nanonesteiden efektiiviseen konvektiolämmönsiirtoon

Koulutusohjelma Energia- ja LVI-tekniikka

Pää-/sivuaine Energiatekniikka **Koodi** K3007

Työn valvoja Asst Prof. Ville Vuorinen

Työn ohjaajat TkT Ari Seppälä, DI Salla Puupponen

Päivämäärä 5.8.2015 **Sivumäärä** 83 **Kieli** Englanti

Tiivistelmä

Nanonesteet ovat uudentyyppisiä lämmönsiirtonesteitä, joissa nanokokoisia partikkeleita (d < 100nm) on dispergoitu perinteiseen lämmönsiirtonesteeseen, kuten veteen tai öljyihin. Aiemmissa tutkimuksissa nanonesteiden konvektiolämmönsiirron on havaittu olevan poikkeuksellisen tehokasta, eikä ilmiötä ole pystytty selittämään perinteisten lämmönsiirtokorrelaatioiden avulla. Jo muutaman tilavuusprosentin partikkeliosuuden on todettu kasvattavan Nusseltin lukua kymmenillä prosenteilla veteen nähden Reynoldsin lukujen ollessa yhtä suuret. Lisäksi useiden tutkimusten mukaan nanopartikkelien lisäys tehostaa konvektiivista lämmönsiirtoa ilman merkittävästi kasvaneita painehäviöitä.

Tässä diplomityössä tutkitaan kokeellisesti konsentraation, partikkelikoon sekä partikkelien lämmönjohtavuuden vaikutusta nanonesteiden pakotettuun konvektiolämmönsiirtoon. Työssä mitattiin sisäkkäisputkilämmönsiirtimessä vesipohjaisia SiO_2-, miselli-, polystyreeni- ja Al_2O_3-nanonesteitä, joiden pitoisuus vaihteli välillä 0,09-1,81 til-% ja partikkelikoko välillä 8-58 nm. Lämmönsiirtomittausten yhteydessä mitattiin myös painehäviöt, jotta nesteiden tehokkuutta käytännön lämmönsiirtosovelluksissa pystyttiin arvioimaan. Tulosten luotettavaa analysointia varten mitattiin myös tarvittavat nanonesteiden aineominaisuudet: partikkelikokojakauma, zeta-potentiaali, viskositeetti, lämmönjohtavuus sekä tiheys. Lisäksi kehitettiin analysointimenetelmiä kokeellisten virheiden minimoimiseksi.

Mittaussarjoissa kaikkien nanonesteiden todettiin käyttäytyvän tavanomaisille nesteille kehitetyn Gnielinskin korrelaation mukaisesti, eikä poikkeavaa tehostumista havaittu. Nanonesteiden Nusseltin luvut olivat hieman suurempia kuin veden yhtä suurilla Reynoldsin luvuilla verrattuina, mutta eroja ei havaittu, kun Prandtlin luvun vaikutus otettiin huomioon analysoinnissa. Yhtä suurilla pumppaustehoilla verrattuna tutkittujen nanonesteiden lämmönsiirtotehokkuus oli vastaavaa tai heikompaa kuin veden. Partikkelikonsentraation lisäämisen havaittiin heikentävän lämmönsiirtotehokkuutta kaikissa tapauksissa. Tämän heikentävän efektin havaittiin kuitenkin olevan vähäisempi pieniä partikkeleita sisältäville nanonesteille viitaten pienen partikkelikoon olevan edullista nanonesteiden lämmönsiirron kannalta. Partikkelimateriaalin lämmönjohtavuudella ei havaittu olevan merkittävää vaikutusta konvektiolämmönsiirtoon tutkituilla pienillä konsentraatioilla ($\leq$1 til-%).

Tässä työssä tutkitut nanonesteet eivät vaikuta lupaavilta lämmönsiirtonesteiltä pakotetun konvektiolämmönsiirron sovelluksiin. Nesteen lämmönjohtavuuden kasvattaminen nanopartikkelien avulla saattaa silti olla potentiaalinen tapa tehostaa konvektiolämmönsiirtoa, sillä nanonesteiden havaittiin käyttäytyvän lämmönsiirtokorrelaatioiden mukaisesti.

Avainsanat nanoneste, konvektiolämmönsiirto, lämmönsiirrin, painehäviö, pumppausteho, konsentraatio, partikkelikoko, lämmönjohtavuus, viskositeetti

Aalto University
School of Engineering

Aalto University, P.O. BOX 11000, 00076
AALTO
www.aalto.fi

Abstract of master's thesis

Author Valtteri Mikkola

Title of thesis Impact of concentration, particle size and thermal conductivity on effective convective heat transfer performance of nanofluids

Degree programme Energy technology and HVAC

Major/minor Energy technology **Code** K3007

Thesis supervisor Asst Prof. Ville Vuorinen

Thesis advisor(s) D.Sc Ari Seppälä, M.Sc Salla Puupponen

Date 5.8.2015 **Number of pages** 83 **Language** English

Abstract

Nanofluids are a modern type of heat transfer fluids, in which typically solid nano-sized particles (d < 100 nm) are dispersed in conventional heat transfer fluid, such as water or oils. In earlier studies, nanofluids have shown anomalous enhancement of convective heat transfer that cannot be explained with conventional correlations. Water-based nanofluids with volume fraction of only a few percents have typically yielded tens of percents higher Nusselt numbers than water when compared with equal Reynolds numbers. In addition, several studies suggest that the addition of nanoparticles enhances convective heat transfer without significant penalty in pressure losses.

In this Master's Thesis, impacts of concentration, particle size and thermal conductivity of particle material on convective heat transfer of nanofluids are experimentally examined. For this purpose, water-based nanofluids containing SiO_2, micelle, polystyrene or Al_2O_3 particles were prepared and measured with an annular tube heat exchanger. The heat transfer measurements also included the pressure losses in order to study the suitability of nanofluids for practical heat transfer applications. The fluids were characterized thoroughly for the sake of an accurate analysis: viscosities, thermal conductivities, densities, particle sizes and zeta potentials of the samples were measured. Furthermore, analysis methods were developed in order to minimize the experimental errors.

In the experimental series, all nanofluids performed as Gnielinski correlation predicts and thus, no anomalous enhancement was observed. The nanofluids reached slightly higher Nusselt numbers than water when compared on the basis of equal Reynolds numbers, but no difference was observed when the effect of Prandtl number was taken into account. In comparison on the basis of equal pumping powers, the nanofluids showed equal or poorer performance than water. Increasing particle concentration was observed to lower the heat transfer performance of the fluids in all cases. However, the magnitude of this deteriorating effect was smaller for nanofluids with smaller particle size indicating that small particle size is beneficial for heat transfer of nanofluids. The thermal conductivity of particle material did not have a notable impact on the convection heat transfer with the studied relatively small particle concentrations ($\leq$1%).

Based on the results of this work, the performance of the nanofluids studied herein do not seem suitable for practical forced convection applications. However, enhancing thermal conductivities of fluids via the addition of nanoparticles might still offer potential for improved convective heat transfer, since behavior of nanofluids was observed to follow conventional correlations.

Keywords Nanofluid, convective heat transfer, heat exchanger, pressure loss, pumping power, concentration, particle size, thermal conductivity, viscosity

Preface

This Master's thesis symbolizes the completion of the long lasting period of my life as a student of energy technology. These years have truly rewarded me with knowledge and abilities related to the field, but also with fortune and beatitude in my personal life. However, being content about my development as a scientist, musician and as a human being, I feel ready to move on to the next chapter of my life. I am sincerely grateful to all of the people who have been part of this journey.

Several people deserve my gratefulness for their effort in this Master's thesis. Firstly, I would like to express my gratitude to Ari Seppälä for providing me this opportunity and for working as my advisor with expertise and enthusiasm. Secondly, Salla Puupponen receives my sincerest thanks for her help and effort in nanofluid preparation, as well as for working as my advisor. Thirdly, I would like to thank Henrika Granbohm for synthesizing the SiO_2 particles and lastly, Ville Vuorinen receives my gratitude for supervising this thesis.

This thesis was a part of EXPECTS-project that was funded by Aalto energy efficiency –program.

Espoo 5.8.2015

Valtteri Mikkola

Table of Contents

Symbols

A	surface area, m^2
c_p	specific heat, J/kgK
D	diffusion constant, m^2/s
d	diameter, m
f	friction factor
G	conductance, W/K
g	gravitational acceleration, m/s^2
h	heat transfer coefficient, W/m^2K
h	enthalpy, J/mol
h	height, m
K	ball constant
k	surface roughness, mm
k	Boltzmann constant, $m^2kgs^{-2}K^{-1}$
L	length, m
M	molecular weight, kg/mol
m	mass, kg
$\dot{m}$	mass flow, kg/s
N	Avogadro number, mol^{-1}
Nu	Nusselt number
P	pumping power
Pr	Prantl number
p	pressure, Pa
p	perimeter, m
Re	Reynolds number
r	radius, m
T	temperature, K
t	time, s
u	velocity (parallel to x-axis), m/s
V	volume, m^3
$\dot{V}$	volumetric flow, m^3/s
v	velocity, m/s
η	dynamic viscosity, kg/sm
η	heat transfer efficiency
θ_{ln}	logarithmic temperature difference
λ	thermal conductivity, W/mK
ρ	density, kg/m^3
τ	shear stress, Pa
v	kinematic viscosity, m^2/s
ϕ	volume fraction
ϕ	heat transfer power

Subscripts

ave	average
bf	base fluid
f	fluid
i	inner
i	ordinal number
in	inlet
max	maximum
nf	nanofluid
o	outer
out	outlet
p	particle
s	solid

1 Introduction

Various types of heating and cooling systems are used widely in industry operation as well as in everyday life. Effective performance of these systems is a requirement for maintaining and developing an energy efficient society. Most of the heat transfer applications, such as transferring thermal energy from a power plant to district heating consumers, are based on convective heat transfer. Properties and heat transfer performance of the fluids utilized in these systems have therefore an extremely essential role in practical heat transfer systems. Typically, water or other conventional heat transfer fluids fulfill the requirements and are considered sufficient for operation of the system. However, development of more effective heat transfer fluids would result in smaller heat transfer systems with reduced capital costs and improved energy efficiencies.

Thermal conductivity of liquids is typically orders of magnitude lower than that of solids. For example, the thermal conductivity of water at room temperature is only 0,598 W/mK [1], whereas the thermal conductivity of silver is 408 W/mK [1]. Thus, it is natural to consider improvement of thermal properties of conventional heat transfer fluids by addition of solid particles. Such dispersions of small solid particles are generally referred as solid-liquid colloids or sols. *Nanofluids* are a modern class of colloids, in which typically solid particles with a very small diameter of 1-100 nm are suspended in a liquid medium.

According to literature, addition of nano-sized particles has been noticed to cause anomalous enhancement in thermal conductivity and convective heat transfer performance of a fluid. Several experiments suggest that the increment of thermal conductivity is significantly larger than the predicted enhancement according to well-known Maxwell equation for thermal conductivity of heterogeneous solutions [2-5]. In addition, the convective heat transfer performance of nanofluids has been stated to increase even beyond the effect of enhanced thermal conductivity [6-11]. The concept of nanofluids was first proposed by Choi *et al.* in 1995 [12] and since then the research in relation to nanofluids has been thriving. The subject has been studied keenly and the amount of annually published articles has been increasing almost exponentially, as elucidated in Figure 1.

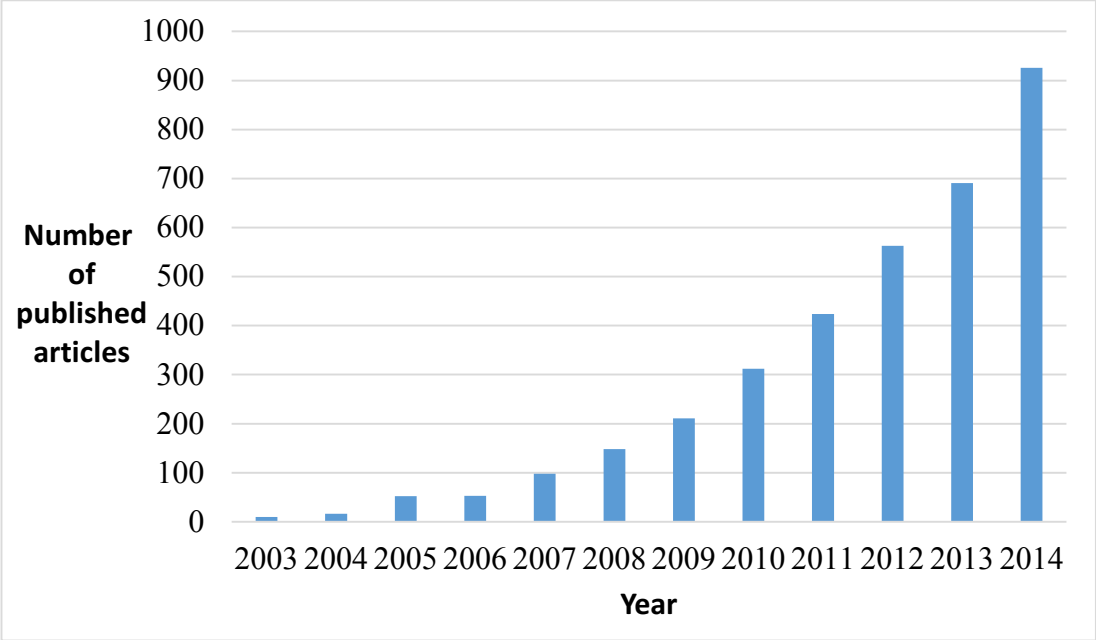

Figure 1. The amount of annually published articles with "nanofluid" in topic. Data was obtained 10.5.2015 [13].

Different research groups agree that the thermal properties of nanofluids are very different than those of conventional heat transfer fluids even with relatively low particle concentrations of only a few vol-%. Typically the addition of nanoparticles has been observed to increase the following three properties by even tens of percents: thermal conductivity, convective heat transfer and viscosity. However, an ongoing debate about the magnitudes of these changes exists, since the results of different groups are often contradictory. In some publications, such anomalous behavior has not been observed at all [14-16]. In spite of the large amount of research, no theory has been able to provide a solid and well-established explanation for physical basis of the heat transfer enhancement of nanofluids.

The aim of this study is to experimentally examine the impact of concentration, particle size and thermal conductivity on convective heat transfer of nanofluids. Nine nanofluid samples are prepared, characterized, measured and analyzed for this purpose. The convective heat transfer performance is studied with an annular tube -type heat exchanger. The measurements cover both laminar and turbulent regime with Reynolds number varying in the range of 1000-11000. In addition to the convective heat transfer, the analysis includes the change in required pumping power due to the increased viscosity and friction factor caused by nanoparticles. The studied nanofluids are also characterized thoroughly; particle sizes, shapes, fluid stabilities, viscosities, densities

and thermal conductivities are measured. Furthermore, analysis methods are developed in order to minimize the experimental errors.

A comprehensive literature review concerning nanofluids is presented in Chapter 2. The experimental methods and materials used in this work are explained in Chapter 3, and the results are reported and discussed in Chapter 4. Finally, Chapter 5 presents the most important conclusions of the work.

2 Structure, properties and behavior of nanofluids

2.1 Characteristics of nanofluids

Nanofluids are suspensions of nanoscale particles in liquids. Vast variety of materials can be used in nanofluids. The most researched particle materials are metals (Cu, Al, Fe, Au and Ag), inorganic oxide materials (Al_2O_3, CuO, Fe_3O_4, TiO_2, and SiO_2) and carbon nanotubes [6]. In addition to solid nanoparticles, some research groups have also studied nanoscale liquid particle suspensions i.e. nanoemulsions [17, 18] Liquids, in which nanoparticles are suspended, are called *base fluids*. Typical studied base fluids are water, oils, acetone and ethylene glycol. Table 1 presents a few examples of previously studied nanofluid systems.

Table 1. Examples of nanofluid systems reported in literature [19].

Particle material	Basefluid	Concentration (vol-%)	Particle size (nm)
Cu	Ethylene glycole	0,3	10
Cu	H_2O	7,5	100
Fe	Ethylene glycole	0,55	10
Ag	Toluene	0,001	60-80
Ag	Ethanol	0,6	4
Fe_3O_4	H_2O	4	10
TiO_2	H_2O	5	15
Al_2O_3	H_2O	5	20
Al_2O_3	Ethylene glycole	0,05	60
CuO	H_2O	5	33
SiC	H_2O	4,2	25
Carbon nanotube	Engine oil	2,0	20-50

Several parameters have an impact on the thermal characteristics of nanofluids. Naturally, the chemistry of particles and base fluid affect the thermal properties of nanofluids. In addition, the geometry of the particles and the suspension (concentration, particle size and shape, size distribution and fluid stability) have an influence on the nanofluid properties. Therefore, a precise and comprehensive characterization of the measured nanofluids is essential in order to obtain reliable and comparable results.

2.1.1 Size of a nanoparticle

A nanoparticle is a particle that has at least one dimension smaller 1 μm. In several occasions, however, nanofluids are defined as suspensions consisting of particles of 1-100 nm in size.

The shape of a nanoparticle is often approximately spherical. In that case, the size of the particle can be simply and comprehensively defined as its diameter. However, in case of non-spherical shape, the particle size naturally cannot be unambiguously explained with a single value. Such value of size is a subject of interpretation and should be well defined. Several methods for defining the effective diameter of non-spherical particles have been proposed. Methods to define the particle diameter as a diameter of a sphere with equal volume, surface area or perimeter are presented in equations 1, 2 and 3, respectively.

$$d_V = \sqrt[3]{\frac{6V}{\pi}} \tag{1}$$

$$d_A = \sqrt{\frac{4A}{\pi}} \tag{2}$$

$$d_P = \frac{p}{\pi} \tag{3}$$

where V is volume, A is surface area and p is perimeter of the particle.

Nevertheless, none of these diameters is able to describe particles comprehensively. Therefore, usage of any correlations that are defined for spherical particles should be avoided if possible. Several different particle shapes have been studied in previous experimental work, including at least spherical, polygonal, cylindrical, tubes, fibers and irregular particles.

In real suspension, particles are never equal in terms of size or shape. The nature of the particle size and shape is in fact a statistical average, rather than the exact size of all particles. The size distribution is therefore preferred to be determined in order to verify the quality of a sample. Evidently, a single value for the particle diameter only describes the fluid accurately if the size distribution of particles is sufficiently narrow.

Particle size distribution can be measured with Dynamic Light Scattering (DLS) or determined from microscope images. An example of size distribution obtained with DLS is presented in Figure 2.

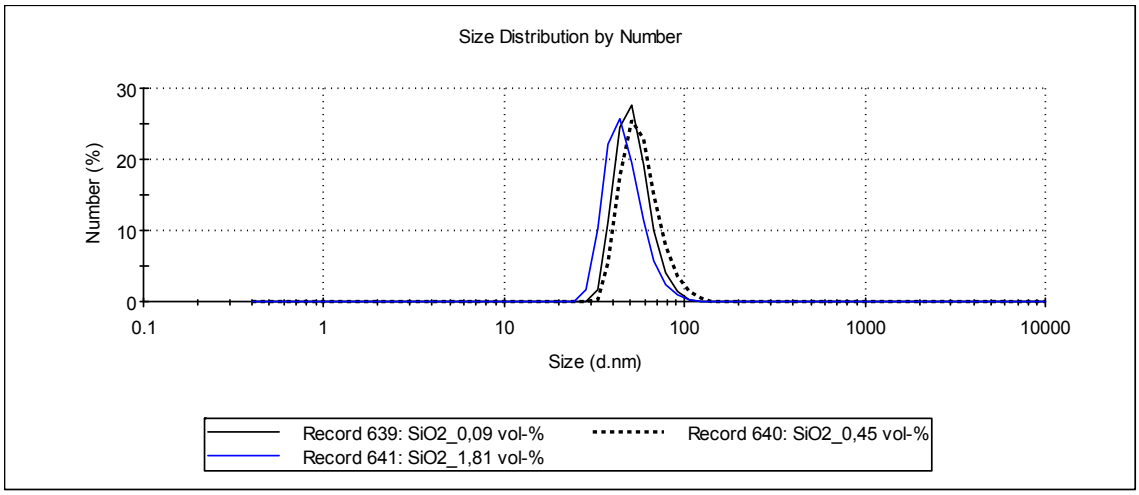

Figure 2. Particle size distributions of three SiO_2 nanofluids

The disadvantage of DLS is that it assumes particles to be spherical in shape. Such assumption may obviously result in serious measurement error in case of non-spherical particles. Moreover, DLS does not provide data concerning the particle shape and thus, DLS results should be verified with microscopy images to avoid uncertainty.

Commonly, particle size distribution and particle shape are determined with electron microscopy techniques. An example of Transmission Electron Microscope (TEM) image is presented in Figure 3.

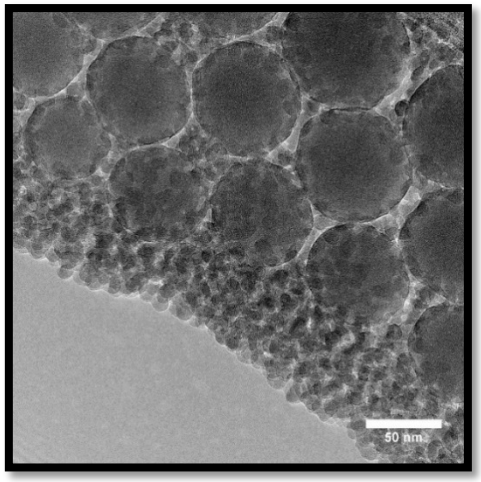

Figure 3. Transmission Electron Microscope image of SiO_2 nanoparticles

Approximate values of particle diameters can be obtained by electron microscopy. The size distribution can be determined if the images cover sufficient amount of particles and the images can be assumed to describe the whole suspension comprehensively. In addition, electron microscopy also provides data concerning particle shape and agglomeration making it an important technology for characterization of nanofluids.

The disadvantage of conventional electron microscopy is that the images represent the size distribution of dry powder and thus, it cannot be positively known whether the particle distribution is exactly similar in suspension. Consequently, both electron microscopy images and DLS should be used to obtain indisputable data of the particle geometry. However, the best method for studying the particle size and shape of nanofluids is a so called cryo-TEM, in which the fluid is rapidly freezed and the whole fluid is imaged. Quick freezing ensures that water (if used as a base fluid) does not crystallize but remains as amorphous phase making the imaging possible. In addition, rapid freezing prevents the particles from agglomeration as they are engaged quickly in the solid base fluid.

2.1.2 Stability, aggregation and zeta potential

Practical exploitation of nanofluids obviously requires the fluids to remain stable. Instability of colloids is in fact one of the most serious problems of nanofluids. Unstable nanoparticles may not stay separated in colloids, but form larger clusters, agglomerates or longer chains. This may obviously have a severe harmful impact on performance of nanofluid, since aggregation affects the size, shape and amount of particles. In this section, the theory of aggregation is presented based on the book "Nanofluidics: Thermodynamic and transport properties" by Eftathios Michaelides [6]

Several mechanisms may cause the particles to come close to one another. These mechanisms include at least the following:

1. Bulk motion of the fluid
2. Lift or other transverse forces
3. Electrical interactions
4. Hydrodynamic interactions
5. Chemical potential forces
6. Brownian motion
7. Flow shear

If particles get to close proximity, they may form bonds resulting in clustering of the particles. General theory of aggregation was originally presented by Derjaguin and Landau 1941 [20] and Verway and Overbeek 1948 [21] and is referred as DLVO-theory. In this theory, all attractive and repulsive forces of particles are taken into account in a single potential energy function. An example of such so called DLVO-curve is presented in Figure 4. Typically, a dimensionless potential energy function has

two minimums: a primary and a secondary minimum. These minimums represent the stable states of the particles. Naturally, these two minimums are separated by a local maximum, which represents an unstable state and functions as an energy barrier between the two minimums.

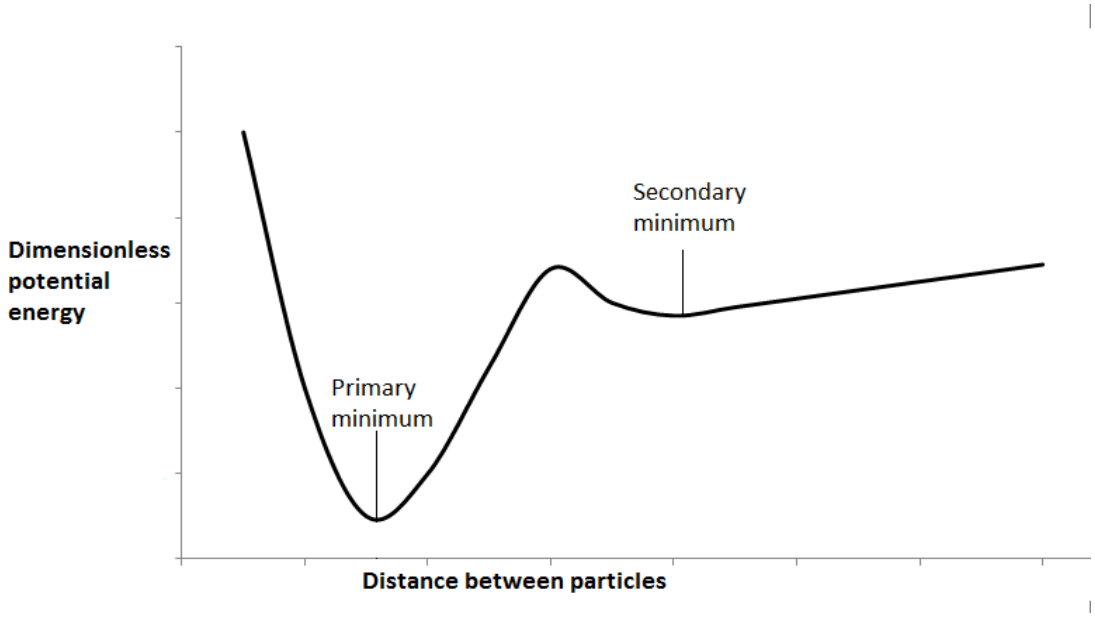

Figure 4. Illustrative example of DLVO-curve

Let us consider two particles with a large initial distance. Brownian motion or other reason causes the particles to begin to approach each other. The two particles fall into the secondary minimum of potential energy, in which they achieve a more stable state. In this state the particles are moving together as one pair. The process is called *flocculation* and the formed clusters are called *flocs*. However, the secondary minimum of potential energy is quite shallow, which means that flocs are relatively unstable clusters. Even a weak repulsive force may cause a floc to break and separate the flocculated particles from each other. Likewise, if the force is attractive, it may cause the particles to further approach each other. The particles would then fall into the primary minimum of potential energy and achieve significantly more stable state. This stronger binding process at the primary minimum of potential energy is called *coagulation*. The primary minimum of potential energy is deep, which means that *coagulants* are quite stable and do not break easily. Particles can now be separated only by a strong chemical, electrical or mechanical force.

The precise form of the potential energy curve is naturally dependent on the situation. For example, magnitude of the barrier between flocculation and coagulation can be modified by altering ion concentration of the fluid. If the barrier is low, coagulates will be more likely to form. Consistently, a large barrier would cause coagulation to become difficult and thus, no stable aggregates would be formed.

In order to maintain the stability of a colloidal system, sufficient repulsive forces between the particles are required to prevent the particles from getting excessively close to one another. Two mechanisms for increasing dispersion stability exist: steric stabilization and electrostatic stabilization. These mechanisms are depicted in Figure 5.

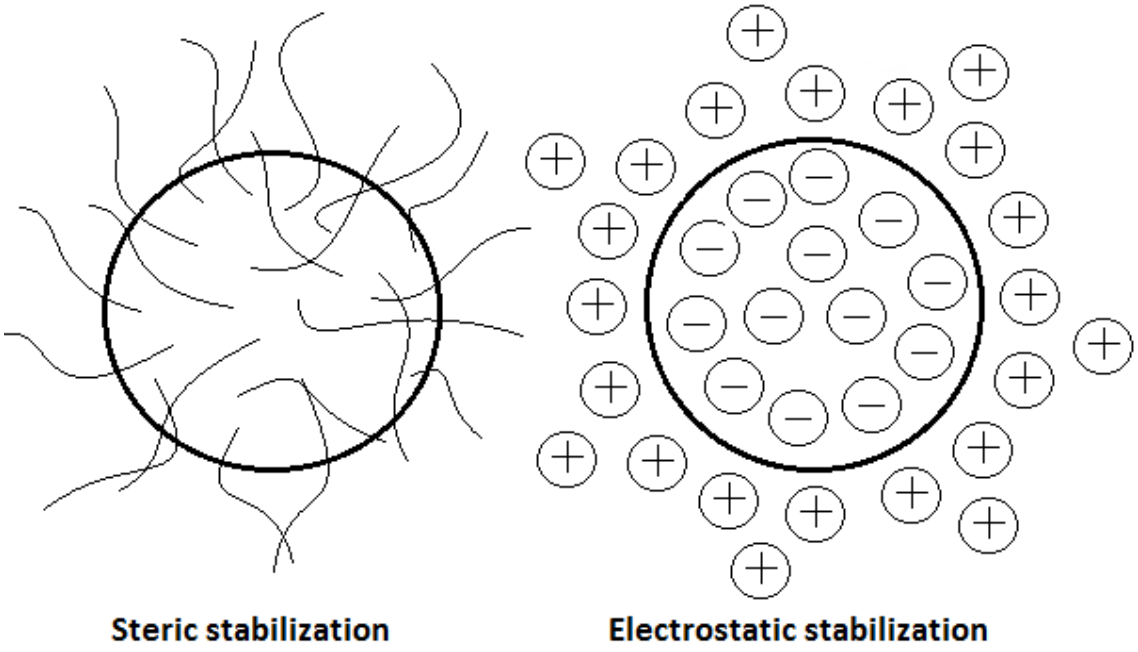

Figure 5. Dispersion stability can be increased by addition of polymeric surfactants (left) or by altering the ion concentration (right)

In steric stabilization, polymeric surfactants are adsorbed onto particle surfaces. If thickness of this layer is sufficient, steric repulsion between the polymeric surfactants prevents the particles from reaching close contact with one another. This process is relatively simple, requiring only the addition of a suitable polymer. However, subsequently flocculating the system will be difficult if desired. The polymer can also be expensive. In electrostatic or charge stabilization, the distribution of charges keep the particles separated. This can be accomplished with ionic surfactants or by altering the ion concentration of the system. Similarly, the system can also be flocculated by

altering the ion concentration if desired. In addition to enhanced stability, both of these stabilization mechanisms obviously affect the system and its behavior by other means as well. Therefore, the stabilization mechanisms such as addition of surfactants should always be reported in order to maintain reasonable comparability between studies.

The particle surfaces in most colloidal dispersions are electrically charged. This surface charge also affects the ion distribution in the surrounding interfacial region. For example, a negatively charged particle would be surrounded by an increased concentration of positive ions, as illustrated in Figure 6.

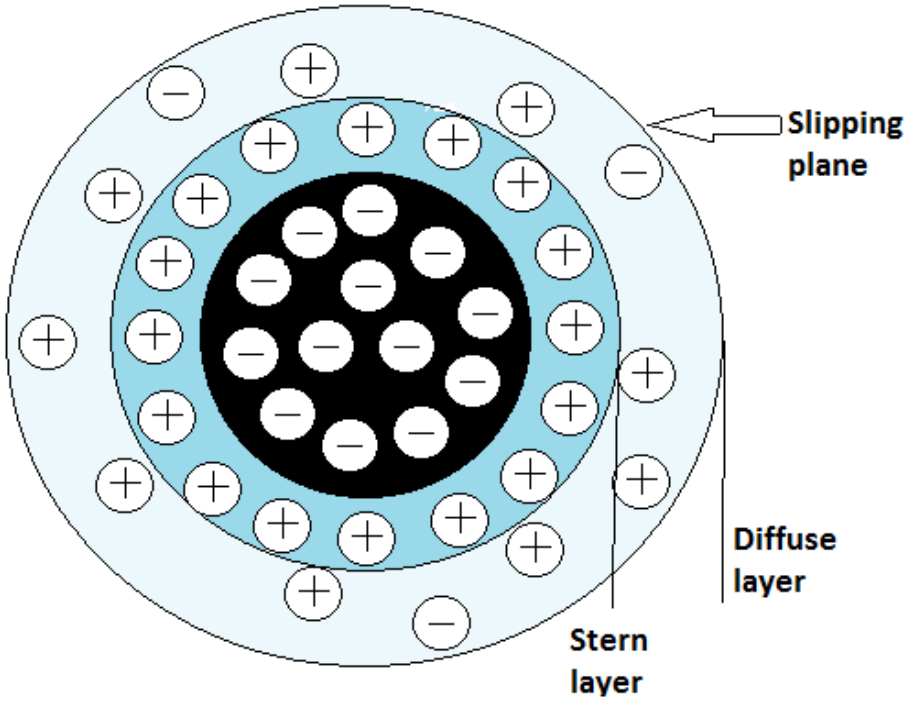

Figure 6. Charge distribution close to a negatively charged particle surface

The liquid layer surrounding the particle can be divided into two parts: an inner region called the Stern layer and an outer region called the diffuse layer. In the Stern layer ions are strongly bound to the particle, whereas in the diffuse layer they are less organized and allowed to move more freely. Inside a certain notional boundary of the diffuse layer the ions and particles form a stable entity. This means that the ions within this boundary are moving together with the particle. The electric potential at this boundary is called the *zeta potential.*

The zeta potential functions as an index of magnitude of electrostatic interaction between colloidal particles. Therefore, zeta potential measurements are commonly used to evaluate the stability of colloidal systems. The value of zeta potential may be positive or negative, but the magnitude of the potential determines the stability based on electrostatic repulsion. If the particles have a large zeta potential in suspension, the repulsive forces between them are sufficient to keep them separated. Generally, a suspension is considered stable if the absolute value of zeta potential is greater than 30 mV. However, this is naturally only an approximate limit, and does not have an exact and justifiable physical basis. Particularly, sedimentation or creaming may eventually occur if the density difference between the liquid and the particles is large.

2.1.3 Density

Nanofluids are heterogeneous mixtures of solid and liquid materials. Let us consider a nanofluid, in which solid nanoscale particles occupy volume V_s and liquid base fluid occupies volume V_f. The system is illustrated in Figure 7.

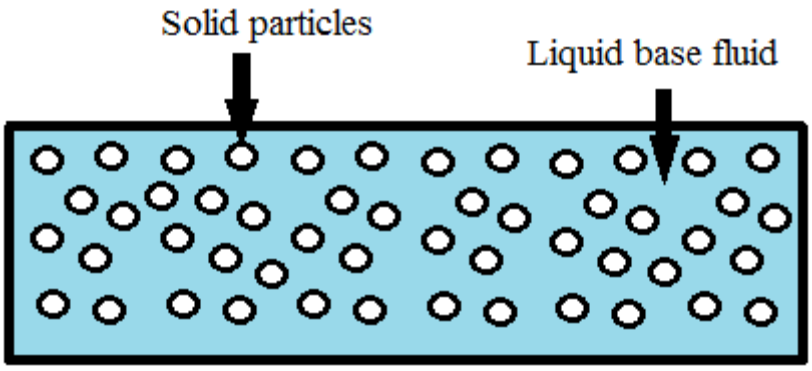

Figure 7. Nanofluid systems consist of solid nanoparticles that occupy volume V_s and liquid base fluid that occupies volume V_f

According to the conservation of volume in heterogeneous mixtures we obtain the following expression for nanofluid volume V.

$$V = V_s + V_f \tag{4}$$

The volume fraction of solid particles ϕ is defined as

$$\frac{V_s}{V} = \phi \tag{5}$$

and volume fraction of liquid base fluid is therefore

$$\frac{V_f}{V} = 1 - \phi \quad (6)$$

The mass that is enclosed within the volumes V_f and V_s can be expressed in terms of densities of the solid particles and the basefluid ρ_s and ρ_f, respectively. The total mass m can thus be expressed as

$$m = m_s + m_f = \rho_s \phi V + \rho_f (1 - \phi) V \quad (7)$$

The *average density* of heterogeneous mixture ρ_{ave} can be achieved as the ratio of mass and volume.

$$\rho_{ave} = \frac{m}{V} = \rho_s \phi + \rho_f (1 - \phi) \quad (8)$$

It must be noted that this derived density ρ_{ave} is in fact an average density of the whole fluid. Density in any local point of the heterogeneous nanofluid is either the density of the base fluid or the nanoparticle, or discontinuous at the particle surface. Similarly, the average density within a very small volume is not necessarily equal to the average density, since the concentration of solid particles may vary slightly locally.

2.1.4 Specific heat

The specific heat of nanofluids $c_{p,nf}$ can be obtained as mass-based weighted average of the specific heats of the nanoparticles $c_{p,s}$ and the base fluid $c_{p,bf}$. In general form, the specific heat of a nanofluid $c_{p,nf}$ can be expressed as [6]

$$c_{p,nf} = \frac{1}{\rho_{nf}} [\rho_s \phi c_{p,s} + \rho_{bf} (1 - \phi) c_{p,bf} + \rho_s \phi \frac{\partial (\Delta h_{mix})}{\partial T}] \quad (9)$$

The mixing enthalpy Δh_{mix} is most commonly assumed to be insignificant for nanofluids containing solid particles, in which case the Equation reduces to form

$$c_{p,nf} = \frac{1}{\rho_{nf}} [\rho_s \phi c_{p,s} + \rho_{bf} (1 - \phi) c_{p,bf}] \quad (10)$$

In Equation 10 one can observe that if the specific heat of the particle material ρ_s is higher than that of the base fluids $c_{p,bf}$, the heat capacity of the mixture $c_{p,nf}$ will increase when the nanoparticles are introduced. Likewise, the heat capacity of the mixture will decrease if the specific heat of the solid material is lower than that of base fluids.

The specific heats of common base fluids and particle materials are presented in table 2. Specific heats of solid particle materials is typically lower than those of base fluids. Therefore, addition of nanoparticles usually causes the heat capacity of the fluid to decrease and consequently, the specific heat of a nanofluid is usually slightly lower than that of base fluids.

Table 2. Specific heats of typical base fluids and solid particle materials [1]

Base fluid	c_{p_fluid} (J/kgK)	Particle material	c_{p_solid} (J/kgK)
water	4183	Alumina (Al_2O_3)	1110
Ethylene glycol	2740	Aluminum (Al)	945
Ethyl alcohol	2430	Copper	385
Toluen	1700	Gold	128
Silicon oil	1470	Lead	131
Refrigerant R134a	1410	Silver	234

2.2. Viscosity of nanofluids

Viscosity is a material property that has a considerable impact on convective heat transfer performance of fluids. In forced convection applications, a more viscose fluid requires higher velocity in order to obtain equally turbulent flow. In addition, larger viscosity increases pressure losses resulting in larger pumping powers. Therefore, low viscosity is beneficial for heat transfer fluids.

Generally, dynamic viscosity η of a Newtonian fluid is defined as [7]

$$\eta = \frac{\tau}{(\frac{\partial u}{\partial y})} \tag{11}$$

where τ is the local shear stress and $(\frac{\partial u}{\partial y})$ the local velocity gradient.

The kinematic viscosity v can be obtained as ratio of dynamic viscosity η and density ρ

$$v = \frac{\eta}{\rho} \tag{12}$$

The Equation (11) can be applied to any point of the fluid. With homogeneous and incompressible fluids in isothermal conditions, this usually results in constant value of viscosity in every point. However, this is not exactly true for heterogeneous nanofluids.

At any point inside a solid nanoparticle, the velocity gradient equals to zero. This means that the viscosity inside the solid particles is infinite, which can be interpreted as the obvious fact that solid materials do not flow. Therefore, the viscous behavior at the solid-liquid interfaces is discontinuous.

Because of the discontinuities at the solid-liquid interfaces, the viscosity in each point of nanofluid cannot be accurately expressed with a single value. Therefore, the viscosity of nanofluid actually refers to an *effective viscosity*, which is a value that represents the viscous behavior of the whole heterogeneous macroscale nanofluid. A single value of effective viscosity is generally assumed to be able to comprehensively describe the viscous behavior of the nanofluid, but no solid evidence exists to prove that such value would apply for instance in turbulent conditions. Viscous behavior in the turbulent regime is also very difficult to study, since all viscosity measurements must be conducted in laminar flow conditions.

Accurate and well-established general theories for calculating the viscosity of a heterogeneous fluid do not seem to exist. Therefore, researchers have to use experimental methods or rely on existing models to determine the viscosity. However, several factors seem to affect the measurements, since no general consensus concerning viscous behavior of nanofluids has been obtained so far. The results shown in literature indicate trends of the effects, but the magnitudes reported in different articles tend to be controversial. The impacts of concentration, particle size, temperature and particle shape on viscosity of nanofluids are discussed in this section.

2.2.1 Effect of concentration, particle size and shape

The addition of nanoparticles has been observed to have a strong increasing effect on the fluid viscosity. Even a relatively small concentration of nanoparticles causes viscous behavior of the fluid to change substantially [21-24]. Typically, increments of tens of percents are observed for nanofluids with a volume fraction of only a few percents. For instance, Mohammad Esfe *et al.* [22] studied the effect of ZnO particle concentration on viscosity of ethylene glycol based nanofluid. For volume fractions of 1%, 2%, 3%, 4% and 5%, they reported viscosity increments of 7%, 9%, 17%, 23% and 29%, respectively. Usually, the increasing concentration causes the viscosity to grow exponentially [25,26], but also linear increment has been reported [27,28]. Volume fractions of the studied nanofluids are typically between 0-10 %, but also concentrations of up to 35% have been studied [29].

Overall, the magnitudes of the reported viscosity increments vary significantly and thus, no solid conclusions can be drawn based on the literature. Several correlations have been proposed based on the experimental results, but none of them can be considered as well-established. These correlations will be further discussed in section 2.2.6. Nevertheless, the experimental results indicate that the viscous behavior of nanofluids cannot be comprehensively explained with concentration alone, but several other parameters such as particle size and shape have a significant influence on the viscosity as well. The only generally acknowledged fact concerning the concentration effect seems to be that the viscosity naturally increases with increasing particle fraction. However, even this is disagreed in some articles, which describes the lack of consensus in the research field. Indeed, increasing particle concentration has also been claimed to even lower the viscosity of base fluid [30]. Such result is naturally unexpected, since the viscosity of solid particles is infinite, and therefore the viscosity must eventually approach infinity with increasing concentration.

Particle size has been observed to have a significant impact on viscosity of nanofluids in a few studies [31-34]. Typically, particle size reduction with a fixed concentration causes the viscosity to increase [31-33]. However, the magnitude of this effect varies notably between different studies. In addition, completely opposite results have also been reported: for example, He *et al*. observed viscosity to grow with increasing particle size [34]. Nevertheless, the amount of articles in which the effect of particle size is purposefully studied is still relatively small. The effect of size is usually rather difficult to study, since it requires investigation of nanofluids that have different particle sizes but are similar in terms of other parameters, such as material, concentration and particle shape. Therefore, more high-quality research concerning the subject is required in order to clarify the exact impact of the particle size on the nanofluid viscosity.

Although a single smaller particle causes less resistance to the flow, the smaller size with a fixed concentration also leads to larger amount of particles. Therefore, the solid-liquid boundary surface area increases substantially with decreasing particle size. The most important effects concerning the viscosity should occur at the boundary surface rather than inside the particles, since the velocity gradient inside the solid material is always zero. Therefore, the boundary surface area should be the most important geometric factor affecting the viscosity of nanofluids, rather than the volume of particles. In this sense, it seems a reasonable result that the viscosity increases with decreasing particle size.

The impact of particle shape on viscosity of nanofluids have been studied in a few articles [35-38]. However, convincing comparisons of the shape effect are difficult to obtain, since different shaped particles also differ in terms of size. Neglecting this effect of different particle sizes is practically impossible. In addition, synthesizing differently shaped particles from the same material is often difficult, due to which some comparisons are conducted with varying materials. Nevertheless, at least the following shapes have been studied: spherical, polygonal, cylindrical and fiber-like. The impact of shape on nanofluid viscosity has been reported to be significant. Typically, the spherical shape is considered to increase the viscosity the least [35,36]. For instance, Venerus et al. studied oil-based Al_2O_3 nanofluids (3 vol-%) with different particle shapes and reported that the relative viscosity of the nanofluid containing spherical (d=100nm) particles was only 1,5 whereas the viscosity of similar fluid containing rod-like particles (l=80nm, d=10nm) was 3,1 [36]. Similarly, Yu et al. reported the relative viscosities of 1 vol-% nanofluids with spherical (d=60nm) and rod-like (l=85nm, d=7nm) Al_2O_3 particles in polyalphaolefin to be 1,2 and 1,4, respectively [35]. A well-established physical explanation for the effect of particle shape does not seem exist. However, the differences could explained at least partially by the differences in particle surface areas. With a fixed volume fraction, spherical particles have the smallest possible surface area resulting in the smallest viscosity increment. However, no solid conclusions of the shape effect can be drawn due to the aforementioned difficulties in comparison and relatively small amount of research conducted. Therefore, more comparable research concerning the effect of particle shape on viscosity of nanofluids is definitely required.

2.2.2 Impact of temperature and hysteresis effect

Similarly to conventional fluids, viscosity of nanofluids is heavily dependent on temperature. However, relative viscosity ratio of nanofluid and base fluid has typically been observed to remain somewhat constant regardless of the temperature [17,22,25]. On the contrary, a few studies claim the relative viscosity to change as a function of temperature; both decrease [39] and increase [28] of relative viscosity with increasing temperature have been reported.

In some articles, so called *hysteresis* behavior has been observed to occur during the viscosity measurements [26,40,41]. In this phenomenon, heating the fluid up to a critical temperature causes a permanent increment on the viscosity. The hysteresis effect probably derives from the instability of studied nanofluids. The elevated temperature causes irreversible agglomeration to occur. One reason for this behavior could be

thermal degradation of surfactants at high temperatures. Obviously, such behavior is harmful for practical utilization of nanofluids as heat transfer fluids.

2.2.3 Non-Newtonian behavior

Most fluids behave as *Newtonian fluids*. For this type of fluid the dynamic viscosity η is not dependent on the shear rate ∂u/∂y. Viscous behavior of a Newtonian fluid can be therefore explained comprehensively with a single value. However, in the case of non-Newtonian fluid, the value of viscosity varies depending on flow conditions. Although most of the base fluids are Newtonian fluids, experiments indicate that the addition of nanoparticles may cause the heterogeneous mixture to behave as non-Newtonian fluids [26,42-46]. Typically, dilute nanofluids with small particle fraction are observed to behave as Newtonian fluids, but increasing concentration above certain limit may cause the fluid to behave as non-Newtonian. However, the phenomenon may also be related to larger polydispersity or agglomeration that is typical for concentrated nanofluids. Indeed, some studies suggest that the nanofluids behave in more Newtonian manner when more efficient mixing is applied [45]. The non-Newtonian behavior is observed particularly at low shear rates, but the increasing shear rate often causes the fluid behavior to approach Newtonian [26,44,46]. Non-Newtonian behavior obviously affects the heat transfer performance of the fluid. Therefore, the viscosities of nanofluids are often preferred to be measured with varying shear rates in order to verify the Newtonian behavior.

2.2.4 Empirical and theoretical viscosity correlations

Several models for estimating the viscosity of a colloid exist. The first widely established viscosity model for colloids with low particle concentrations was derived by Einstein in 1906 [47].

$$\eta_r = 1 + 2{,}5\phi \tag{13}$$

where ϕ is the solid particle volume fraction and η_r is the relative viscosity of the colloid. However, experimental studies indicate that equation (13) typically underestimates the viscosity of a nanoscale colloid. Therefore, the equation has been further developed to obtain more suitable models for nanofluids. Batchelor introduced Brownian motion effect and added a quadratic term to the equation as following [48]

$$\eta_r = 1 + 2{,}5\phi + 6{,}5\phi^2 \tag{14}$$

In the Batchelor equation, the added second order term causes the impact of concentration to be significantly larger than in the case of Einstein equation (13). However, experimental results indicate that the viscosity of nanofluid cannot be explained solely with particle volume fraction and thus, a proper correlation should include also other variables. Krieger and Dougherty [49] proposed an equation that can be also used to predict behavior of partially agglomerated nanofluids:

$$\eta_r = (1 - \frac{\phi}{\phi_{max}})^{-\eta_{int}\phi_{max}} \quad (15)$$

where ϕ_{max} is the maximum particle packing fraction, which usually varies from 0,495 to 0,54 and η_{int} is the intrinsic viscosity that has a value of 2,5 for monodispersed suspensions of non-elastic spheres [49]. Corcione considered the effect of particle size and formed the following viscosity correlation [25].

$$\eta_r = ((1 - 34{,}87\frac{d_p}{d_f})^{-0,3}\phi^{1,03})^{-1} \quad (16)$$

where d_p is the particle diameter and d_f is the diameter of a base fluid molecule, given by

$$d_f = 0{,}1(\frac{6M}{\mathrm{N}\pi\rho_{f0}})^{1/3} \quad (17)$$

where M is the molecular weight of the base fluid, N is the Avogadro number and ρ_{f0} is the mass density of the basefluid at 20°C.

Generally, the four above-mentioned correlations are used as theoretical comparison references for experimental results. In addition to these, dozens of other empirical or theoretical based models have been suggested to explain the viscous behavior of nanofluids [50]. However, experimental results often deviate significantly from these suggested correlations and thus, no correlation can be considered as well-established. In addition, predictions of different correlations also deviate from each other [51]. Therefore, experimental data should always be used in analysis of convective heat transfer results.

2.3 Convective heat transfer of nanofluids

In most industrial processes heat is transferred by forced convection. Therefore, performance of the heat transfer fluids utilized in these systems has a remarkable impact

on energy efficiency of practical applications. Significant economic and environmental benefits could be obtained by exploitation of more effective heat transfer fluids.

In several studies, anomalous enhancement in convective heat transfer performance of nanofluids has been reported [6-11]. Exploitation of nanofluids could thus offer a major potential in improving the practical convective heat transfer processes. However, the convection heat transfer of nanofluids is a complex phenomenon that is difficult to be explained comprehensively. In addition to all conventional factors, the convection heat transfer of heterogeneous nanofluids is also dependent on factors such as particle material, concentration, particle size and particle shape. In this section, the effects of different parameters on the convective heat transfer of nanofluids are discussed.

2.3.1 General overview of convective heat transfer

Convection is a type of heat transfer, in which thermal energy is transferred by movement of fluids. In practice, forced convection systems include two mechanisms of heat transfer: thermal conduction and advection. Due to advection, convection heat transfer is a significantly more complex phenomenon than thermal conduction. Analytical solving of convection requires solutions for the continuity equations of mass, momentum and energy. Convection in laminar flow is quite well understood and analytical solutions exist for several geometries. However, a generally established momentum equation for turbulent flow does not exist and thus, the heat transfer coefficients cannot be accurately determined analytically. Due to the lack of analytical solutions, the heat transfer coefficients in turbulent flow are often determined with experimental correlations. However, the heat transfer coefficients obtained using these correlations are not accurate, but include a large possible error of approximately 5-15% [7]. Some of the most used correlations for fully developed turbulent forced convection through a circular duct are presented in Table 3.

Table 3. Correlations for fully developed turbulent forced convection through a circular duct [7]. Abbreviations: Nu - Nusselt number, Re - Reynolds number, Pr - Prandtl number and f - friction factor.

Dittus-Boelter	$Nu = 0{,}023Re^{0,8}Pr^{k}\ ,\ k = 0{,}3\ for\ cooling\ and\ 0{,}4\ for$ heating
Colburn	$Nu = 0{,}023Re^{0,8}Pr^{1/3}$
McAdams	$Nu = 0{,}021Re^{0,8}Pr^{0,4}$
Prandtl	$Nu = \frac{\left(\frac{f}{2}\right)RePr}{1 + 8{,}7(\frac{f}{2})^{0,8}(Pr - 1)}$
Petukhov and Kirillov	$Nu = \frac{\left(\frac{f}{2}\right)RePr}{1{,}07 + 12{,}7(\frac{f}{2})^{1/2}(Pr^{2/3} - 1)}$
Gnielinski	$Nu = \frac{\left(\frac{f}{2}\right)(Re - 1000)Pr}{1 + 12{,}7(\frac{f}{2})^{1/2}(Pr^{2/3} - 1)}$

Several previous experiments indicate that heat transfer behavior of nanofluids does not follow the conventional correlations, but higher Nusselt numbers are reached instead. Consequently, specific correlations for convective heat transfer of nanofluids have also been proposed. For example, Pak and Choi [52] suggested that the heat transfer of nanofluids could be explained as

$$Nu = 0{,}021Re^{0,8}Pr^{0,5} \tag{18}$$

However, the experimental results of convection heat transfer of nanofluids tend to vary significantly and thus, no correlation is generally considered to predict the behavior of nanofluids accurately.

2.3.1.1 Factors affecting the convective heat transfer

Generally, heat transfer coefficient h is a function of six factors [53]:

1. thermal conductivity λ
2. characteristic length (typically the diameter of the pipe), L
3. dynamic viscosity, η
4. density, ρ
5. velocity, v
6. specific heat, c_p

This dependence can be also presented in a form of an unknown function as

$$F\ (k, \lambda, L, \eta, \rho, v, c_p) = 0 \tag{19}$$

The seven variables in the function (19) contain four primary dimensions: mass, time, length and temperature. According to the basic theorem of dimension analysis (Buckinham's π-theorem), the connection between these seven variables can be presented with only three (seven variables – four primary dimensions) dimensionless variables [53]. Several forms for these variables can be formulated, but in the most general form the three dimensionless variables are the Nusselt number Nu, the Reynolds number Re and the Prandtl number Pr.

$$Nu = \frac{kL}{\lambda} \tag{20}$$

$$Re = \frac{vL\rho}{\eta} \tag{21}$$

$$Pr = \frac{c_p \eta}{\lambda} \tag{22}$$

The connection between these dimensionless variables can be written in a form of an unknown function

$$Nu = g(Re, \mathrm{Pr}) \tag{23}$$

Different forms for the function g have been suggested based on experiments. These proposed equations correspond to the existing experimental correlations. The most significant benefit of such correlations is that they produce general information that provides quite accurate estimates for different fluids and heat exchangers [53]. Consequently, all convection heat transfer results are typically presented in dimensionless form.

A remarkable fact considering the heat transfer of nanofluids is that the dependence of Nu on only two other factors, Re and Pr, is based on the assumption of the six above presented factors of the heat transfer coefficient (λ, L, η, ρ, v, c_p). The expression (23) holds true only if no additional factors exist. However, the factors do not include any parameters concerning the special geometry of heterogeneous nanofluids, such as particle size or shape. In this sense, the convection heat transfer behavior of nanofluids could in fact deviate from the conventional heat transfer correlations, as suggested in several articles.

Due to the heterogeneous nature of nanofluids, several additional factors may have an impact on the heat transfer coefficient. These factors include at least the following:

1. Particle size (distribution)
2. Particle shape
3. Amount of particles (concentration)
4. Zeta potential
5. Other interactive forces between the particles
6. Elasticity of particles
7. Density difference between particles and base fluid

The addition of nanoparticles obviously affects the material properties of the fluid and therefore also affects its convective heat transfer behavior. However, no consensus exists whether these changes cause the fluid to behave anomalously and deviate from the correlations.

Generally, the convection heat transfer correlations are considered to have rather poor accuracy of 5-15% [7]. This means that the exact effects of different parameters on the convective heat transfer are not known accurately. In addition, several practical factors affect the performance of real heat transfer systems thus reducing the accuracy of the correlations. These practical factors contain at least the following:

1. Impurities of fluid or heat transfer surfaces
2. Air bubbles
3. Surface roughness
4. Surface material
5. Pressure losses (describe the contact between the fluid and the surface)
6. Temperature and temperature gradient (material properties change with temperature)
7. Development of flow profile

2.3.1.2 Factors affecting the pressure loss of forced convection

Generally, pressure loss of fully developed incompressible flow in a straight pipe can be expressed with Darcy-Weisbach equation [1]

$$\frac{\Delta p}{L} = \frac{f \rho v^2}{2d} \tag{24}$$

where f is the friction factor, that is a generally considered to be a function of Reynolds number and surface roughness k of the pipe as f(Re, k). According to this, pressure loss is a function of the following five variables:

1. Velocity v
2. Density ρ
3. Diameter d
4. Dynamic viscosity η
5. Surface roughness k

In practical systems, the pressure loss is also affected by other factors, such as impurities of the fluid, imperfection of the tube surface and air bubbles. In special case of heterogeneous fluids, the presence of solid particles naturally affects the flow behavior. In addition to direct effect on material properties, also factors such as particle size, shape and elasticity, concentration, density difference of solid and liquid material, zeta potential and other interactive forces between the particles may have an effect on the pressure losses of heterogeneous fluids.

2.3.2 Comparison of the heat transfer performances

The heat transfer coefficient itself yields little information about the suitability of the fluid for practical applications; insufficient heat transfer coefficient can always be increased by increasing the flow velocity. In practice, this can be conducted by simply increasing the pump frequency. The actual utility cost of heat transfer is therefore the electrical energy consumed by the circulation pumps. Consequently, the final practical aim of improving convective heat transfer performance of fluids is to decrease the power of pumps or alternatively the size and financial cost of heat exchangers.

Experimental results of convective heat transfer of nanofluids are most commonly presented by plotting Nusselt number as a function of Reynolds number. Nanofluids have been noticed to typically reach higher Nusselt numbers than water when compared on this basis. However, such “enhancement” does not state that utilizing nanofluids would necessarily improve the performance of real heat exchangers, since this comparison method does not take into account the fact that the two compared fluids differ in terms of flow velocities and pumping powers. Since the viscosity of a nanofluid is higher than that of the base fluids, the flow velocity of the nanofluid is also larger if Reynolds numbers are set equal. The required pumping power is roughly

directly proportional to the third power of velocity ($P \sim v^3$) meaning that the more viscous nanofluid would require substantially larger pumping power than the reference base fluid at the point of comparison. For example, a nanofluid with 20% higher viscosity also has 20% higher velocity resulting in almost 73% larger pumping power with equal Re of nanofluid and base fluid, if the densities and friction factors of the two fluids are considered to be roughly equal. Therefore, the fluid that performs lower in terms of this comparison method may in fact be the more efficient heat transfer fluid in practice. In addition, this presentation method (Nu as a function of Re) is also incapable of explaining the relation of dimensionless variables accurately, since the effect of Prandl number is ignored. Due to these reasons, the method has been criticized in several recent publications [16, 54-56]. It can be concluded that different comparison methods are required to obtain useful information about practical effectiveness of heat transfer fluids.

In addition to heat transfer coefficients, a practically oriented analysis of heat transfer performances requires information about pumping powers. However, the real electricity consumption of the pump is insufficient for such analysis, since the pump efficiencies vary significantly depending on flow conditions. Therefore, ideal pumping power P should be determined as

$$P = \dot{V}\Delta p \tag{25}$$

where $\dot{V}$ is volumetric flow and Δp is pressure loss. The volumetric flow data is typically required for any type of heat transfer analysis. However, an analysis that includes the required pumping powers introduces an additional experimental challenge, since accurate pressure loss measurement is also required.

The practical efficiency of nanofluids can be evaluated with several methods. Each of these methods has its own assets and disadvantages. Often, convective heat transfer efficiency is defined as [37, 62]

$$\eta = \frac{\phi_{nf}/P_{nf}}{\phi_{bf}/P_{bf}} \tag{26}$$

where ϕ_{nf} and ϕ_{bf} are the heat transfer powers and P_{nf} and P_{bf} are the ideal pumping powers of the nanofluid and base fluid, respectively. In literature, the convective heat transfer efficiency η is presented as a function of various variables, such as Reynolds number or concentration. However, this method contains some uncertainty, depending

on the choice of the comparison variable. For instance, comparison between fluids at equal Reynolds numbers leads to aforementioned risk of comparing different pumping powers, whereas comparison of equal concentrations results in comparison of average efficiencies of the selected comparison area, such as fixed range of velocity or Reynolds numbers.

Some authors prefer to simply compare the heat transfer powers as a function of pumping power in order to prevent these errors resulted from the above-mentioned comparison method [52]. This straightforward method is in fact very effective to express whether the fluid would be useful for practical application or not. However, the comparison of heat transfer powers is slightly difficult due to its extreme sensitiveness to temperature differences. It is therefore essential to keep the temperature difference exactly similar in each measurement.

Several research groups prefer to reduce the sensitiveness to temperature ranges by comparing heat transfer coefficients instead of heat transfer powers as a function of pumping power [16,17,57,63]. Such comparison offers a useful overview to thermal performance of the fluid, due to its simplicity and relatively little uncertainty. In this method, the pumping power or heat transfer coefficient ratios of nanofluid and base fluid can be used as well. Although the direct effect of temperature difference is neglected while transforming heat transfer powers to coefficients, the temperature still affects the results via material properties. Therefore, equal temperature levels must still be met as accurately as possible. Nevertheless, this method leaves the differences in specific heats slightly inconclusively assessed, since the effect of the temperature change of the fluid is diminished in the calculation of heat transfer coefficients. Large specific heat is beneficial for heat transfer fluids, since the specific heat determines the amount of heat that the fluid can receive or release with certain temperature change. With equal flow rates, a fluid with larger specific heat would be able to retain higher temperature difference and thus, obtain larger heat transfer power in real applications.

The disadvantage of all these aforementioned practically oriented methods is, however, that none of them provides general information that would hold true in different heat transfer systems. Quantities such as pumping power are related to the original pipe geometry and thus, measurements with a different heat exchanger would yield different values. This is contrary to conventional method of presenting a relation of

dimensionless numbers, which provides very general information that holds true for every system with equal dimensionless numbers.

2.3.3 Effect of concentration, particle size and shape

Particle concentration i.e. the fraction of dispersed phase is naturally one of the parameters affecting the convective heat transfer on nanofluids. The amount of research concerning the impact of concentration is rather significant, since similar samples with different concentrations can be obtained easily [9-11,14-16,55-63]. Typically, even rather small particle volume fractions of 1-5vol-% are observed to increase the Nusselt number by tens of percents, when compared on the basis of equal Reynolds numbers [6-8,52,54-56]. However, the reported magnitudes vary rather significantly and thus, no agreement concerning the magnitude of the effect exists. Furthermore, in some articles such convection enhancement was not observed at all [11-13]. The fluid properties change greatly as the concentration is increased. Particularly, the viscosity of a nanofluid is typically significantly larger than that of the base fluids meaning that velocity and pumping power are also larger if Reynolds numbers are set equal. In order to obtain a proper comparison concerning the practical efficiency of the fluids, pumping powers must also be considered.

Varying results of practical potential of nanofluids have been obtained in literature. In some occasions, nanofluids have been observed to perform significantly better than the base fluids [60,61], whereas in some cases the effect is the opposite [62]. Often, relatively small particle concentrations have been observed to improve the fluid performance, but excessively large amount of solid particles causes the negative effect of increasing pumping powers to dominate deteriorating the practical performance [57]. This is a reasonable result, since the practical efficiency must naturally eventually worsen with increasing fraction of solid material. However, some studies have also reported that addition of nanoparticles deteriorate the heat transfer efficiency of fluids in all cases, regardless of the concentration [17,63].

Several studies have investigated the impact of particle size on convective heat transfer of nanofluids. The experimental results indicate that the particle size has a significant effect on heat transfer performance of a nanofluid. Typically, small particle size is suggested to be beneficial for convective heat transfer [33,34,57,64]. For example, Meriläinen *et al.* reported that 6,5 nm SiO_2 and 8,2 nm Al_2O_3 nanofluids required 25% less pumping power to reach equal heat transfer coefficients with water, whereas other

nanofluids with larger particle sizes showed only deteriorated performance [57]. However, also contradictory results concerning the size effect exist. For example, Abbasian Arani and Amani [65] observed 20nm to be an optimal particle size for TiO_2 particles, whereas the fluids with smaller or larger particle sizes (10nm, 30nm, 40nm and 50nm) had poorer performance. He *et al.* [66] did not observe any remarkable changes in convective heat transfer or pressure losses when the particle (agglomerate) size was altered. Overall, the majority of results seems to indicate the small particle size to be beneficial for nanofluids, but no widespread consensus concerning the effect or its magnitude exists.

Several different particle shapes have been studied in previous experiments, including at least spherical, polygonal, cylindrical and fiber-like particles. However, the impact of particle shape on convective heat transfer performance of nanofluids has been studied in relatively few articles. This results from the fact that convincing comparisons considering the shape effect are difficult to obtain: differently shaped particles are also different in terms of size. In addition, synthesizing differently shaped particles from a single material is difficult, due to which in some studies the shape effect is studied by comparing nanofluids that contain different particle materials. Consequently, the comparisons are often questionable. In some publications, non-spherical particle shape has been stated to be beneficial for heat transfer performance of nanofluids [35,37]. Ferrouillat *et al.* [37] observed that the practical heat transfer efficiency of nanofluids containing rod-like particles was higher than that of nanofluids containing spherical particles. However, none of the studied nanofluids reached the performance of water. In addition, Yu *et al.* [35] reported that nanofluids containing fiber-like particles reached higher Nusselt numbers than the fluids containing spherical particles when Reynolds numbers were set equal. However, the pressure losses of fiber-like or tube-like particles have usually been observed to be rather large [67,68]. Overall, no well-established consensus concerning the effect of particle shape on effective heat transfer performance exists.

2.4. Overview of the previous experimental studies

Previous studies have been unsuccessful in comprehensively explaining the behavior of nanofluids. In spite of significant amount of research work, no consensus concerning the heat transfer or viscous behavior has been obtained. The inconsistencies between

different publications are remarkable, and a reader should not draw any general conclusions based on only a few publications.

At least three possible reasons for the contradictions exist. Firstly, the nanofluids are often characterized insufficiently or the characterization is even completely disregarded. Secondly, some experimental devices may be incapable of accurately measuring the heterogeneous nanofluids. For example, the falling ball type viscometer measurements may be extremely sensitive to even minor agglomeration resulting in measurement errors. Thirdly, the comparisons are often conducted only on basis of dimensionless numbers. By far the most used comparison method of convective heat transfer is to present Nusselt numbers as a function of Reynolds number. However, this method disregards the effect of Prandtl number and thus, is unable to explain whether the performance of nanofluids follow conventional correlations. The information value of this comparison method is in fact rather poor, since it also ignores the required pumping powers leaving the practical heat transfer potentials unassessed. Furthermore, use of dimensionless numbers may also result in amplifying possible measurement errors in material properties. For example, a measurement error in viscosity may distort the convective heat transfer results notably, if the comparison is conducted on the basis of Reynolds numbers. Such concern may be justifiable, since the reported nanofluid viscosities are often in disagreement with one another.

3 Experimental methods

In this chapter, fabrication, characterization and experimental methods applied in this work are discussed.

3.1 Preparation of nanofluids

Several different types of nanofluids were investigated in this study. The measurements were divided into three sets according to their objectives. In the first measurement set, three different concentrations of SiO_2-nanofluids with average particle sizes of ~50 nm were measured to study the effect of concentration on convective heat transfer of nanofluids. The SiO_2 nanoparticles were synthesized by The Department of Material Science and Engineering of Aalto university (AFM group). In the second set, nanofluids with very small particle size of ~10nm were studied. Polystyrene-in-water nanofluids and micelle-in-water fluids were prepared and measured. Micelles were formed using polysorbate20 (Tween20) and sorbitan trioleate (Span85) surfactants. In the third set, the effect of thermal conductivity of particle material on the convective heat transfer behavior of nanofluids was studied. Two equal concentrations of Al_2O_3- and polystyrene nanofluids with similar particle size distributions were compared. Thus, the effect of concentration and particle size was attempted to keep similar in order to obtain fair comparison between the two types of nanofluids with different thermal conductivities of particle materials. A commercial dispersion of Al_2O_3(aq) (Nanostructured & Amorphous Materials Inc.) was used for Al_2O_3 nanofluid preparation. The polystyrene nanofluids were prepared by the research group of Applied Thermodynamics at Aalto University. All nanofluids studied in this work are presented in Table 4.

Table 4. Composition of the measured nanofluids

Series	Dispersed material	Concentration	Surfactant	Diameter (nm)
1.set	SiO_2	0,09	-	52
	SiO_2	0,45	-	58
	SiO_2	1,81	-	47
2.set	Polystyrene	1,0	SDS	17
	Tween 20 / Span 85	0,5	-	8
3. set	Al_2O_3	0,5	-	10
	Al_2O_3	1,0	-	10
	Polystyrene	0,5	SDS	12
	Polystyrene	1,0	SDS	12

3.1.1 Silica nanofluids

The SiO_2 nanoparticles were synthesized by the Stöber method [69]. In brief, ethanol, water and ammonia (25%) were mixed in a beaker under magnetic stirring. Tetraethyl orthosilicate (TEOS) was added dropwise and kept under constant stirring for 18 h. The dispersion was then distilled to remove ethanol and ammonia, after which water was added to obtain the desired concentration. To break any formed agglomerates, the fluids were mixed with ultrasonic mixer for approximately 1h. Before the heat transfer measurements SiO_2 nanofluids were filtered with robust paper filters.

3.1.2 Tween20-Span85 -micelles

Nanosized micelles were formed by mixing two nonionic surfactants together; hydrophilic polysorbate20 (Tween20) and lipofilic sorbitan trioleate (SPAN 85). Hydrophilic-lipophilic balance (HLB) describes the ratio of polar 'head' and nonpolar 'chain' in the surfactant molecule. The more polar the head group is, the more the surfactant has affinity towards water, and the larger the HLB value is. The HLB value of 11 was found to be adequate to obtain sufficient fluid stability, which resulted in fractions of 81,9 w-% of Tween20 and 18,1 w-% of SPAN 85. After dilution to desired concentration, the fluid was mixed with ultrasonic processor (Hielscher 400UPS, 400W) for approximately one hour 200 ml at a time. Before the measurements, the fluid was filtered with 0,2 μm filter paper.

3.1.3 Alumina nanofluids

A commercial Al_2O_3-water dispersion (20 w-%) was purchased from Nanostructured & Amorphous Materials Inc (reported particle size of 10±5 nm). In this study, the dispersion was simply diluted to desired concentrations and mixed ultrasonically for approximately one hour 700ml at a time. Before the measurements, the fluids were filtered with 0,45 μm filter paper.

3.1.4 Polystyrene nanofluids

Polystyrene nanofluids were prepared by adopting the method from Kaiyi and Zhaoqun [70]. The method allows formation of very small polystyrene nanoparticles with narrow size distribution using relatively small amount of surfactant. The initial solution was prepared by dissolving used surfactant, sodium dodecyl sulfate (SDS) to deionized water. Surfactant and water mass fractions were 1.4-2.8 wt-% and 83 wt-% of the final sample mass, respectively. The solution was heated to 80 °C and purged with nitrogen

for ~15 minutes, after which polymerization initiator, polar potassium persulfate (KPS) was added. KPS amount was 500 ppm of the final sample mass. Polymerization solution was stirred for ~15 min under N_2 atmosphere, after which the first part of styrene (30 wt-%) together with 1-butanol (co-surfactant, 1500ppm of the final sample mass) was added slowly in drops to the hot solution during ~30 min. Small polystyrene nuclei were let to form for ~1 h at 80 °C after which the rest styrene was added to the solution in one batch. Finally, the temperature was raised to 85 °C and the polymerization was continued for ~2 h. The total styrene amount was 4,6 w-% of the overall fluid mass.

3.2 Characterization of nanofluids

Heat transfer information of partially unknown fluid is useless and thus, accurate characterization of nanofluids is essential in order to analyze the convective heat transfer measurements correctly. The most important properties of nanofluid are the particle size distribution, specific heat, viscosity and thermal conductivity. Methods concerning these factors are discussed in this chapter. In addition, calculation methods utilized in the analysis of heat transfer and pressure loss measurements are reported.

3.2.1 Particle size distribution and zeta potential

Dynamic light scattering (DLS) is a method to experimentally determine particle size distribution of a fluid sample. A DLS apparatus directs a laser to the sample and analyzes fluctuations in the pulse scattering. The size distribution of sample is obtained from the scattering data.

The small nanoscale particles scatter the incoming laser pulse to all directions. However, the particles are constantly moving because of the Brownian motion. This causes the scattering profile of the laser to fluctuate over time allowing the determination of the particle size distribution, since the movement of particles is dependent on their size via Stokes-Einstein equation for diffusion of a spherical particles through a viscous medium.

$$D = \frac{kT}{6\pi\eta r} \tag{27}$$

where D is the diffusion constant, k is the Boltzmann constant, η is the dynamic viscosity and r is the radius of the sphere. The Stokes-Einstein equation assumes the particles to be spherical, which may result in measurement error in case of non-spherical particles.

In this work, DLS measurements were conducted at temperatures of 20°C and 60ºC in order to study the stability of fluids in the temperature range used in the convective heat transfer measurements. In addition, the size distribution of each sample was verified after the convective heat transfer measurements. The size distribution measurements consisted of at least 4 parallel measurements, each of which further consisted of 13 sub runs. The reported size distributions represent an average of such measurement data.

Dynamic light scattering is not an ultimately accurate and trustworthy method and thus, the results should be verified with another method, i.e. electron microscopy. In this work, particle size distribution was determined with both DLS and TEM-images.

In addition to particle size distributions, DLS was used to determine zeta potentials of the nanofluids. The zeta potentials were measured at temperatures of 20°C and 60ºC. The zeta potential measurements consisted of at least 4 parallel measurements, each of which furher consisted of 10-100 sub runs. The reported zeta potentials represent an average of such data.

3.2.2 Viscosity measurements

The viscosity measurements were conducted with two different types of viscometers in order to ensure the measurement reliability and to compare the functionality of different measurement methods. The two measurement devices were Haake falling ball type C viscometer and Brookfield DV3TLVCJ0 cone/plate rheometer. The temperature range in both viscosity measurements was 20°C-60°C, which is roughly equal to the temperature range of the convective heat transfer measurements.

3.2.2.1 The falling ball viscometer

In the falling ball viscometer, a ball falls through a less dense sample fluid pillar. The viscosity is determined by measuring the time required for the ball to fall a particular measurement length. The falling velocity of the ball is directly proportional to the viscosity of a fluid and the density difference between the ball and the sample. The viscosity is calculated as:

$$\eta = K(\rho_b - \rho_f)t \tag{28}$$

where K is the constant determined in calibration, ρ_b is the density of the ball, ρ_l is the density of the sample and t is the measured time.

Prior to measurements, the device was calibrated with water with temperature range 14°C-70°C, which corresponds to viscosity range 0,41-1,14 mPas. The recommended measuring range with the used ball is 0,6–10 mPas.

Each reported measurement point is an average of at least three parallel points measured at same temperature consecutively. Deviation between these parallel measurements was less than 1,5 % and deviation in temperature was at most 0,1°C.

The falling ball viscometer was observed to ber very sensitive to any agglomeration or larger particles. The measured viscosities of SiO_2-nanofluids increased several percents when the samples rested in the viscometer overnight.

3.2.2.2 The rotational viscometer

The viscosities were also measure with Brookfield DV3TLVCJ0 cone/plate rheometer. In this rotational-type rheometer, a plate rotates against a thin film of sample. In this manner, the fluid is forced to non-slipping Couette-flow between two parallelly moving plates. The upper surface of the fluid cylinder rotates along with the rotating plate, whereas the lower surface sticks with the stationary cone. The device measures the resisting torque that is caused by the sample.

Measurements were conducted at the temperature range of 20°C-50°C. The temperature was controlled using Haake K50 water bath. Shear rate of 1500 1/s was used in the measurements. In addition, Newtonian behavior of the samples was verified by varying shear rate in range of 1125-1875 1/s.

Repeatability of measurements was usually within $\pm$2%. Because of these deviations at least two parallel measurements of each sample were conducted through the whole temperature range. The maximum error of temperature was assumed to be less than 0,05°C.

At higher temperatures, rapid evaporation of the sample fluid caused the measurement quality to deteriorate. Since the initial amount of the sample is very small, the system is extremely sensitive to evaporation of the fluid. Therefore, the sample was changed between every measurement point at higher temperatures. Using this procedure, the error caused by evaporation was mostly prevented.

Rounding of the values caused a notable error on the measurements. Particularly at high temperatures, the viscosity values of water-based nanofluids are small with magnitude

of only ~0,50 cP. The measurement device yields values with only two decimals, which causes the rounding error of second decimal to be ~1%. However, the character of the rounding error is random and thus, such error can be decreased by measurement repetition. Therefore, three parallel measurements were conducted at 50 ºC in order to diminish the rounding error.

Alumina nanofluids were not able to be measured with the cone/plate –viscometer. The Al_2O_3 nanofluid samples agglomerated rapidly during the viscosity measurements, and results were not obtained. In order to investigate this phenomenon, the sample was inserted without starting the motor. Also in this case, agglomeration occurred. It was concluded that the reason for agglomeration was not the shear stress caused by the rotating spindle, but instead the chamber material, aluminium. The surface of reactive aluminium always oxidizes to alumina when in contact with air. Therefore, the Al_2O_3-nanofluid may agglomerate easily on the identical bulk surface of the sample holder. Usage of surfactants could possibly prevent this behavior, but the surface chemistry was not desired to be altered since it would have affected the viscous and thermal behavior of the fluid as well. However, Chandrasekar *et al.* [71] measured Al_2O_3 nanofluids without surfactants with similar cone/plate viscometer thus arguing with this theory. However, there are numerous other factors which may impact on the fluid stability, such as particle size, shape or even crystal phase of Al_2O_3. Therefore, comparison with even slightly dissimilar fluids is difficult. Tue to the stability issues, the Al_2O_3-nanofluids were measured only with Haake falling ball viscometer.

3.2.3 Thermal conductivity measurements

Thermal conductivities of nanofluids were measured with C-therm TCi-3-A thermal conductivity analyzer, based on modified transient source plane technique. In this device, the sensor releases a small thermal pulse into the sample. The effusivity is analyzed based on the disappearance of the pulse, after which the thermal conductivity is determined based on the measured effusivity.

All samples were measured in three parallel measurements, each of which further consisted of ten single points. Average values of all measurement points are reported in this study. The thermal conductivities were measured at room temperature.

3.3 Convective heat transfer and pressure losses

The experimental apparatus is presented in Figure 8. The convective heat transfer measurements were conducted in a tube-in-tube type heat exchanger, in which nanofluid sample flows in the inner tube and hot water flows in the outer section. The inner and outer tubes of the heat exchanger were 1,47m long acid-resistant steel pipes with inner diameters of 6mm and 13mm, respectively. The thickness of the inner pipe, which corresponds to the wall separating the two fluids, was 1mm.

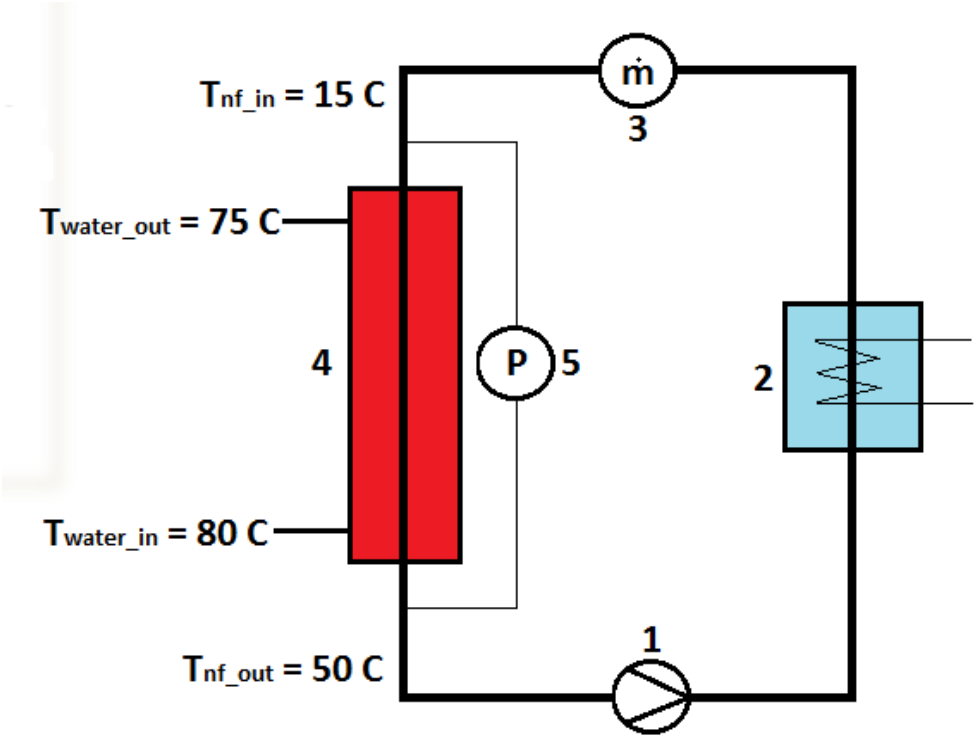

Figure 8. The convection heat transfer measurement apparatus consists of pump (1), cooler (2), flow meter (3), tube-in-tube type heat exchanger (4) and pressure meter (5).

In the first and second measurements sets, the temperature of incoming nanofluid was set to ~ 15°C. The cooling was arranged using a heat exchanger with cold tap water flowing in the external side. In the third measurement set, the inlet temperature was raised to 20 °C in order to verify that the same temperature could be reached in subsequent measurements regardless of the season, since the temperature of cold tap water varies slightly depending on current season.

The outlet temperature of the heated sample varied between 45°C and 78°C, depending on the flow rate. In the first measurement set, the volumetric flow of nanofluid was varied in the range of 0,13-1,34 l/min. In the second and third measurement sets, a more

effective pump was purchased to reach even higher flow rates. In these measurement sets the maximum flow rate was 2,17 l/min. Flow rates were controlled with pump frequency controllers.

The hot water in the outer section entered to the heat exchanger at the temperature of 80°C and cooled to 75°C-80°C, depending on the flow rate of the nanofluid. The flow rate of hot water was kept constant at ~8 l/min in all measurements. The heat capacity flow of the hot water was set to heavily dominate that of nanofluids. This reduced possible errors by forcing the heat releasing temperature of water to remain almost constant and by diminishing significance of the thermal resistance of the outer surface.

In order to prevent natural convection, the warming nanofluid was arranged to flow upwards in the vertically positioned heat exchanger. Consistently, water flow on the external side was set to flow downwards. Consequently, the measurement device was a counter-flow type heat exchanger.

The temperatures of the nanofluids were measured with two thermometers at the inlet point and another two at the outlet. Before reaching the outlet thermocouples, the fluids were strangled in a narrow gap of only 1mm of diameter in order to ensure complete mixing of the fluids. With such arrangement, cross-sectional temperature gradients were diminished thus improving the quality of outlet temperature measurement. The temperature of hot water was measured with one thermometer on each side of the tube. Apparatus for measuring pressure loss (Yokogawa DP Harp pressure transmitter) was connected to each side of the inner tube of the heat exchanger, with the distance of 1,68m.

Velocities of nanofluid and water flows were measured with Optiflux 4000 electromagnetic flow sensor. The velocity measurements were performed at the inlet temperature. Because of this, the measured flow rate values were further corrected to obtain the flow rates at the heat exchanger temperature as

$$\dot{V}_{heat\ exchanger} = \frac{\rho_{in}\dot{V}_{measured}}{\rho_{ave}} \tag{29}$$

The temperature of water side altered very little and thus, the correction for velocity measurement of outer section was not required.

3.3.1 Calculation of heat transfer coefficient

Heat transfer coefficients of nanofluids were calculated using the measured inlet and outlet temperatures, mass flows and fluid properties. First, the logarithmic temperature difference is calculated using its definition.

$$\theta_{ln} = \frac{(T_{water,in} - T_{nf,out}) - (T_{water,out} - T_{nf,in})}{ln\frac{T_{water,in} - T_{nf,out}}{T_{water,out} - T_{nf,in}}} \quad (30)$$

where $T_{i,j}$ are inlet and outlet temperatures of fluids. Subscript *nf* refers to nanofluid. The logarithmic temperature difference θ_{ln} represents the effective temperature difference between the heat exchanging fluids. Conductance G of heat exchanger is defined as the ratio of heat transfer power ϕ and logarithmic temperature difference θ_{ln} as

$$G = \frac{\phi}{\theta_{ln}} = \frac{\dot{m} c_p \Delta T}{\theta_{ln}} \quad (31)$$

where $\dot{m}$ is the mass flow, c_p is the specific heat calculated based on well-established Equation (10) and ΔT the temperature change of the fluid. Conductance per length can be also expressed as

$$\frac{1}{G/L} = \frac{1}{\pi d_i h_i} + \frac{\ln(\frac{d_o}{d_i})}{2\pi\lambda_{tube}} + \frac{1}{\pi d_o h_o} \quad (32)$$

where d_i and d_o are the inner and outer diameter of the tube, respectively, h_i and h_o are the inner and outer heat transfer coefficients, respectively, and λ is the thermal conductivity of the tube material (15 W/mK). The first term represents the thermal resistance between the nanofluid to the inner surface of the tube, second term is the thermal resistance of the tube wall and the third term is the thermal resistance between outer surface of the tube and water. Except h_i and h_o, all factors in equation (32) are known. Heat transfer coefficient of nanofluid, h_i can thus be calculated after h_o is obtained using well-known correlations for Nusselt number of turbulent flow. In this work, Dittus-Boelter correlation for cooling fluids [7] was used to determine the Nusselt number of the external water side.

$$Nu_{DB} = 0{,}023 Re^{0,8} Pr^{0,3} \quad (33)$$

where Nu_{DB} is the Nusselt number according to Dittus-Boelter correlation, Re is the Reynolds number and Pr is the Prandtl number of the hot water flow. The Nusselt

number was further corrected to correspond to the geometry of the duct between the annular tubes. This was conducted with a method suggested by Petukhov and Roizen [72].

$$Nu_{ann} = \frac{h_o d_o}{\lambda_{water}} = 0{,}86 Nu_{DB} \frac{d_o}{d_i}^{0{,}16} \quad (34)$$

3.3.2 Determination of the mean temperature

Some material properties of fluids, particularly viscosity, are strongly dependent on the temperature. For instance, viscosity of water at 20°C is 1,01 mPas [1], whereas at 70°C the viscosity is only 0,41 mPas [1]. Therefore, the correct mean temperature accurately representing the conditions inside the heat exchanger is required for the result analysis.

The axial temperature profile inside the heat exchanger is logarithmic and thus, usage of average of inlet and outlet temperatures as the mean temperature of the fluid yields excessively low values. Particularly in the laminar measurements, in which the temperature changes are the largest, use of such value for mean temperature would result in error of almost 10°C in experimental conditions of this study.

More accurate average mean temperature value would be obtained, if the temperature was measured in several points instead of only two. Due to the lack of such metering, the axial temperature profile inside the heat exchanger was numerically determined by dividing the tube into a thousand computation cells with equal lengths. The conductance per length and the heat transfer power of the heat exchanger were calculated according to Equation (31). The conductance was assumed to be constant along the length of the tube. Starting from the entrance point of nanofluid with measured temperature values $T_{nf,\,in}$ and $T_{water,\,out}$, the heat transfer power of the cell *i* is calculated with equation

$$\phi_i = \left(T_{water,i} - T_{nf,i}\right) \frac{G}{L_{tot}} L_{cell} \quad (35)$$

where *G* is the conductance, L_{cell} is the length of the computation cell, L_{tot} is the total length of the tube and subscript *i* refers to the number of the cell. If the heat capacity flow is assumed to be constant, the temperature change of nanofluid in the cell can now be calculated as

$$\Delta T_{nf,i} = \frac{\phi_i}{\phi_{TOT}} \left(T_{nf,out} - T_{nf,,in}\right) \quad (36)$$

Consistently, the temperature change of water in the cell is calculated as

$$\Delta T_{water,i} = \frac{\phi_i}{\phi_{TOT}}(T_{water,in} - T_{water,out}) \quad (37)$$

Temperature values of the next cell can now be obtained simply by summing

$$T_{nf,i+1} = T_i + \Delta T_i \quad (38)$$

This algorithm is repeated for all thousand cells. The temperature values of the last cell obtained this way are bound to be very close to the measured values $T_{nf,\,out}$ and $T_{water,\,in}$, since the calculation method is based on the experimentally determined conductance. Infinite amount of computation cells would yield an accurate result, within the frames of the assumptions, naturally.

The mean temperatures were obtained as averages of these thousand computational temperature points. Mean Reynolds numbers were also calculated as average values of these points in order to prevent the error caused by heavily temperature-dependent viscosity value.

3.3.3 Pressure loss measurements

The pressure loss measurements were conducted during convective heat transfer experiments using Yokogawa dp harp transmitter. The device was connected with 1 mm tubes on each side of the inner tube of the heat exchanger. The tube length for pressure loss measurements was 1,68 m.

3.3.3.1 Calibration

The pressure meter was calibrated prior to the measurements in order to verify the reliability of results. The calibration was conducted by measuring hydrostatic pressure differences of stationary water pillars at room temperature. One side of the pressure meter was filled with 5 cm high water pillar and the height of the pillar on the other side was varied between 5 cm-95 cm.

The measured values were compared with analytical values. The hydrostatic pressure difference of a water pillar is

$$p_{h2} - p_{h1} = \rho g(h_2 - h_1) \quad (39)$$

where p is the hydrostatic pressure and h_1 and h_2 are the pillar heights, respectively.

The calibration indicated that the readings of the pressure meter were systematically 2,0918 kPa higher than the real values. When this systematic error was corrected

computationally, the results were very close to real values, as is shown in Figure 9. The zero pressure difference value of p_0 = 2,0918 kPa remained constant regardless of the pressure level, when equally tall water pillars with height of up to 1,0m were set to both sides. The equipment was thus considered to provide accurate values, when the p_0 was subtracted from the experimental values. The pressure difference range of calibration covered the entire pressure loss range of the heat transfer measurements.

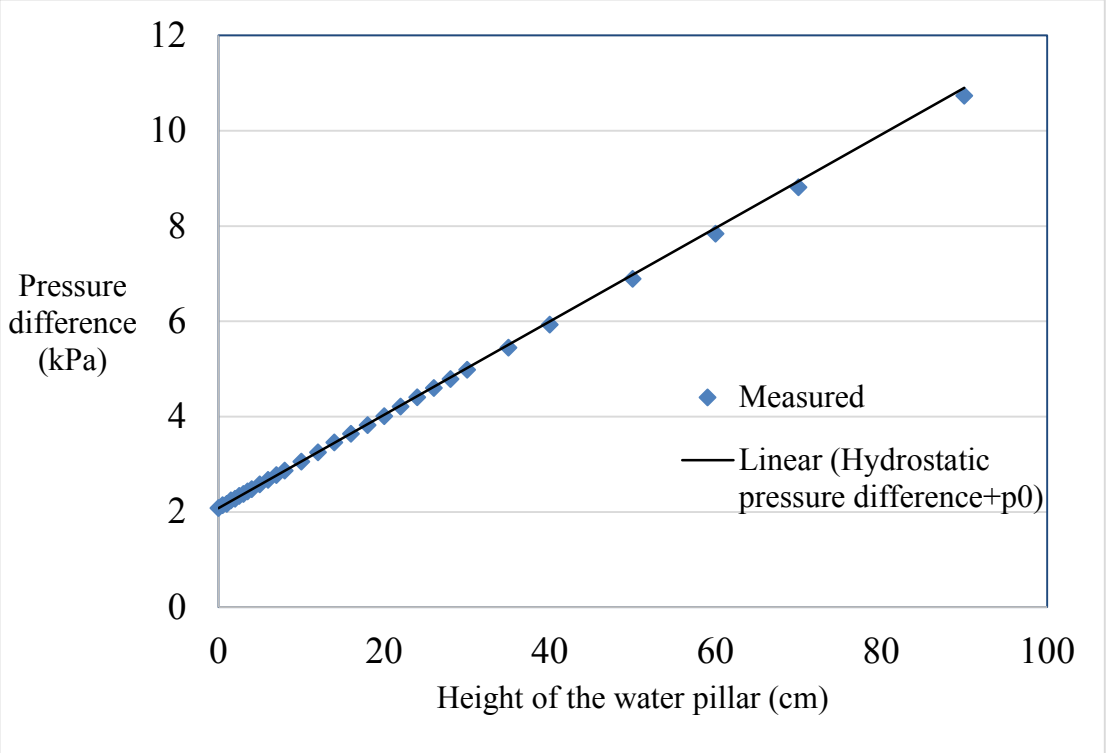

Figure 9. Measured pressure difference of water pillars compared to analytically determined values.

3.3.3.2 Correction of dynamic pressure loss considering temperature change

The vertical position of the tube used to prevent natural convection caused a problem concerning pressure loss measurements. In real dynamic measuring situation one side of the pressure meter experiences a high-temperature fluid pillar, while the pillar on the other side of the apparatus remains constant at room temperature. Although these pillars are equal in terms of height, density difference caused by differing temperatures results in unequal hydrostatic pressures on each side of the pressure difference indicator, as illustrated in Figure 10.

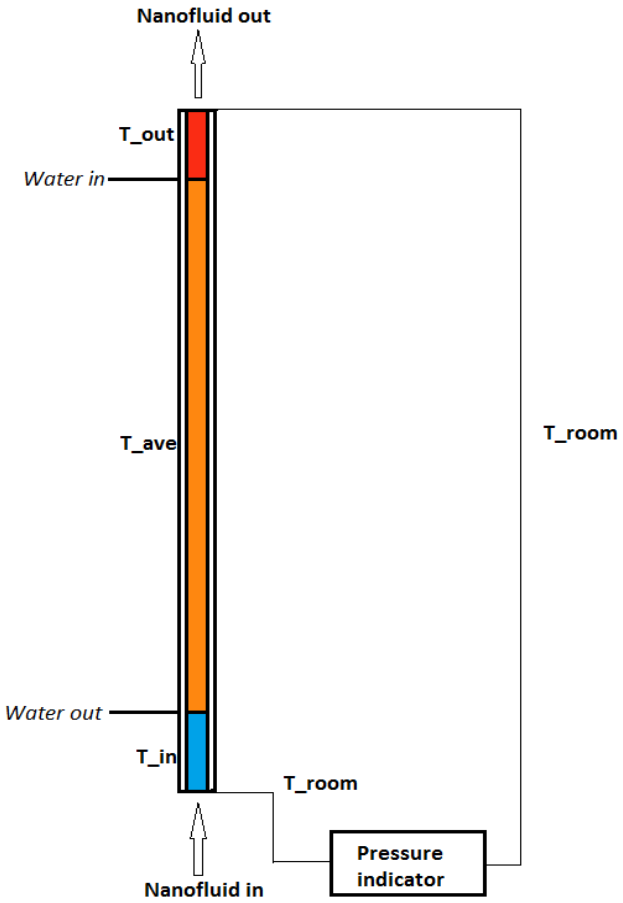

Figure 10. Illustrative picture of temperature levels on each side of the pressure indicator

The difference in hydrostatic pressure caused by the temperature difference is

$$\Delta p = \left(\rho_T - \rho_{T\_ambient}\right) g h \tag{40}$$

where ρ_T is the density of fluid inside the vertical heat exchanger tube. Since the fluid densities vary slightly as a function of temperature, the temperature profile inside the tube is required in order to obtain an accurate ρ_T value.

In this work, a function for fixing the error caused by this effect was formulated. In the function, the tube was divided into three separate parts. The first part of the function covers the short distance between the first pressure meter joint and the inlet of the heat exchanger, where the temperature of the fluid is the measured inlet temperature. The second part is the actual heat exchanger, inside which the fluid temperature changes constantly. The average temperature of this part is calculated with methods as explained in Section 3.3.2. The third part covers the distance between the outlet point of the tube

and the second joint of the pressure meter. In this part, the fluid is constant at the outlet temperature.

Although this effect is rather insignificant in turbulent flow, it may completely ruin the measurements in laminar flow region. The temperature difference resulted in the pressure loss error of ~0,127 kPa with the smallest used fluid flow. Therefore, a notably large error of even 117 % would have been encountered if the corrective method was not applied. In addition to laminar flow regime, the method naturally increases accuracy in transition and turbulent regime as well.

4 Results

Several different types of nanofluids were experimentally investigated in this study. The objective was to determine the impacts of concentration, particle size and thermal conductivity of particle material on convective heat transfer performance of nanofluids. The measurements were divided into three sets according to their objectives. In the first set, the impact of concentration was studied by measuring three different concentrations of SiO_2-nanofluids with average particle size of ~50 nm. In the second set, polystyrene and micelle nanofluids with very small particle size of ~10 nm were measured. The purpose was to compare the performance of nanofluids composed of small particles to that of SiO_2 nanofluids with significantly larger particle sizes. In the third set, the effect of thermal conductivity on convective heat transfer behavior of nanofluids was studied. Two concentrations (0,5 and 1,0 vol-%) of Al_2O_3-nanofluids were measured and compared with equal concentrations of polystyrene-nanofluids with equal particle size. Thus, the effect of concentration and particle size were aimed to keep similar in order to obtain a fair comparison between the two types of nanofluids with different thermal conductivities of particle materials.

4.1 Characteristics of nanofluids

The main properties of the studied nanofluids are summarized in Table 5. Further information concerning the properties can be found in corresponding sections.

Table 5. Concentration and the main material properties of the studied nanofluids. Particle size is measured with DLS and reported as the peak value of number distribution. Viscosity (η), thermal conductivity (λ) and density (ρ) values are measured at 25 °C.

Particle material	Concentration (vol-%)	Particle size (nm)	PDI	$\lambda_{nf}/\lambda_{water}$	η_{nf}/η_{water}	ρ_{nf}/ρ_{water}
SiO_2	0,09	52	0,035	1	1,04	1,00
SiO_2	0,45	58	0,063	0,99	1,08	1,01
SiO_2	1,81	47	0,079	0,99	1,22	1,02
Micelle	0,5	8	0,398	1,00	1,01	1,00
Polystyrene1	1,0	17	0,103	1,00	1,03	1,00
Al_2O_3	0,5	10	0,228	1,01	1,09	1,01
Al_2O_3	1,0	10	0,259	1,02	1,21	1,02
Polystyrene2	0,5	12	0,091	1,03	1,04	1,00
Polystyrene2	1,0	12	0,117	1,04	1,09	1,00

4.1.1 Zeta potential

The measured zeta potential data is presented in Figures 11, 12 and 13. Each curve corresponds to the average of at least three parallel measurements. The location in the horizontal axis represents the value of zeta potential, whereas the values of vertical axis correspond to the total counts during the measurements and are not comparable between different fluids.

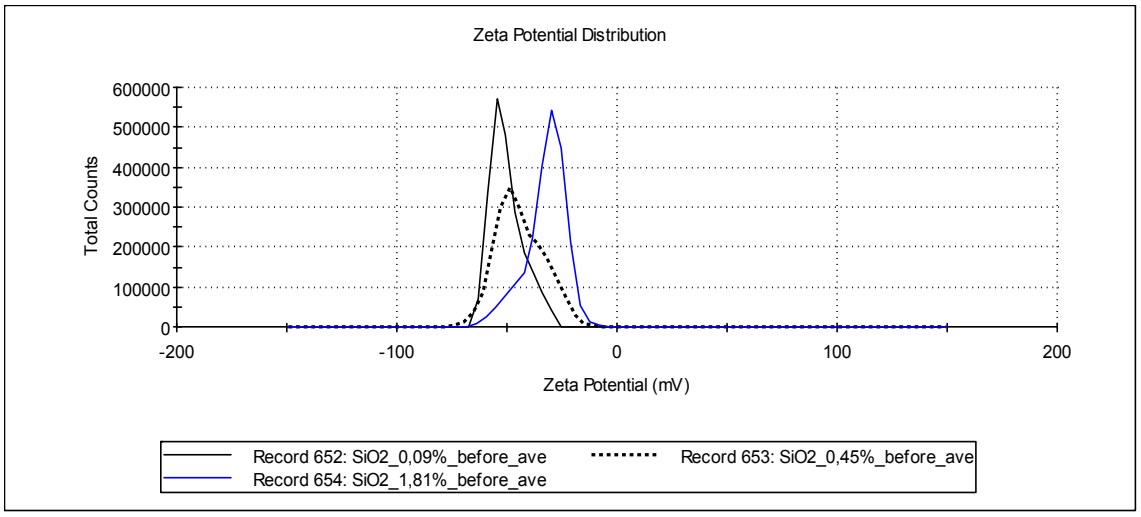

Figure 11. Zeta potentials of SiO_2 nanofluids.

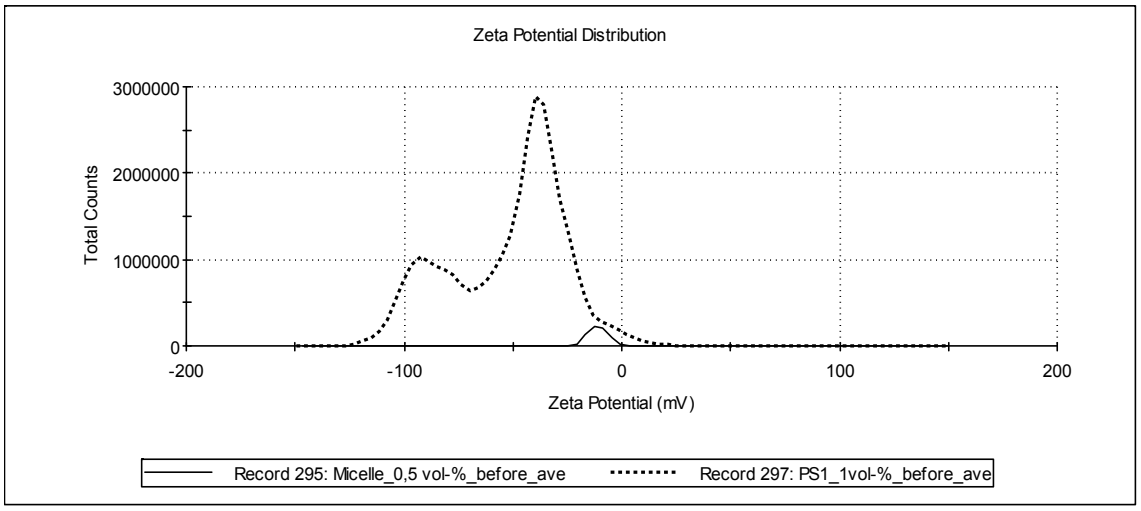

Figure 12. Zeta potentials of micelle and polystyrene 1 nanofluids.

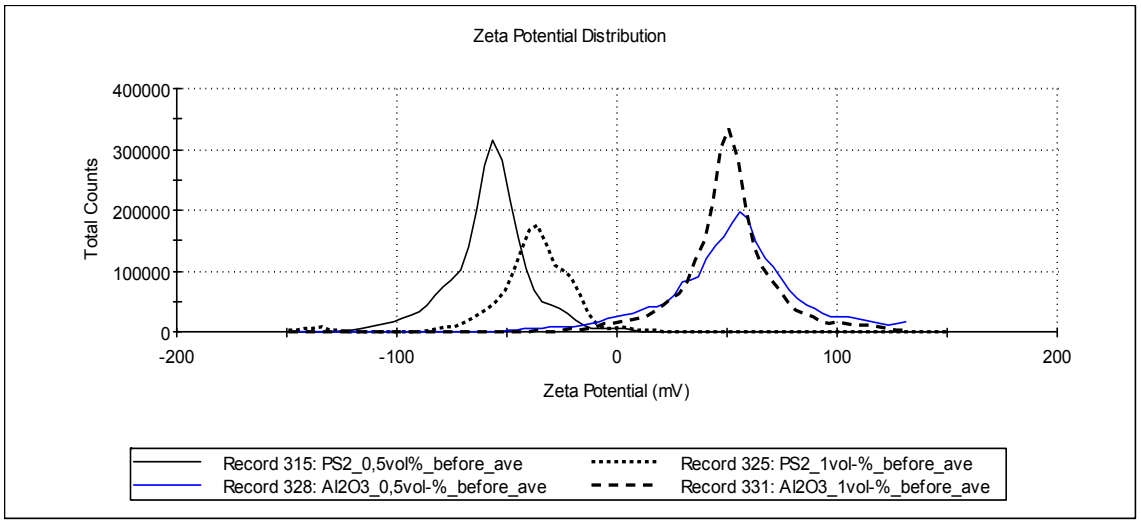

Figure 13. Zeta potentials of Al_2O_3 and polystyrene nanofluids.

The zeta potentials of SiO_2, polystyrene and Al_2O_3 samples were considered to be sufficient for stability since the absolute values exceeded the stability limit of 30 mV. However, for micelle nanofluid a relatively broad zeta potential distribution of 0-45 mV was obtained and thus, its stability was considered to be uncertain. Indeed, the micelle sample was observed to change slightly during the convective heat transfer measurements and thus, have poorer stability than the other samples, as discussed in Section 4.1.2.

4.1.2 Size distribution

The average particle sizes and polydispersity indices of nanofluids measured with DLS are presented in Table 5 (c.f. Chapter 4.1). The size distributions are illustrated in Figures 14, 15 and 16, where each curve is calculated as an average of at least five measurements. These parallel measurements were typically almost identical. The samples were measured at two temperatures, 25 °C and 60 °C, in order to study the effect of temperature on dispersion stability. No significant differences were observed at these two temperatures. The size distributions of the fluids were also measured after the convective heat transfer measurements in order to ensure the dispersion stability during the experiments.

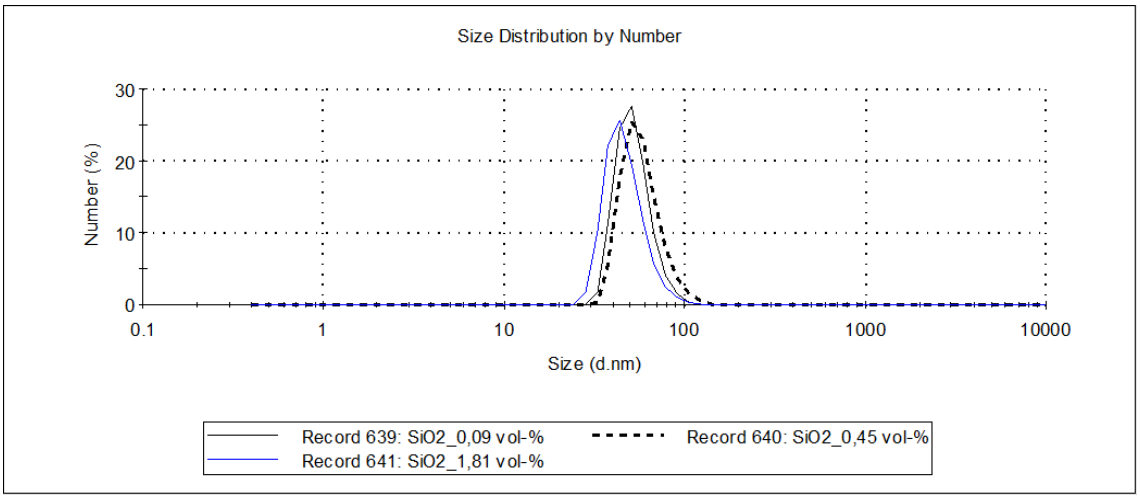

Figure 14. Size distributions of the SiO_2-nanofluids

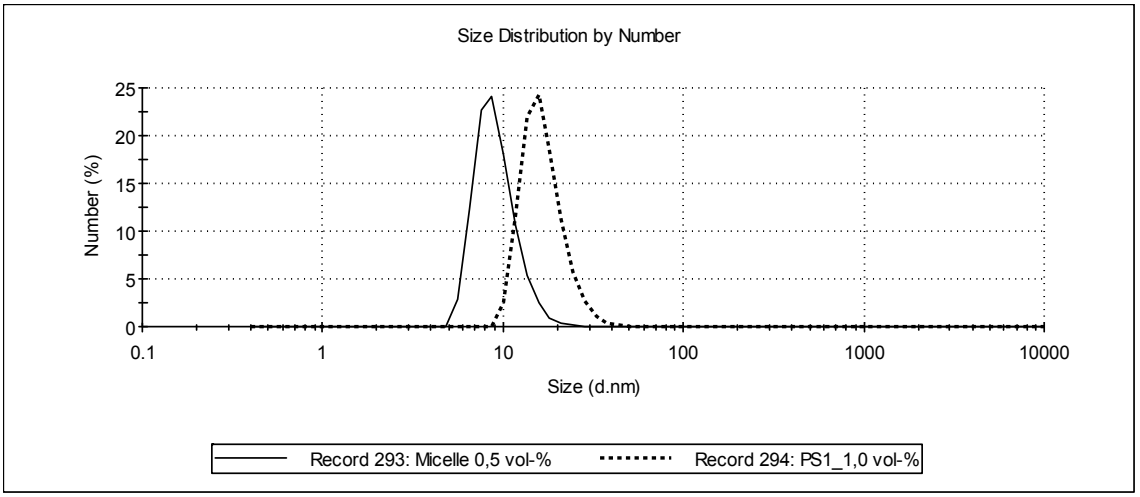

Figure 15. Size distributions of the second measurement set samples; polystyrene and micelle samples with small particle size

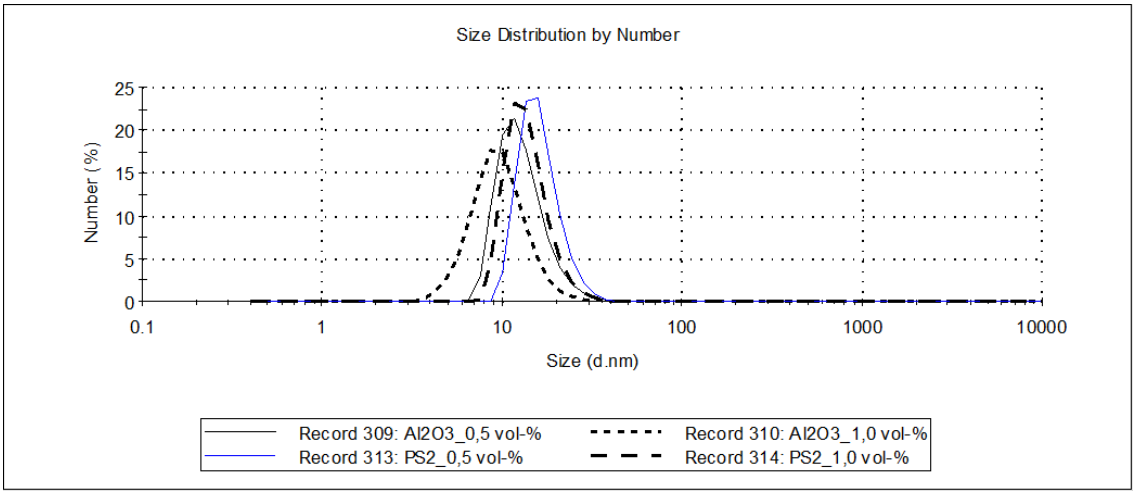

Figure 16. Size distributions of the third measurement set samples; polystyrene and alumina samples with similar particle size distributions

The size distributions of the samples with same particle material but different concentrations were usually very similar. The size distributions of SiO_2 nanofluids differed slightly from each other since the nanoparticles were synthesized in several small batches. However, the magnitude of these differences was only ~10% and therefore the fluids were considered to be suitable for comparison.

Figure 17 presents an unsuccessful attempt to verify the size distribution of micelle sample after the heat transfer measurements. Parallel measurements yielded differing results and thus, the size distribution was not able to be verified. Nevertheless, such behavior indicates that the fluid composition had slightly altered during the heat transfer measurements. Micelles are not strongly bound particles but rather loose assemblies of amphiphilic molecules. Therefore, the micelles may deform in flowing systems. Additionally, temperature may impact on the spontaneous structure into which the surfactants orientate. Therefore, stability of the micelle sample during the heat transfer measurements was be considered slightly uncertain. Other nanofluids were observed to remain unchanged during the heat transfer measurements.

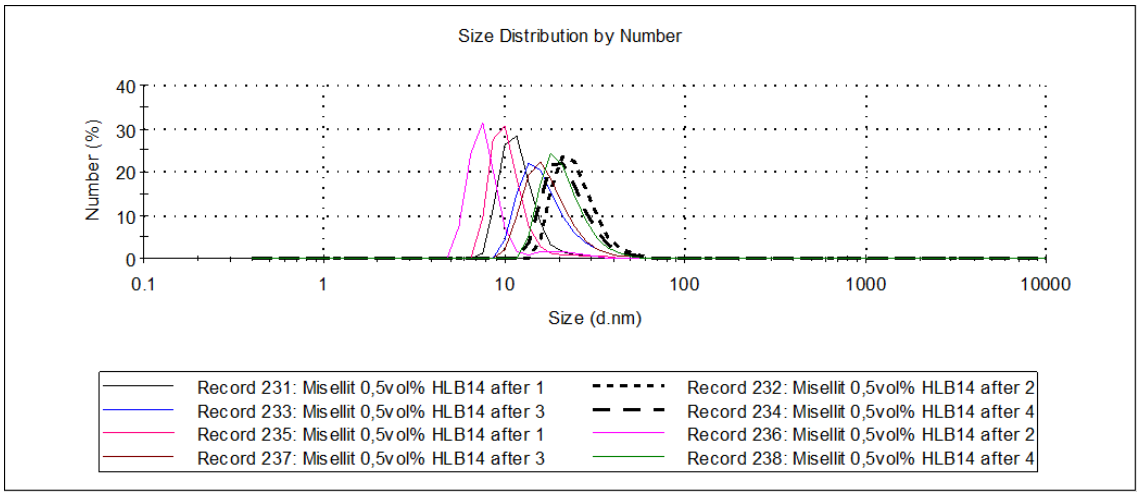

Figure 17. Size distribution of the micelle nanofluid was not able to be verified after the heat transfer measurements

Since DLS assumes the particles to be spherical in shape, the size distributions were verified with Transmission Electron Microscopy. The TEM-images are presented in Figures 18, 19 and 20.

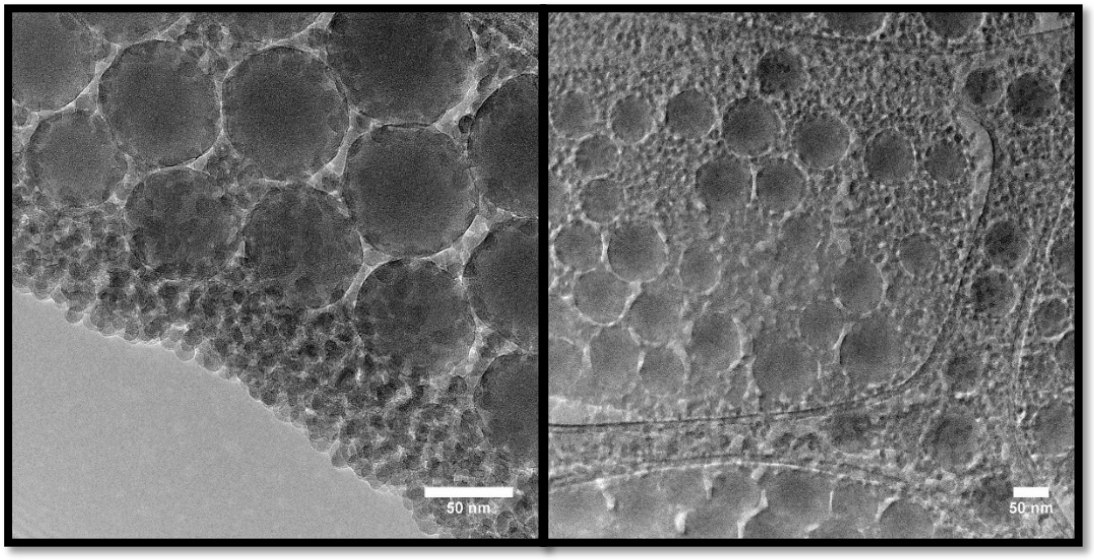

Figure 18. TEM-images of SiO_2 particles

Transmission electron microscope images of SiO_2 particles (Figure 18) show that the particles are spherical in shape. However, the particles can be divided into two groups in terms of size: small particles with average diameter of ~10 nm and large particles with average diameter of ~90nm. These results differ significantly from the DLS measurements that indicated average diameter of ~50 nm. However, DLS measures the suspension whereas TEM images describe the dried sample. Therefore, the differences were probably caused by the drying and long storing of the TEM samples. Nevertheless, doubtless information concerning the size of SiO_2 particles was not obtained.

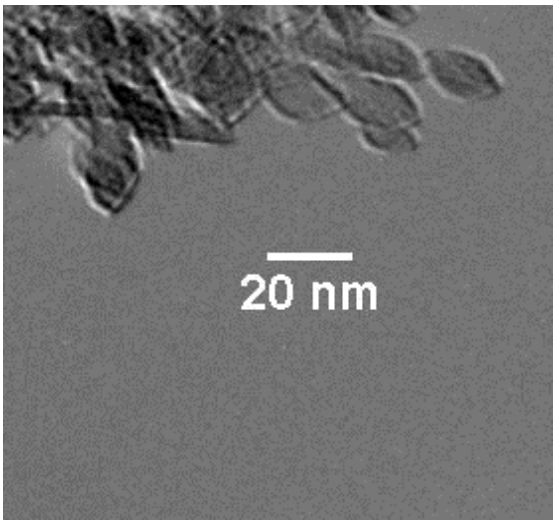

Figure 19. TEM-image of Al_2O_3 nanoparticles

The TEM-image (Figure 19) reveals that the Al_2O_3 particles were somewhat eye-shaped. According to TEM imaging, the average length of the particles was 16,1 nm, whereas the average thickness was 9,9 nm. The size was analyzed based on twenty imaged particles. The result is in good agreement with the DLS result that indicated average size of 10nm (Figure 17). In addition, both of these results match the value that was reported by the manufacturer, 10±5 nm.

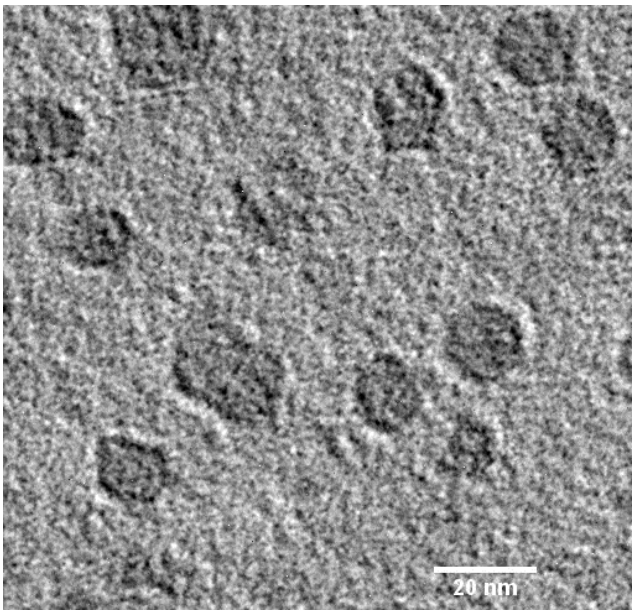

Figure 20. TEM-image of polystyrene2 particles

According to the TEM-image (Figure 20), the polystyrene particles were approximately spherical in shape. An analysis based on thirty imaged particles indicated average particle diameter of 11,5 nm. The result is in good agreement with the DLS result, 12 nm.

4.1.3 Viscosity

The relative viscosities measured at 25 ºC temperature are presented in Table 5 (c.f. Chapter 4.1). The relative viscosities are plotted as a function of temperature in figures 21, 22, 23 and 24.

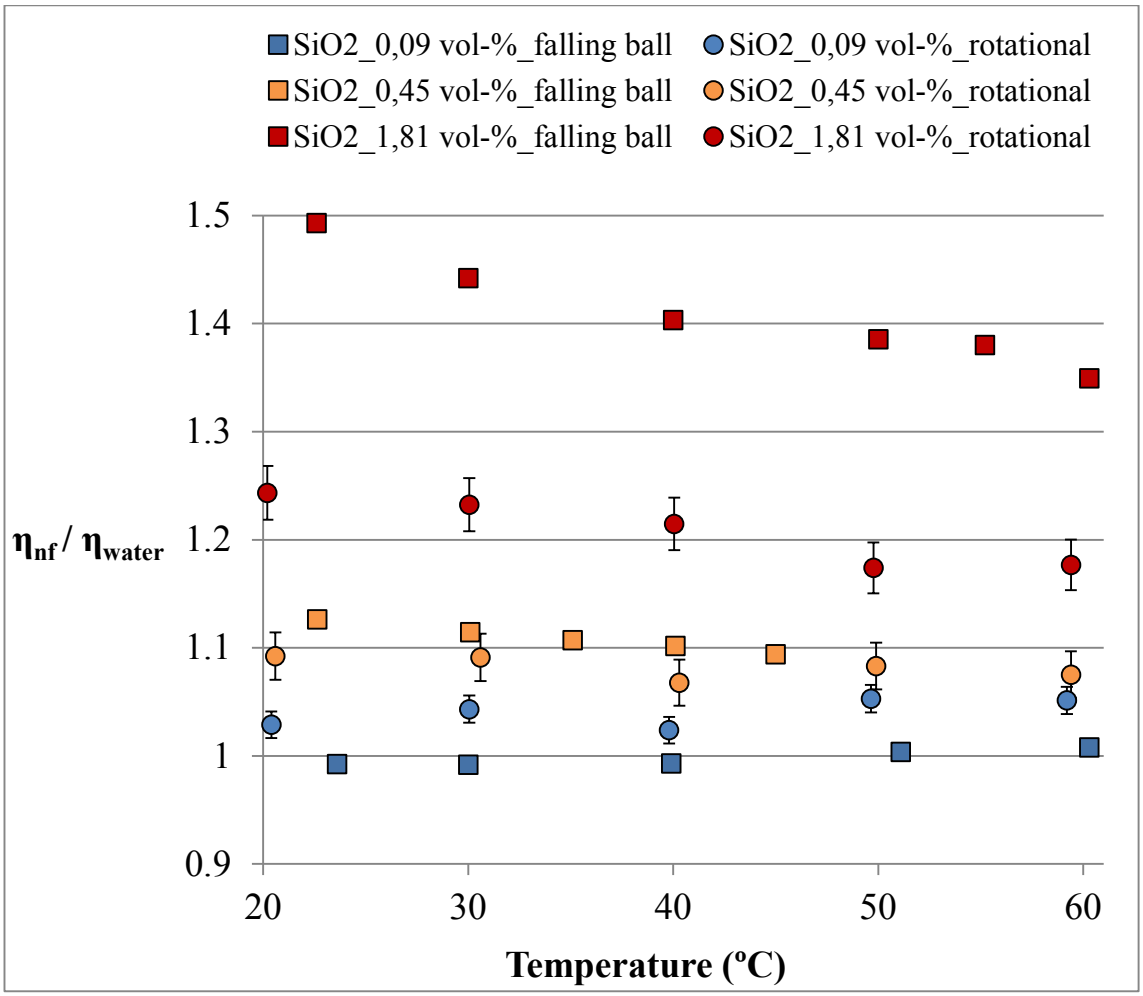

Figure 21. Viscosities of SiO_2 nanofluids. Error bars are estimated based on the differences between parallel measurements. Error bars of viscosities measured with falling ball viscometer are not illustrated as the differences were insignificant.

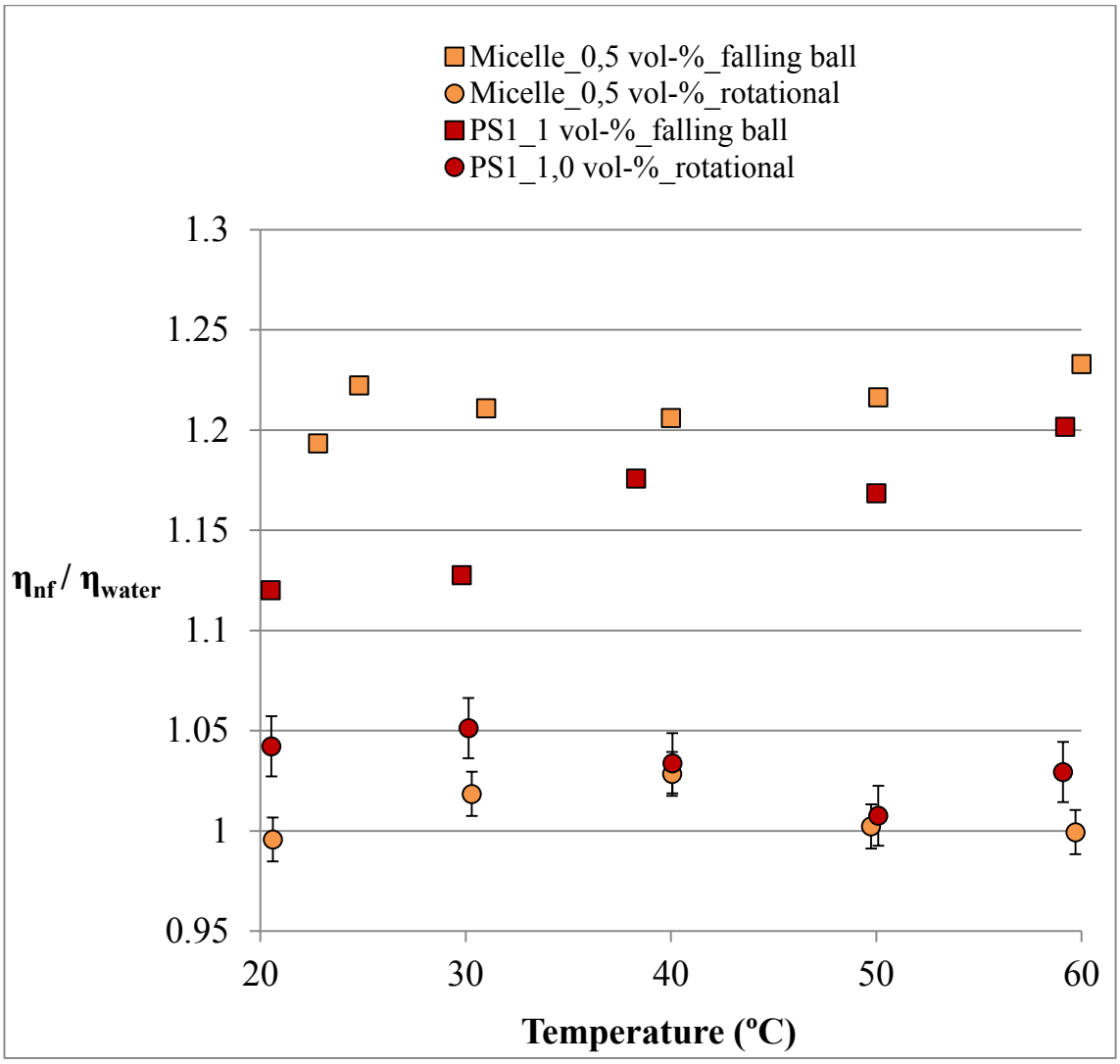

Figure 22. Viscosities of micelle and polystyrene 1 nanofluids. Error bars are estimated based on the differences between parallel measurements. Error bars of viscosities measured with falling ball viscometer are not illustrated as the differences were insignificant.

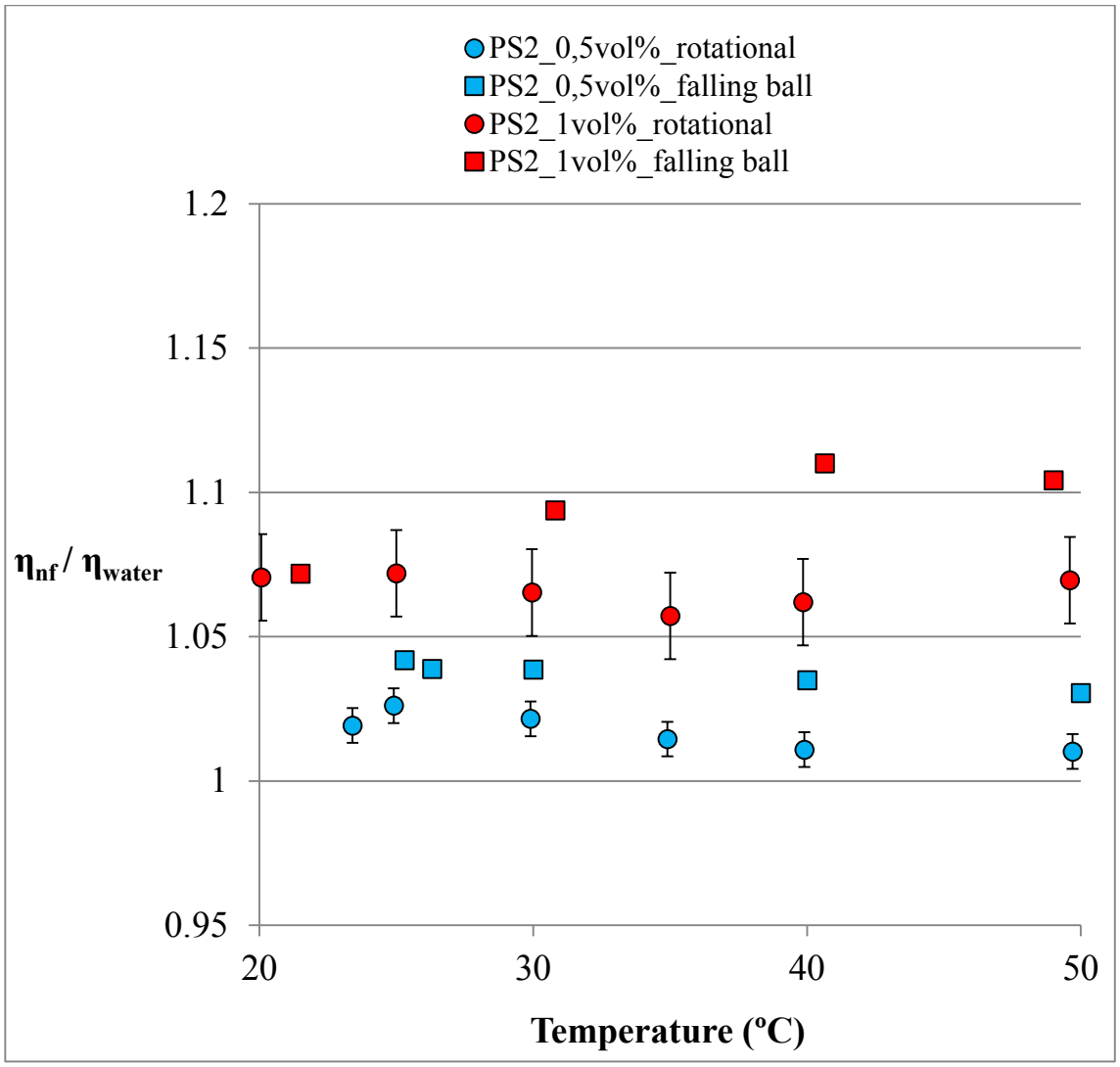

Figure 23. The viscosities of polystyrene 2 nanofluids. Error bars are estimated based on the differences between parallel measurements. Error bars of viscosities measured with falling ball viscometer are not illustrated as the differences were insignificant.

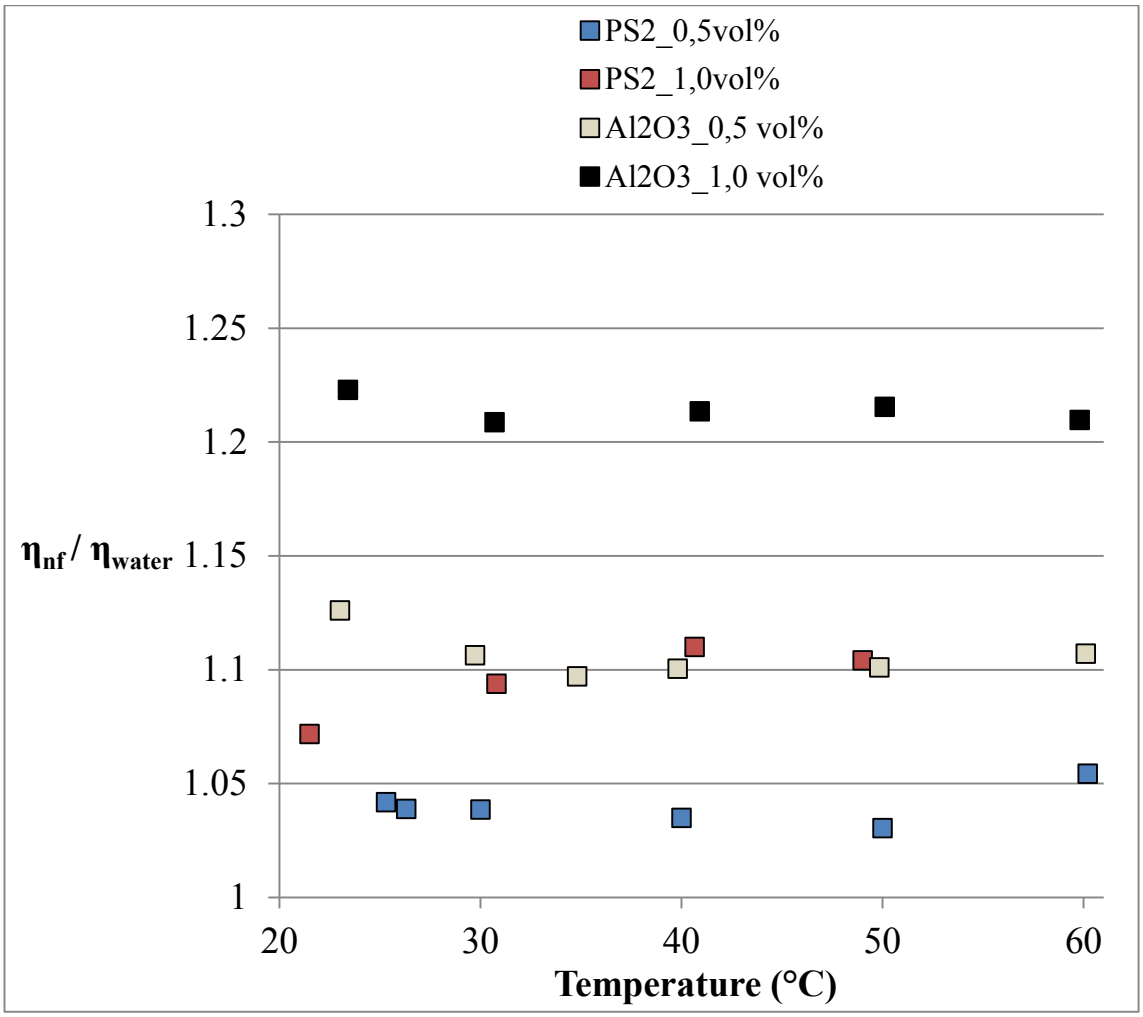

Figure 24. Viscosities of Al_2O_3 and polystyrene 2 nanofluids measured with the falling ball viscometer.

The viscosities were measured with two measurement devices: Haake Type C falling ball viscometer and Brookfield DV3TLVCJ0 cone/plate rotational rheometer. The results differed significantly depending on which measurement technique was used. In all measurements except one (0,09 vol-% SiO_2), the relative viscosities were lower when measured with the rotational rheometer. Relative magnitude of the difference seems to increase with increasing concentration. The largest difference was observed for 1,81 vol-% SiO_2 nanofluid, for which the difference was 20,5% at maximum. A definite reason for these differences was not found. Nevertheless, the sensitiveness of falling ball viscometer to any larger particles or agglomerates may result in excessively high values. In addition, unstable micelles may break in the rheometer due to vigorous stirring, in which case the values would be substantially lower than in the case of falling ball viscometer measurements.

Typically, the measured relative viscosity of nanofluids was independent on the temperature, as proposed in several publications [17,22,27]. However, the relative viscosity of 1,81 vol-% SiO_2 nanofluid was observed to decrease with increasing temperature (Figure 19). This phenomenon was observed with both measurement devices. Similar behavior was observed by Sundar *et al.* [28].

The Newtonian behavior of the samples was verified with the rotational viscometer. However, the studied range of shear rate 1125-1875 1/s was relatively high and narrow, since sufficient shear rates are required to obtain accurate results for low viscosity fluids, such as the water-based fluids studied herein. Thus, viscous behavior of the fluids in extremely low shear rates corresponding to the conditions of the falling ball viscometer was not able to be verified. Therefore, non-Newtonian behavior with very low shear rates cannot be ruled out as a reason for the differences of the results obtained with the two devices, since the conditions of the devices differ from each other in terms of shear rates.

The rotational type cone/plate –viscometer was considered to be more reliable measurement device and thus, those results were used in the data analysis of the convective heat transfer experiments. However, the viscosities of Al_2O_3-nanofluids were not able to be measured with the rotational viscometer as discussed in Section 3.2.2.2. Therefore, the falling ball viscometer values were used in the analysis of alumina nanofluids. In order to obtain a reasonable comparison between the samples of the third measurement set, the falling ball viscometer values were used in the analysis of polystyrene nanofluids as well.

4.1.4 Thermal conductivity

The relative thermal conductivities of samples are presented in Table 5 (c.f. Chapter 4.1). The addition of nanoparticles caused slight increments in thermal conductivities. However, the observed differences were relatively small; the maximum enhancement of 3,5 % was obtained with 1 vol-% polystyrene nanofluid.

In the third measurement set, an interesting phenomenon was encountered. The thermal conductivities of Al_2O_3-nanofluids were observed to be to be slightly lower than those of polystyrene nanofluids with corresponding concentrations. This result is truly unexpected since the literature value of thermal conductivity of bulk Al_2O_3 is 12,1 W/mK [1], whereas the value for bulk polystyrene is only 0,14 W/mK [1]. Naturally, the thermal conductivity in nanoscale is not similar to that of bulk due to distortions in

the crystal structure of extremely small systems as studied herein. In addition, surface chemistries of the two samples differ substantially from each other; in the case of polystyrene nanofluids, high concentration of anionic surfactant was used whereas no surface treatment was used for Al_2O_3 nanofluids. However, no clear conclusion concerning these differences can be drawn due to relatively large inaccuracy of the measurement device, 3 %.

4.2 Heat transfer coefficients

Nusselt numbers of the three measurement sets are plotted as functions of Reynolds numbers in Figures 25, 26, 27 and 28. The nanofluids typically reached higher Nusselt numbers than water with equal Reynolds number. The largest difference of 12,5-20,5 % was obtained for 1,81 vol-% SiO_2 nanofluid. Similar behavior has been widely reported literature as well [6-8,55,57-59]. However, this presentation method has been criticized in several recent publications, since it does not take the required pumping powers into account [16,54-56]. Therefore, the presentation method is unable to describe the suitability of nanofluids for practical applications as discussed in chapter 2.3.2.

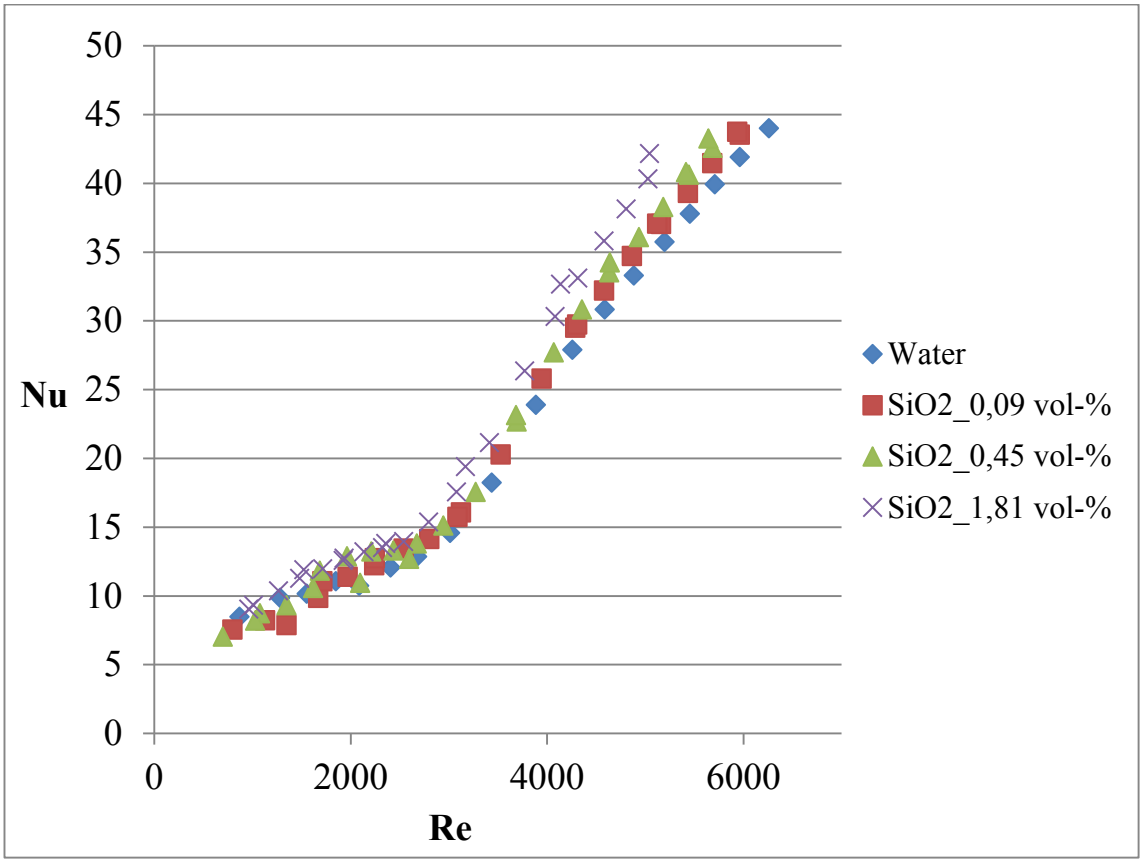

Figure 25. Nusselt numbers of SiO_2-nanofluids plotted as a function of Reynolds number

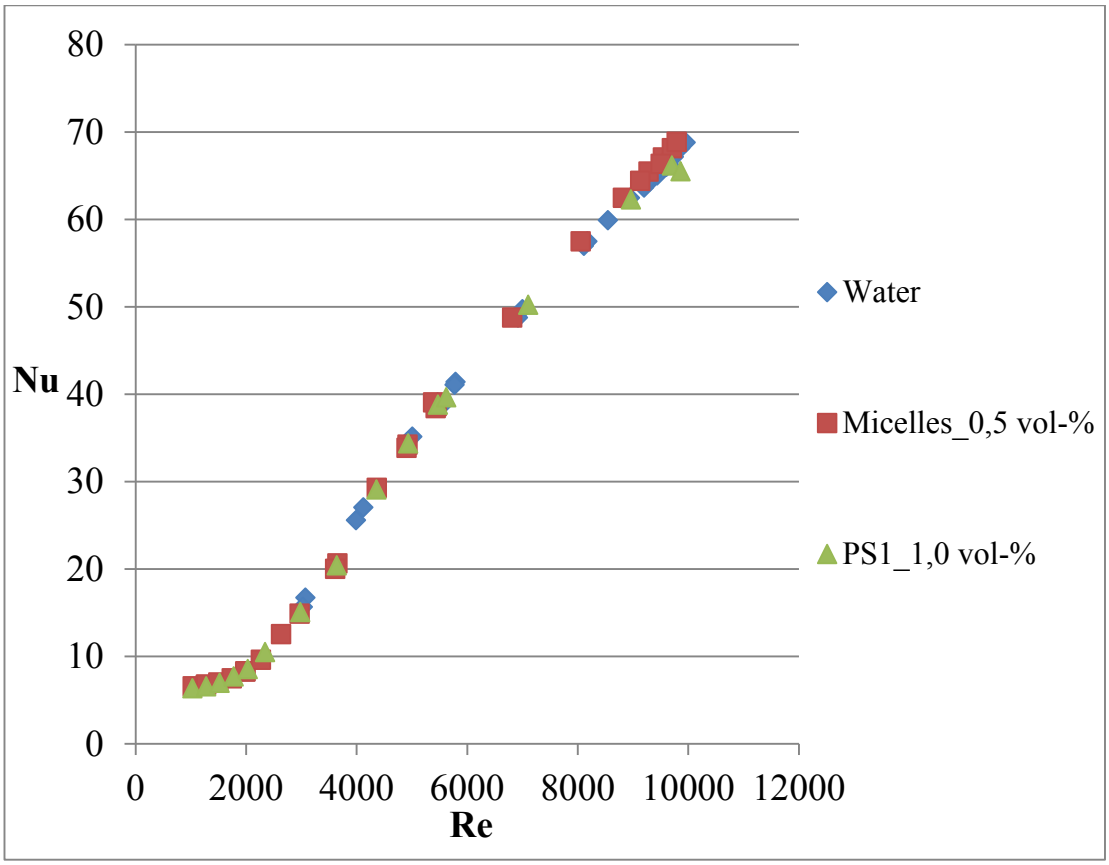

Figure 26. Nusselt numbers of micelles and polystyrene 1 plotted as a function of Reynolds number

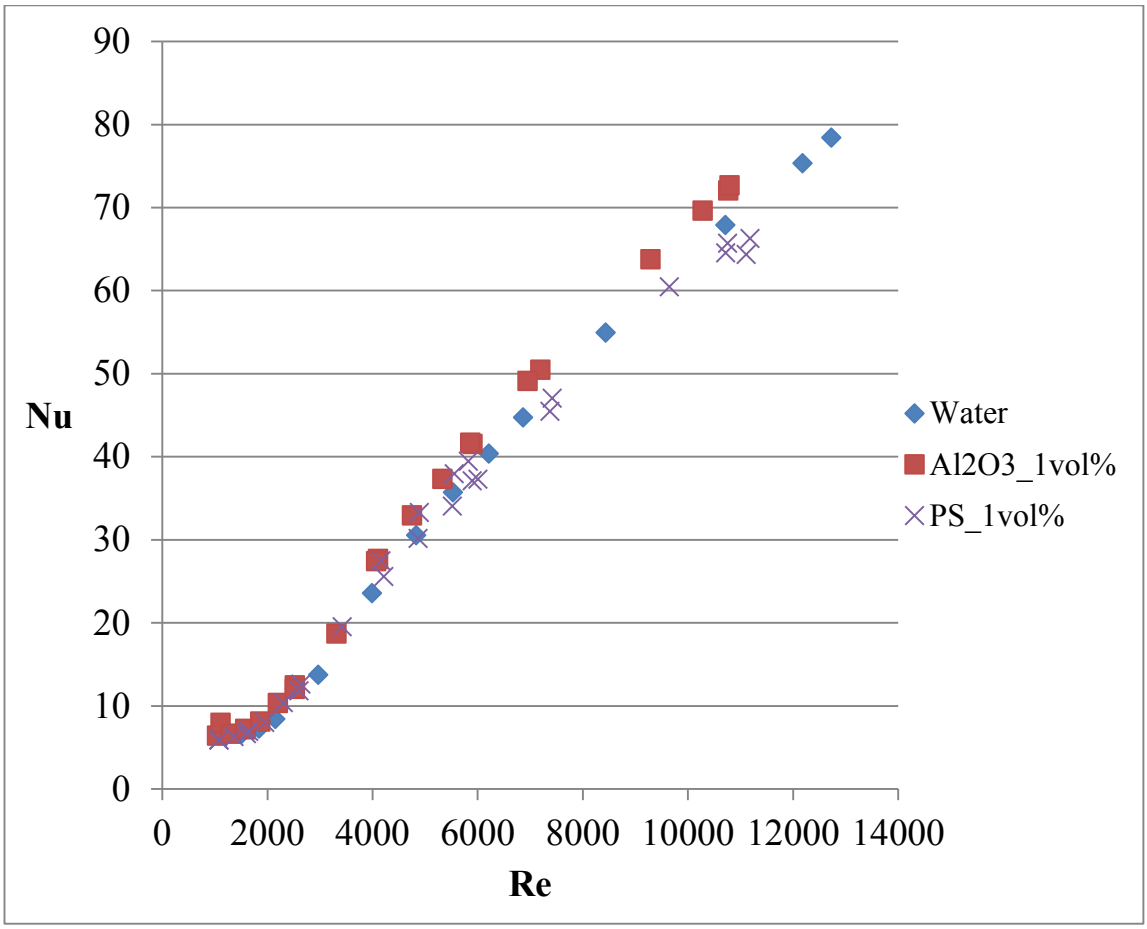

Figure 27. Nusselt numbers of 1,0 vol-% Al_2O_3- and polystyrene2-nanofluids plotted as a function of Reynolds number

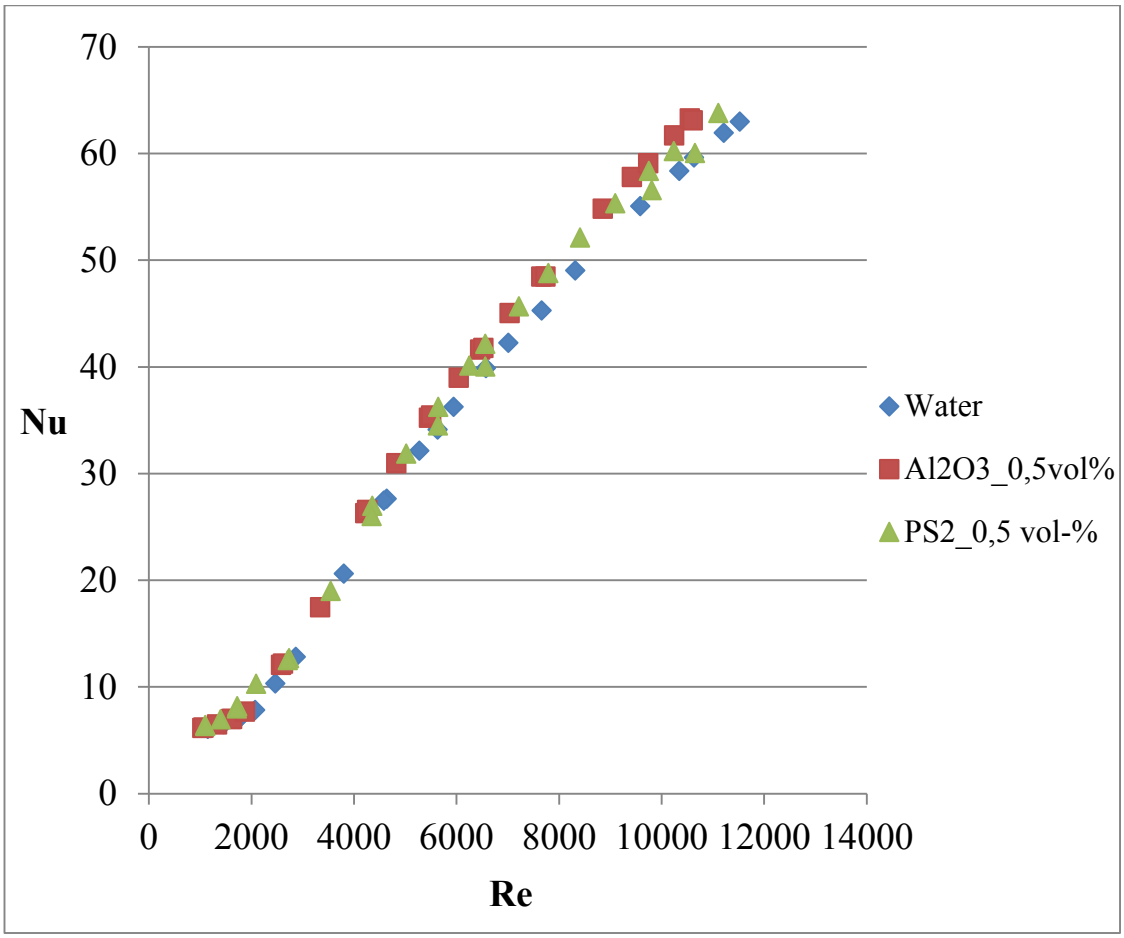

Figure 28. Nusselt numbers of 0,5 vol-% Al_2O_3- and polystyrene2-nanofluids plotted as a function of Reynolds number

The conventional presentation manner shown in Figures 25-28 (Nu is presented as a function on Re) is unable to state whether the performance of the fluids follow conventional correlations, since the effect of Prandtl number is disregarded. Therefore, a direct comparison between the experimental results and correlation values should be presented. In this work, Gnielinski correlation [7] was used as a reference correlation.

$$Nu_{Gnielinski\ correlation} = \frac{\left(\frac{f}{2}\right)(Re-1000)Pr}{1+12{,}7\left(\frac{f}{2}\right)^{1/2}(Pr^{2/3}-1)} \quad (41)$$

Since the purpose was to obtain purely correlation-based reference values, experimental friction factors were not desired to be used in equation (41). Instead, the friction factors for this purpose were determined based on Blausius Law for turbulent flow in a pipe [73], as presented in Equation (42)

$$f = 0{,}316Re^{-0{,}25} \quad (42)$$

In Figures 29, 30 and 31, the measured Nu (Nu_{exp}) are presented as a function of Nu calculated based on Gnielinski correlation ($Nu_{correlation}$). In this presentation method, a fluid behavior that was in perfect agreement with Gnielinski correlation would form the line y=x.

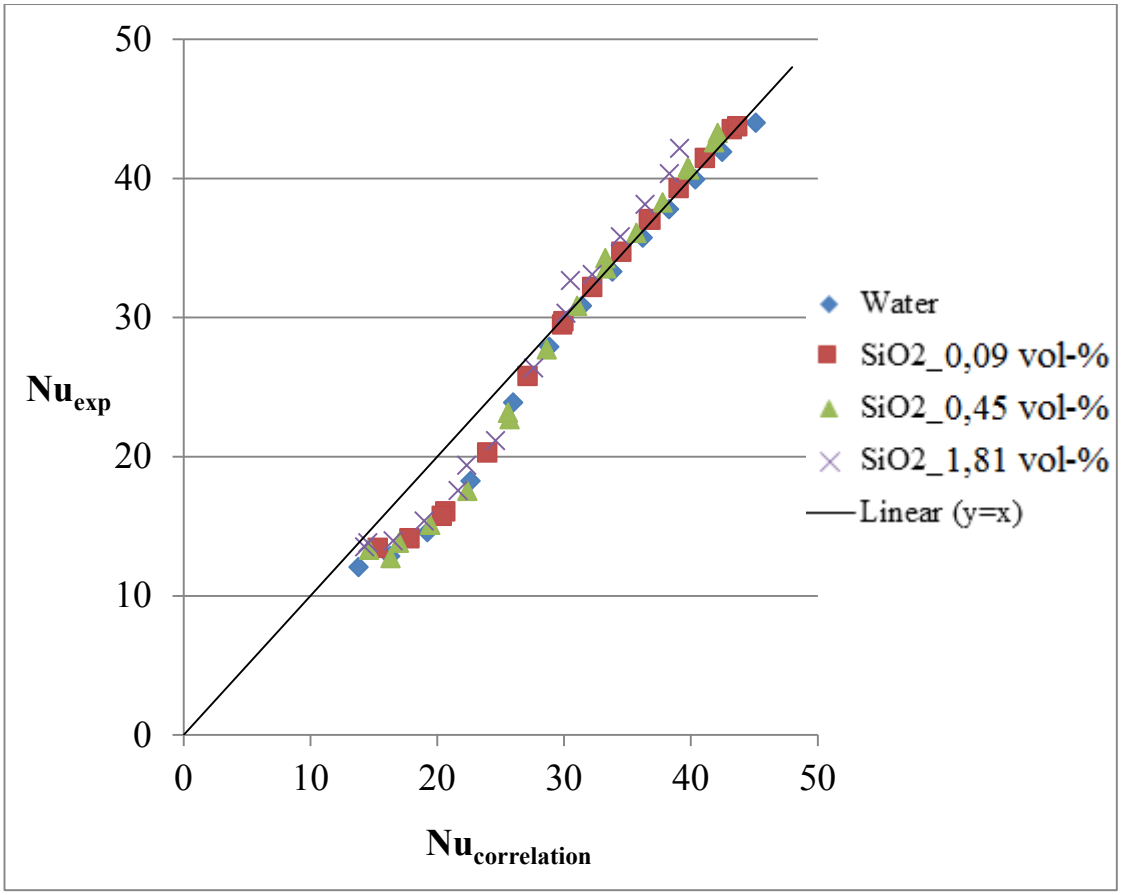

Figure 29. Experimental results of SiO_2-nanofluids compared to Gnielinski correlation

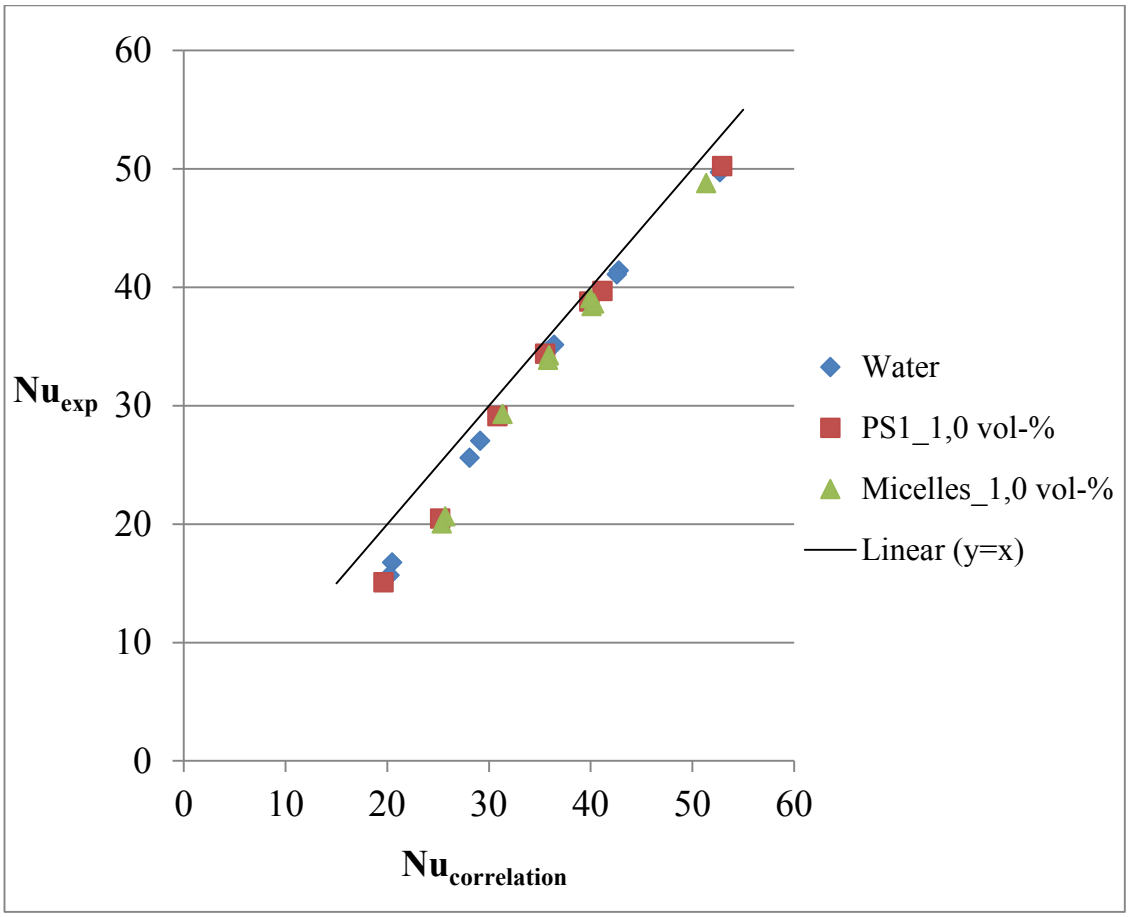

Figure 30. Experimental results of micelle- and polystyrene1-nanofluids compared to Gnielinski correlation

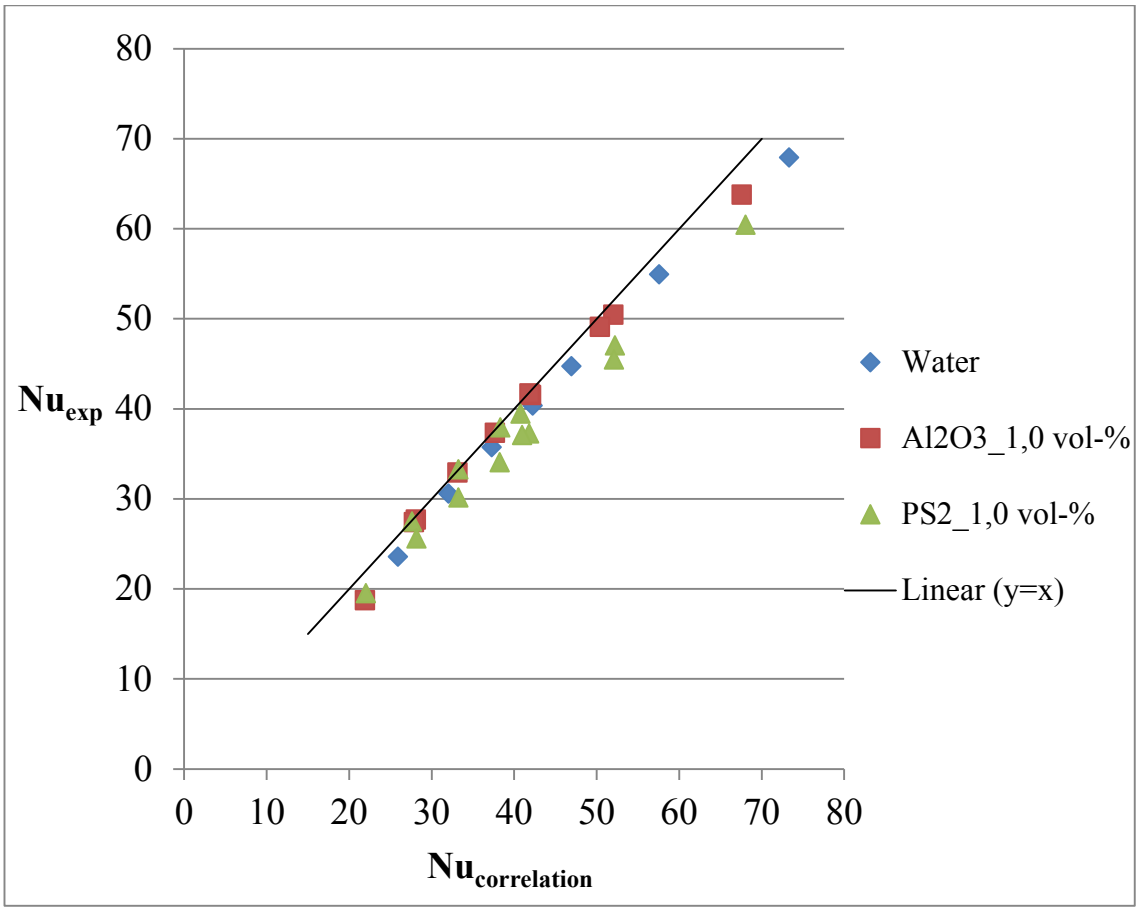

Figure 31. Experimental results of 1,0 vol-% Al_2O_3- and polystyrene2-nanofluids compared to Gnielinski correlation

Figures 29-31 indicate that the conventional correlations seem to be able to explain the heat transfer behavior of the studied nanofluids sufficiently. Particularly with higher Nusselt numbers, where the flow is approaching fully turbulent regime, the measured values equate to the predicted values very accurately. In addition, nanofluids and water behave almost similarly when presented with this method that takes both Re and Pr into account. In all cases, the Nu of a nanofluid was within 5% deviation from that of waters. Overall, no anomalous heat transfer behavior was observed with the studied nanofluids.

In Figure 32, the results of 0,5 vol-% Al_2O_3- and polystyrene2-nanofluids are compared to Gnielinski correlation. In this case, the experimental results do not follow the correlation very well, but the nanofluids show slightly deteriorated heat transfer performance instead. However, the same deterioration of heat transfer performance can be observed for the reference water sample as well and thus, the results of the nanofluids and the reference are similar. The difference between the measured and the predicted values in the Figure 32 can be attributed to a thin thermal resistance layer on inner surface of the measurement tube caused by an earlier measured unstable

polystyrene sample. Shorter polymerization time used for this earlier sample probably caused polymerization to occur inside the measurement device when the temperature of the fluid was elevated. However, regardless of the resistance layer, the measurements are well comparable within the same measurement set. Due to the similar results between the nanofluids and the reference, no anomalous heat transfer behavior was observed in this measurement set either.

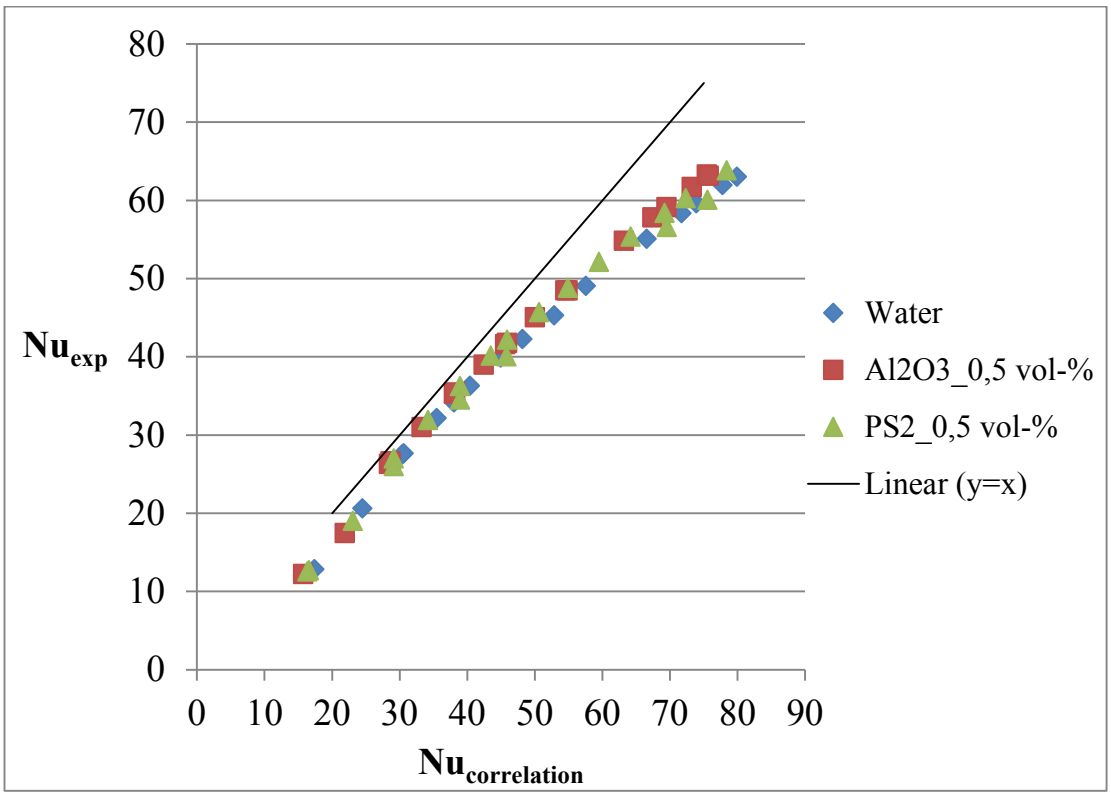

Figure 32. Experimental results of 0,5 vol-% Al_2O_3- and polystyrene2-nanofluids compared to Gnielinski correlation

4.3 Pressure losses and friction factors

The Darcy friction factors are presented in Figures 33, 34, 35 and 36. In all three measurement sets, the friction factors of nanofluids were approximately equal to those of waters. In the turbulent flow regime, the curves unite smoothly. Likewise, the behavior in the transition flow regime was noticed to be somewhat similar for all measured fluids. The only significant differences between the samples were observed in the laminar flow regime, where the accuracy of the pressure loss measurement device is limited.

The pressure loss measurements of 1 vol-% polystyrene nanofluid failed due to fluid instability discussed in previous Chapter and thus, those results are not presented here.

Due to the contamination of the heat exchanger, also the subsequently measured 0,5 vol-% fluids of the third set experienced increased pressure losses (Figure 36). Therefore, the friction factors of these fluids differ from the earlier measurements and the results are not comparable with the other measurement sets due to the altered measurement conditions. However, the friction factors of 0,5 vol-% nanofluids are comparable with each other and with the water reference that was measured in the same conditions.

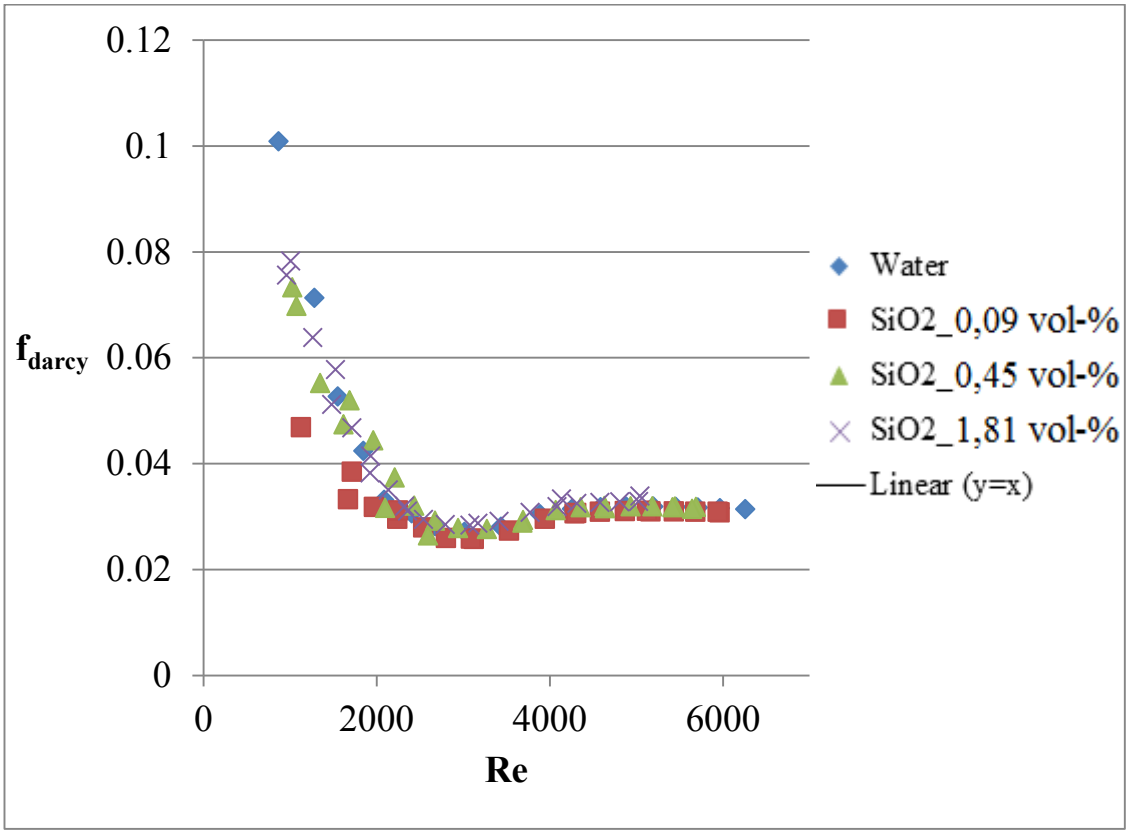

Figure 33. Friction factors of SiO_2-nanofluids

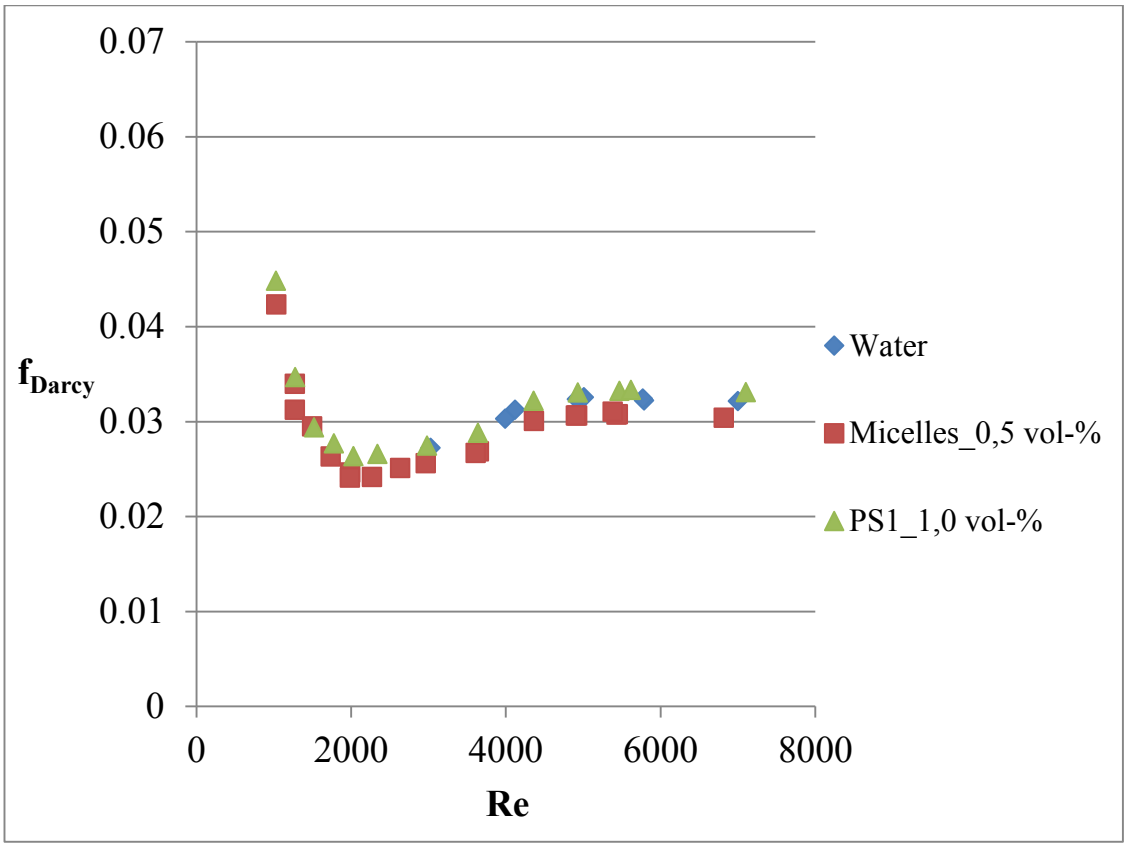

Figure 34. Friction factors of micelle and polystyrene 1 nanofluids

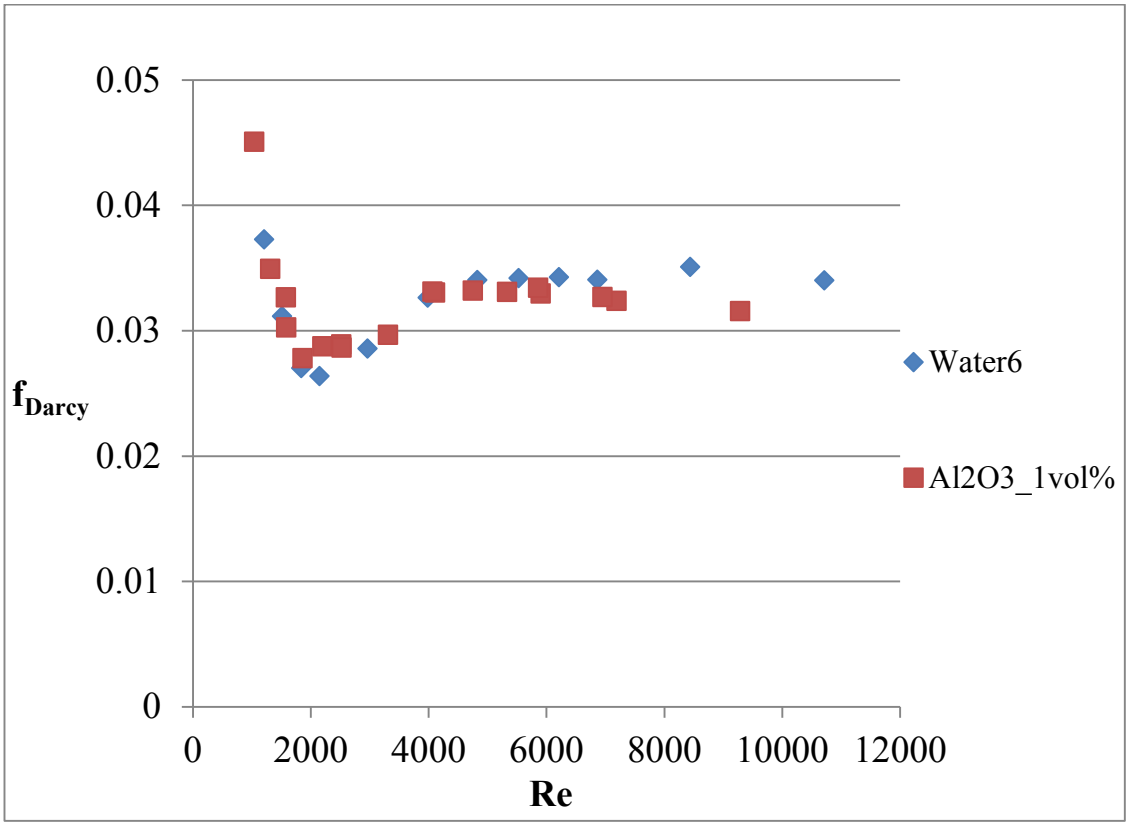

Figure 35. Friction factors of 1 vol-% Al_2O_3 nanofluids

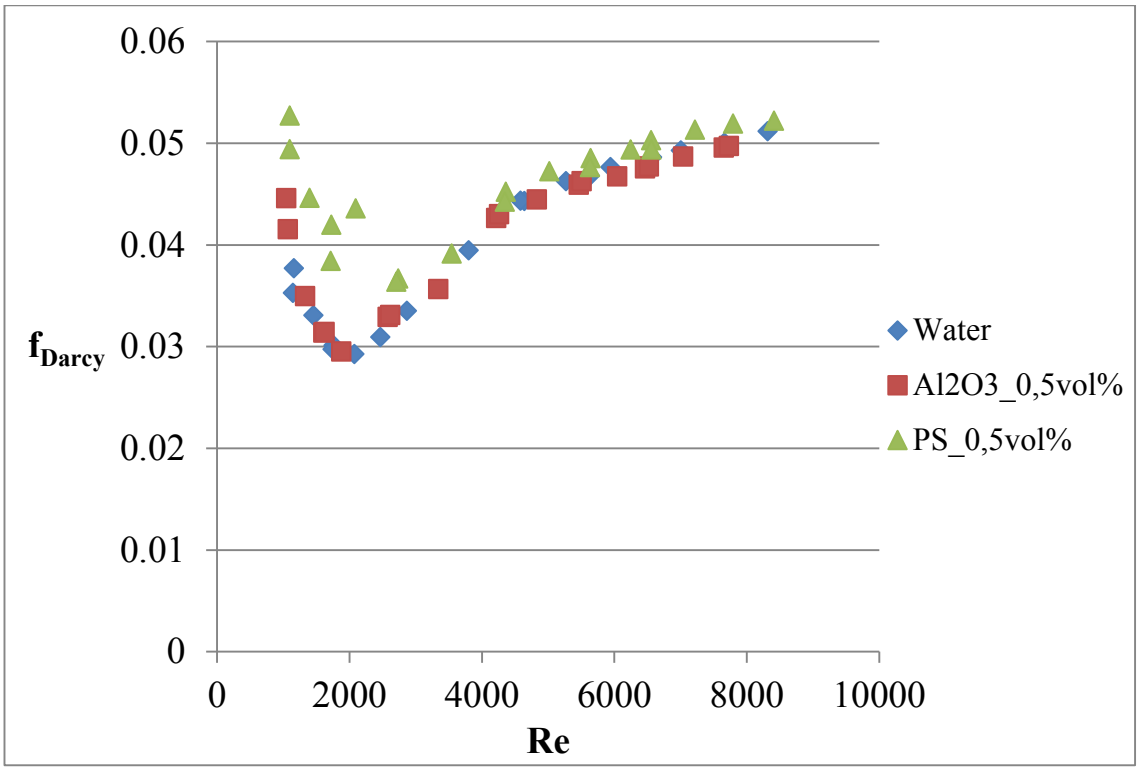

Figure 36. Friction factors of 0,5 vol-% Al_2O_3- and polystyrene-nanofluids

Overall, the observed differences in the friction factors were rather small and thus, all variance in the results was interpreted to be natural fluctuation within the error boundaries. Such results were expected, since no large deviations in pressure losses are expected for nanofluids with relatively low particle fractions if the solid material is well dispersed into the base fluid.

4.4 Effective heat transfer performance

Figures 37, 38, 39 and 40 describe the effective heat transfer performance of the fluids; the heat transfer coefficients are presented as a function of pumping power. On the basis of equal pumping powers, the addition of nanoparticles seems to deteriorate the heat transfer performance of the fluids. In all cases, nanofluids showed lower or similar performance to that of waters. Furthermore, the effect of concentration seems clear: the effective heat transfer performance decreases with increasing concentration as observed also in the earlier experiments of the research group [17]. Similar deterioration has been reported in literature as well [17,37,63].

In addition to the concentration, the particle size was observed to have an influence on the effective convective heat transfer of the nanofluids. Silica nanofluids with the largest particle size of ~50 nm had the lowest performance whereas smaller Al_2O_3,

polystyrene and micelle nanofluids composed of ~10 nm particles performed substantially better. Thus, the results indicate that small particle size would be beneficial for effective convective heat transfer performance of nanofluids. However, the SiO_2 nanofluids differ from the other samples in terms of material as well and thus, no unquestionable conclusions concerning the effect of particle size can be drawn based on the obtained results.

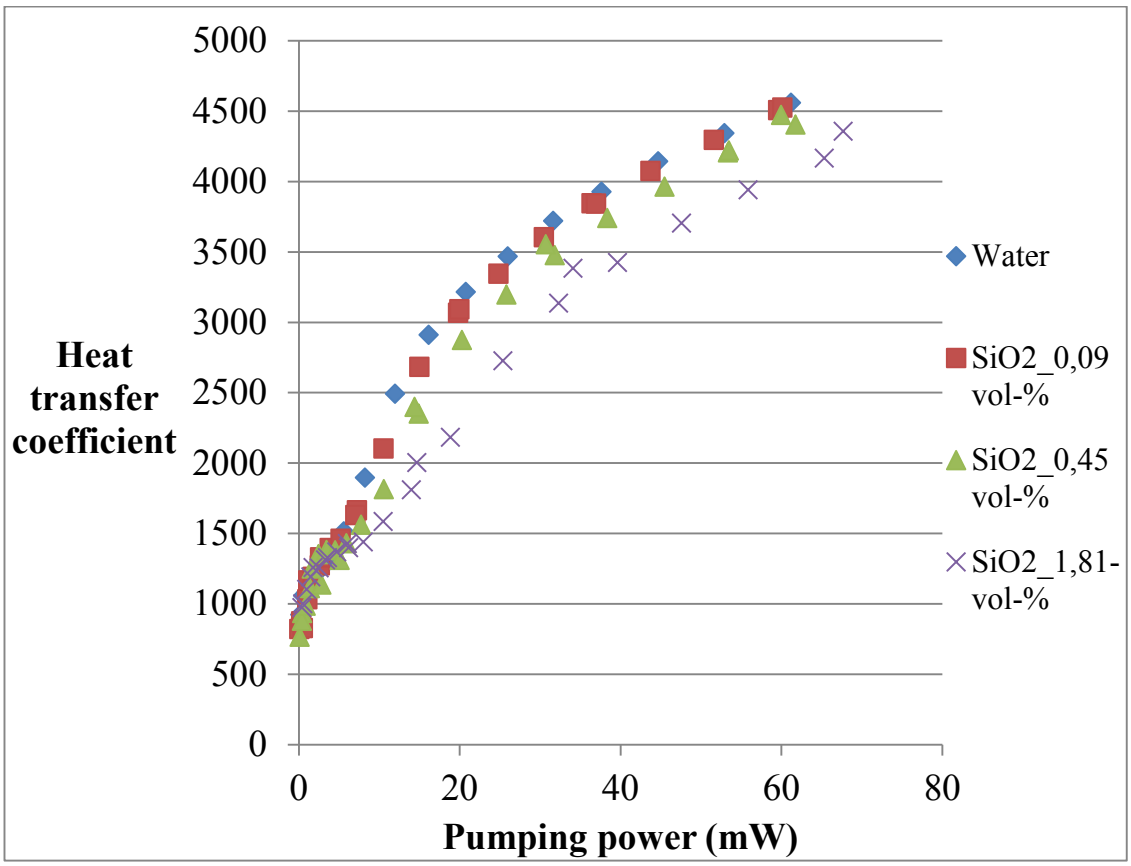

Figure 37. Effective heat transfer performance of SiO_2-nanofluids

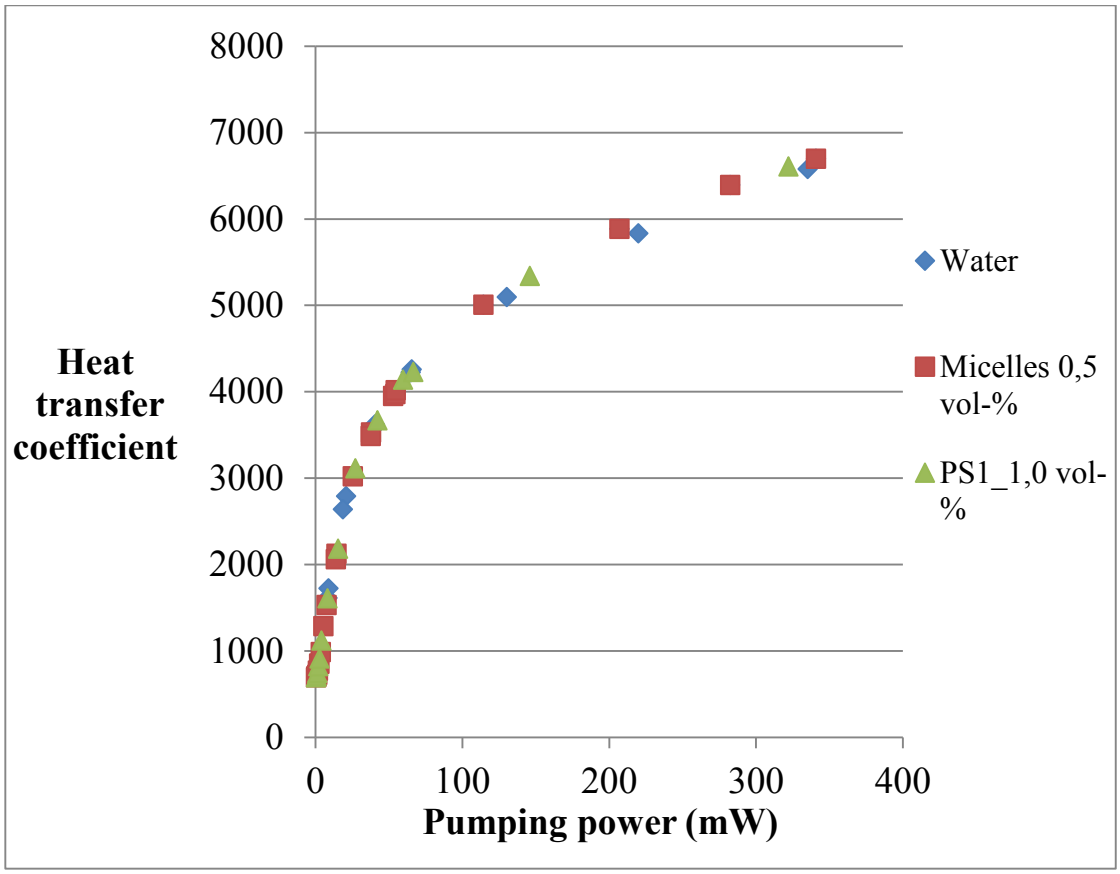

Figure 38. Effective heat transfer performance of micelle and polystyrene nanofluid

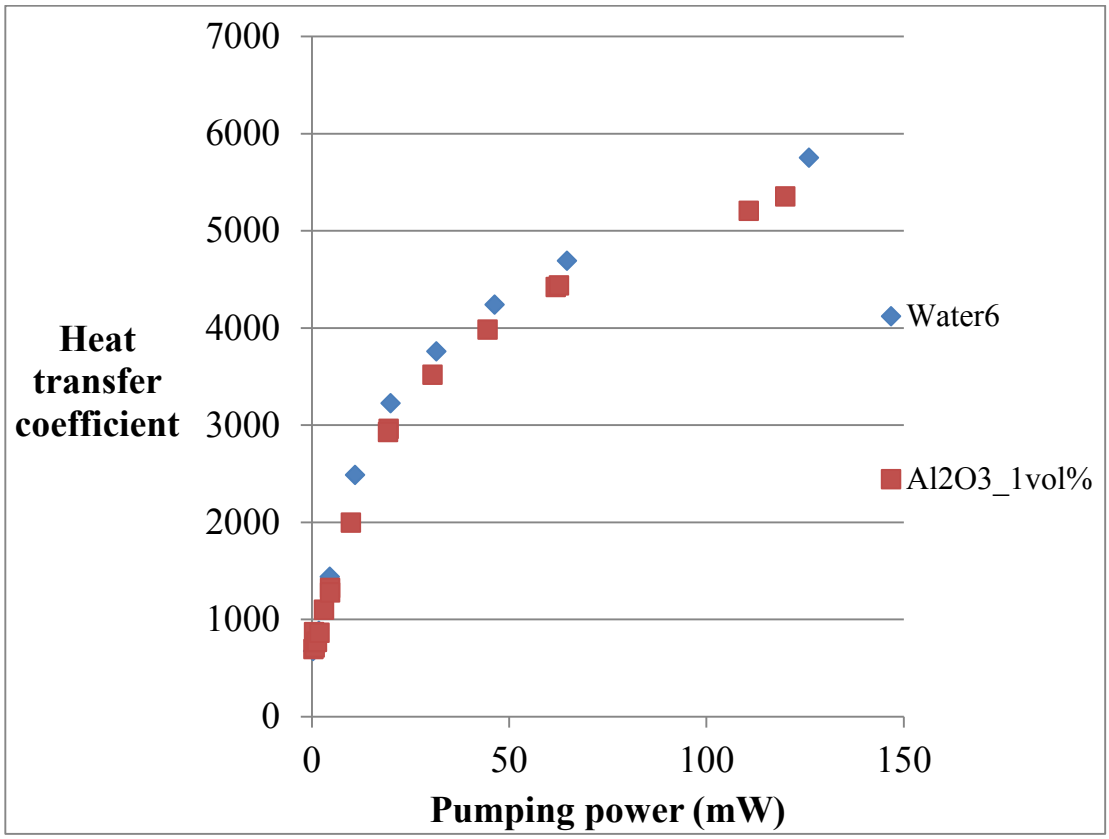

Figure 39. Effective heat transfer performance of 1 vol-% Al_2O_3 nanofluid

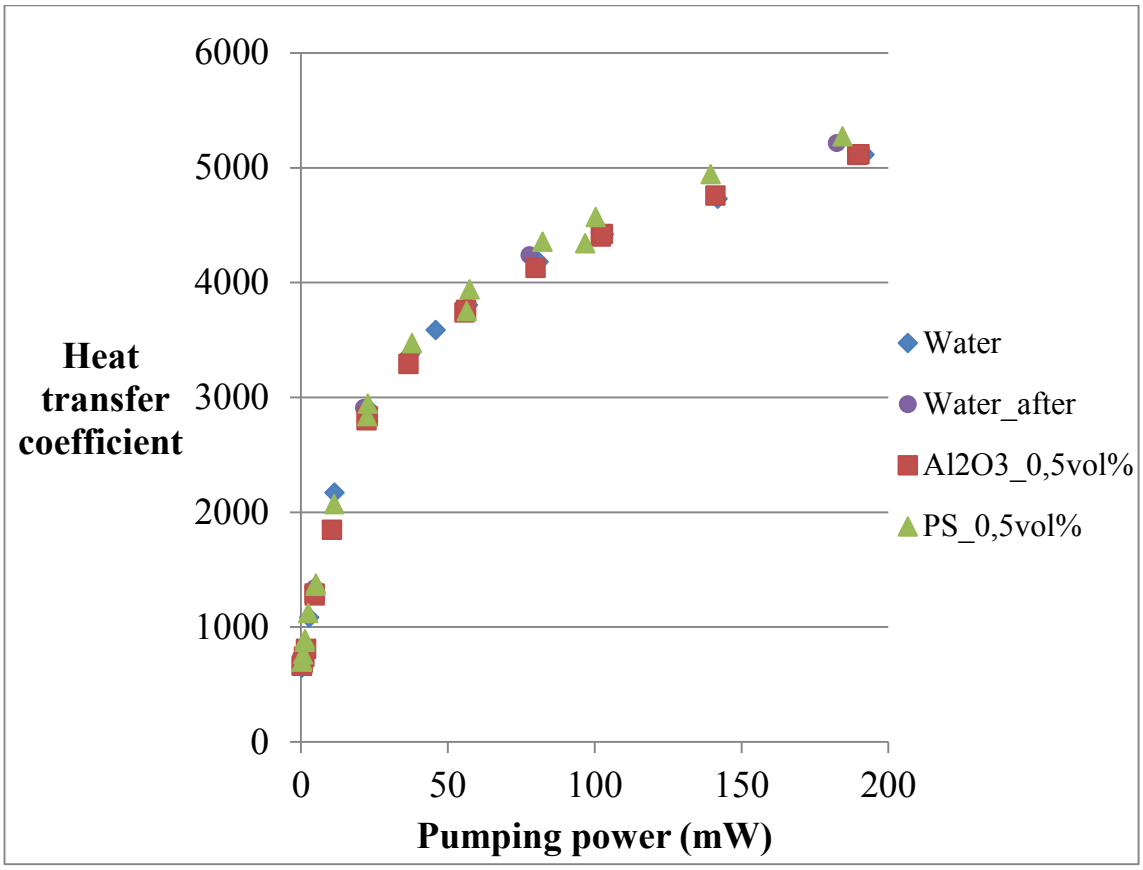

Figure 40. Effective heat transfer performance of 0,5 vol-% Al_2O_3- and polystyrene-nanofluids. The graph "Water_after" corresponds to the parallel measurements of water conducted after the nanofluid experiments.

Figure 41 collects relative pumping powers of all measured nanofluids as a function of heat transfer coefficients. The pumping powers of each nanofluid are compared with the corresponding water samples measured in the same conditions. A relative pumping power value below one would represent improved performance and consistently, values above one can be interpreted as deterioration. This presentation method is very sensitive to any errors in heat transfer coefficient, since such error would result in comparison with false reference value. Consequently, errors are emphasized resulting in larger uncertainty. Nevertheless, Figure 41 clearly suggests that the nanofluids required equal or larger pumping power to reach equal heat transfer coefficients with water. The only exception was 0,5 vol-% polystyrene 2 nanofluid that showed slightly improved performance in the regime of high heat transfer coefficients. However, the parallel measurement of water reached equal performance as can be seen in Figure 40 and thus, the deviation is undoubtedly within the measurement uncertainty. Therefore, no practical improvement was obtained with any nanofluids measured in this study.

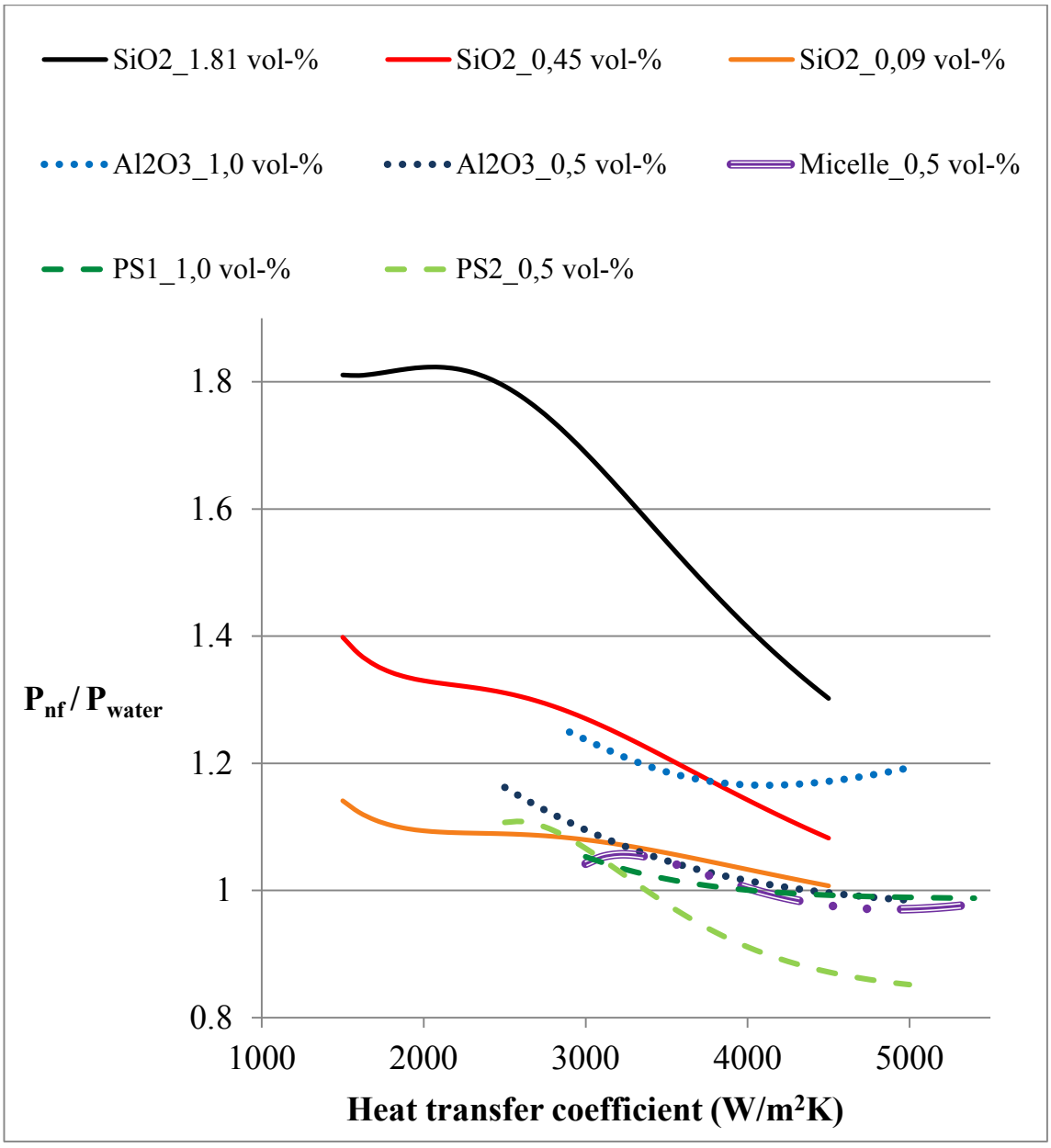

Figure 41. Relative pumping powers as a function of heat transfer coefficient

5 Conclusions

Impacts of particle size, concentration and thermal conductivity of particle material on effective convective heat transfer of nanofluids were experimentally studied in this work. For this purpose, nine different nanofluids were successfully prepared, characterized, and measured with an annular tube heat exchanger. The studied nanofluids were also characterized thoroughly: particle sizes, shapes, fluid stabilities, viscosities, densities and thermal conductivities were measured. Furthermore, analysis methods were developed in order to minimize the experimental errors.

No significant deviations from conventional heat transfer correlations were observed. All measured samples followed the well-known Gnielinski correlation for turbulent flow. A traditional method of presenting Nusselt numbers solely as a function of Reynolds numbers indicated increment in the convection heat transfer, but once differences in Prandtl numbers were considered, no enhancement was observed. Since Nusselt numbers are dependent on both Reynolds number and Prandtl number, the traditional method of presenting results only as a function of Reynolds number was found to be questionable and favor more viscous nanofluids excessively.

An analysis of effective convective heat transfer considering the required pumping powers was also conducted. In all cases, the nanofluids presented similar or lower heat transfer performance than water. According to the experiments, the influence of concentration seems clear; increasing concentration decreased the convective heat transfer performance of all measured nanofluids. With equal velocities, the pressure losses of nanofluids and water were approximately equal, but the nanofluids reached slightly lower heat transfer coefficients. This could be interpreted as the more viscous nanofluids experiencing less turbulence than water with equal velocity, which results in diminished convective heat transfer.

Particle size was observed to have an influence on the heat transfer performance of nanofluids. The decrease in effective heat transfer performance was observed to be weaker for nanofluids with smaller particle size. With equal pumping powers, the samples with particle size of ~10 nm reached approximately equal heat transfer coefficients with water, whereas the fluids with particle size of ~50 nm exhibited deteriorated performance. Therefore, the measurement data indicates that very small particle size would be beneficial for heat transfer performance of nanofluids, as suggested in several publications [33,34,57,64]. However, it has to be acknowledged

that this result is only hypothetical, since fluids with different particle materials were compared.

The effect of thermal conductivity of particle material on convective heat transfer was studied by comparing Al_2O_3-nanofluids to polystyrene nanofluids with equal concentrations and particle sizes. Peculiarly, the thermal conductivities of Al_2O_3-nanofluids were observed to be lower than those of polystyrene samples. Such result is naturally unanticipated since the thermal conductivity of bulk Al_2O_3 is two orders of magnitude higher than that of polystyrenes [1]. However, the observed differences in the thermal conductivities were rather small and no large deviations were even expected, since the particle concentrations of the studied fluids were relatively low ($\leq$1 vol-%). Nevertheless, both nanofluid types performed roughly equally in the convection heat transfer experiments, and no significant effects on convection were observed.

The two devices used in the viscosity measurements (Haake Falling Ball and Bookefield rotational cone/plate) yielded contradictory results. The values obtained with the falling ball viscometer were typically notably higher than those obtained with the rotational viscometer. The largest deviation of 20,5 % was observed with 1.81 vol-% SiO_2-sample. The rotational type viscometer was considered to be more reliable, since the falling ball viscometer was discovered to be extremely sensitive to any agglomerates or larger particles. Similar uncertainty in viscosity measurements could be one of the reasons for inconsistent results in literature [22-46,50,51]. Furthermore, errors in viscosity measurements could also distort the analysis of convective heat transfer experiments, since Reynolds number is heavily dependent on viscosity.

Although anomalous enhancement in convection heat transfer of nanofluids was not observed, enhancement in thermal conductivity caused by the nanoparticles could still be harnessed to improve conventional heat transfer fluids. Significant increment in thermal conductivity might be obtained for instance by using metallic nanoparticles. However, the addition of the particles would result in practical enhancement only if the negative effects caused by increasing viscosity and decreasing specific heat were able to be retained low. Such optimization of material properties naturally requires more comprehensive and specific understanding of nanofluids and thus, further research is definitely needed.

The two viscosity measurement devices used in this work proved to yield contradictory results for heterogeneous nanofluids. Therefore, an inclusive comparison between

different measurement devices would be useful in order to provide insight to uncertainties of the measurement methods. In addition, sensitivity of measurement techniques to agglomeration should be studied.

Phase changing nanofluids are another interesting direction for future research. Such fluids would enable exploitation of latent heat of solid-liquid phase change, which is conventionally impossible due to the non-flowing solid phase. Particularly, phase changing nanofluids could offer major improvement in low-temperature heat transfer applications, in which utilizing liquid-gas phase change is not possible.

6 References

[1] Kotiaho, V., Lampinen, M. and Seppälä, A., Termodynamiikan ja lämmönsiirto-opin taulukoita, Aalto University, Department of energy engineering, 2004. ISBN 951-22-7557-0

[2] Sundar, L. S. et al., Investigation of thermal conductivity and viscosity of Fe_3O_4 nanofluid for heat transfer applications, International communications in heat and mass transfer, vol. 44, pp. 7-14, 2013

[3] Yu, W. et al., Investigation of thermal conductivity and viscosity of ethylene glycol based ZnO nanofluid, Thermochimica Acta, Vol. 491, pp. 92-96, 2009

[4] Yu, W. et al.,Review and comparison of nanofluid thermal conductivity and heat transfer enhancements, Heat transfer engineering, Vol. 29, 2008

[5] Esfe, M. et al., Thermal conductivity of Cu/TiO_2-water/EG hybrid nanofluid: Experimental data and modeling using artificial neural network and correlation, International communications in heat and mass transfer, Vol. 66, pp. 100-104, 2015

[6] Michaelides, E. E., Nanofluidics: Thermodynamic and transport properties, Springer, 2014. ISBN: 978-3-319-05620-3

[7] Kakac, S. et al., Convective heat transfer (Third edition), CRC Press, Taylor&Francis Group, 2014. ISBN: 978-1-4665-8344-3

[8] Sarkar, J., A critical review on convective heat transfer correlations of nanofluids, Renewable and sustainable energy reviews, Vol. 15, pp.3271-3277, 2011

[9] Wu, J.M. and Zhao, J., A review of nanofluid heat transfer and critical heat flux enhancement – research gap to engineering application, Process in nuclear energy, Vol. 66, pp. 13-24, 2013

[10] Hussein, A. M. et al., A review of forced convection heat transfer enhancement and hydrodynamic characteristics of a nanofluid, Renewable and sustainable energy reviews, Vol. 29, pp. 734-743, 2014

[11] Gupta, M. et al., A comprehensive review of experimental investigations of forced convective heat transfer characteristics for various nanofluids, International journal of mechanical and materials engineering, 2014

[12] Choi, S. U. S. and Eastman, J. A., Enhancing thermal conductivity of fluids with nanoparticles, ASME International mechanical engineering congress & exposition, 1995

[13] ISI Web of knowledge

[14] Akhavan-Zanjani, H. et al., Turbulent convective heat transfer and pressure drop of graphene-water nanofluid flowing inside a horizontal circular tube, Journal of dispersion science and technology, Vol. 35, pp. 1230-1240, 2014

[15] Williams, W., Buongiorno, J. and Hu, L., Experimental investigation of turbulent convective heat transfer and pressure loss of alumina/water and zirconia/water nanoparticle colloids (nanofluids) on horizontal tubes, Journal of heat transfer, Vol. 130, pp. 2008

[16] Haghighi, E. B., Single phase convective heat transfer with nanofluids: An experimental approach (Doctoral thesis), KTH industrial engineering and management, Department of energy technology, Division of applied thermodynamics and refrigeration, 2015. ISBN: 978-91-7595-414-1

[17] Saarinen, S. et al., Turbulent heat transfer characteristics in a circular tube and thermal properties of n-decane-in-water nanoemulsion fluids and micelles-in-water fluids, International journal of heat and mass transfer, Vol. 81, pp. 246-251, 2015

[18] Puupponen, S. et al., Preparation of paraffin and fatty acid phase changing nanoemulsions for heat transfer, Thermochimica acta, Vol. 601, pp. 33-38, 2015

[19] Li, Y. et al., A review on development of nanofluid preparation and characterization, Powder technology, Vol. 196, pp. 89-101, 2009

[20] Derjaguin, B. V. and Landau, L., Theory of the stability of strongly charged particles in solutions of electrolytes, Acta Physicochimica, URss, 14, 633-662, 1941

[21] Verway, E. J. and Overbeek, J. T. G., Theory of the stability of lycophobic colloids, Elsevier, 1948

[22] Esfe, M. and Saedodin, S., An experimental investigation and new correlation of viscosity of ZnO-EG nanofluid at various temperatures and different solid volume fractions, Experimental thermal and fluid science, Vol. 55, pp. 1-5, 2014

[23] Mishra, P. C. et al., A brief review on viscosity of nanofluids, International nano letters, Vol 4, pp. 109-120, 2014

[24] Jarahnejad, M. et al., Experimental investigation on viscosity of water-based Al_2O_3 and TiO_2 nanofluids, Rheologica acta, Vol. 54, pp. 411-422, 2015

[25] Corcione, M., Empirical carrelating equations for predicting the effective thermal conductivity and dynamic viscosity on nanofluids, Energy conversion and management, Vol. 52, pp. 789-793, 2011

[26] Said, Z. et al., Experimental investigation of the thermophysical properties of AL_2O_3-nanofluid and its effect on a flat plate solar collector, International communications in heat and mass transfer, Vol. 48, pp. 99-107, 2013

[27] Chen, H. et al., Rheological behavior of ethylene glycol based titania nanofluids, Chemical physics letters, Vol. 444, pp. 333-337, 2007

[28] Sundar, L. S. et al., Viscosity of low volume concentrations of magnetic Fe_3O_4 nanoparticles dispersed in ethylene glycol and water mixture, Chemical physics letters, Vol. 554, pp. 236-242, 2012

[29] Fedele, L. et al., Viscosity and thermal conductivity measurements of water-based nanofluids containing titanium oxide nanoparticles, International journal of refrigeration, Vol. 35, pp. 1359-1366, 2012

[30] Suganthi, K. S. et al., Heat transfer performance and transport properties of ZnO -ethylene glycol and ZnO -ethylene glycol - water nanofluid coolants, Applied energy, Vol. 135, pp. 548-559, 2014

[31] Pastoriza-Gallego, M. J. et al., CuO in water nanofluid: Influence of particle size and polydispersity on volumetric behavior and viscosity, Fluid phase equilibria, Vol. 300, pp. 188-196, 2011

[32] Namburu, P. K. et al., Experimental investigation of viscosity and specific heat of silicon dioxide nanofluids, IET micro & nano letters, Vol 2, s. 67, 2007]

[33] Esfe, M. H. and Saedodin, S., Turbulent convection heat transfer and thermophysical properties of MgO-water nanofluid with concentration of different nanoparticles diameter, an empirical study, Journal of thermal analysis and calorimetry, Vol. 119, pp. 1205-1213, 2015

[34] He, Y. et al., Heat transfer and flow behaviour of aqueous suspensions of TiO_2 nanoparticles (nanofluids) flowing upward through a vertical pipe, International journal of heat and mass transfer, Vol. 50, pp. 2272-2281, 2007

[35] Yu, L. et al., Laminar convective heat transfer of alumina-polyalphaolefin nanofluids containing spherical and non-spherical nanoparticles, Experimental thermal and fluid science, Vol. 37, pp. 72-83, 2012

[36] Venerus, D. et al., Viscosity measurements on colloidal dispersions (nanofluids) for heat transfer applications, Applied rheology, Vol. 20, 2010

[37] Ferrouillat, S., et al., Influence of nanoparticle shape factor on convective heat transfer and energetic performance of water-based SiO_2 and ZnO nanofluids, Applied thermal engineering, Vol. 51, pp. 839-851, 2013

[38] Jeong, J. et al., Particle shape effect on the viscosity and thermal conductivity of ZnO nanofluids, International journal of refrigeration, Vol. 36, pp. 2233-2241, 2013

[39] Moosavi, M. et al., Fabrication, characterization, and measurement of some physicochemical properties of ZnO nanofluids, International journal of heat and fluid flow, Vol. 31, pp. 599-605, 2010

[40] Nguyen, C.T. et al., Viscosity data for Al_2O_3-water nanofluid – hysteresis: is heat transfer enhancement using nanofluids reliable?, International journal of thermal sciences, Vol. 47, pp. 103-111

[41] Said, Z. et al., New thermophysical properties of water based TiO_2 nanofluid - The hysteresis phenomenon revisited, International communications in heat and mass transfer, Vol. 58, pp. 85-95, 2014

[42] Li, X. et al., Rheological behavior of ethylene glycol-based SiC nanofluids, International journal of heat and mass transfer, Vol. 84, pp. 925-930, 2015

[43] Pineiro, M. M. et al., Rheological non-Newtonian behaviour of ethylene glycol-based Fe_2O_3 nanofluids, Nanoscale research letters, Vol. 6, pp. 1-7, 2011

[44] Mariano, A. et al., Thermal conductivity, rheological behaviour and density of nen-Newtonian ethylene glycol-based SnO_2 nanofluids, Fluid phase equilibria, Vol. 337, pp. 119-124, 2013

[45] Sadri, R. et al., An experimental study on thermal conductivity and viscosity of nanofluids containing carbon nanotubes, Nanoscale research letters, Vol. 9, 2014

[46] Pastoriza-Gallego, M. J. et al., Rheological non-Newtonian behaviour of ethylene glycol-based Fe_2O_3 nanofluids, Nanoscale research letters, Vol. 6, pp. 1-7, 2011

[47] Einstein, A., A new determination of molecular dimensions, Annalen der Physik, 19:371-381, 1906

[48] Batchelor, G., The effect of Brownian motion on the bulk stress in a suspension of spherical particles, Journal of fluid mechanics, Vol. 83, pp. 97-117, 1977

[49] Krieger, I. M. and Dougherty, T. J., A mechanism for non-newtonian flow in suspensions of rigid spheres, Transactions of the society of rheology, 3, pp. 137-152, 1959

[50] Sundar, L. S. et al., Empirical and theoretical correlations on viscosity of nanofluids: A review, Renewable and sustainable energy reviews, Vol. 25, pp. 670-686, 2013

[51] Yiamsawas, T. et al., Measurement and correlation of the viscosity of water-based Al_2O_3 and TiO_2 nanofluids in high temperatures and comparisons with literature reports, Journal of dispersion science and technology, Vol. 34, pp. 1697-1703, 2013

[52] Pak, B. C. and Cho, Y. I., Hydrodynamic and heat transfer study of dispersed fluids with submicron metallic oxide particles, A journal of thermal energy generation, transport, storage, and conversion, 11:2, pp. 151-170, 1998

[53] Lampinen, M. J., Mamdouh, E. H. A. and Kotiaho, V., Lämmönsiirto-oppi, Aalto University, Department of energy engineering, 2008. ISBN: 978-951-22-9572-2

[54] Yu, W. et al., Thermophysical property-related comparison criteria for nanofluid heat transfer enhancement in turbulent flow, Applied physics letters, Vol. 96, 2010

[55] Wu, Z. et al., Pressure drop and convective heat transfer of water and nanofluids in a double-pipe helical heat exchanger, Applied thermal engineering, Vol. 60, pp. 266-274, 2013

[56] Yu, W., Comparative review of turbulent heat transfer of nanofluids, International journal of heat and mass transfer, Vol. 55 pp. 5380-5396, 2012

[57] Meriläinen, A. et al., Influence of particle size and shape on turbulent heat transfer characteristics and pressure losses in water-based nanofluids, International journal of heat and mass transfer, Vol. 61, pp. 439-448, 2013

[58] Fotukian, S.M. and Esfahany, M. N., Experimental study of turbulent convective heat transfer and pressure drop of dilute CuO/water nanofluid inside a circular tube, International communications in heat and mass transfer, Vol. 37, pp. 214-219, 2010

[59] Dalkilic, A. S. et al., Forced convective heat transfer of nanofluids – A review of the recent literature, Current nanoscience, Vol. 8, pp. 949-969, 2012

[60] Esfe, M. H. et al., Experimental studies on the convective heat transfer performance and thermophysical properties of MgO-water nanofluid under turbulent flow, Experimental thermal and fluid science, Vol. 52, pp. 68-78, 2014

[61] Samira, P. et al., Pressure drop and thermal performance of CuO/ethylene glycol (60%)-water (40%) nanofluid in car radiator, Korean journal of chemical engineering, Vol. 32, pp. 609-616, 2015

[62] Ferrouillat, S. et al., Hydraulic and heat transfer study of SiO_2/water nanofluids in horizontal tubes with imposed wall temperature boundary conditions, International Journal of Heat and Fluid flow, Vol. 32, pp. 424-439, 2011

[63] Bayat, J. and Nikseresht, A. H., Thermal performance and pressure drop analysis of nanofluids in turbulent forced convective flows, International journal of thermal sciences, Vol. 60, pp. 236-243, 2012

[64] Mehrali, M. et al., Effect of specific surface area on convective heat transfer of graphene nanoplatelet aqueous nanofluids, Experimental thermal and fluid science, Vol. 68, pp. 100-108, 2015

[65] Abbasian Arani, A. A. and Amani, J., Experimental Investigation on heat transfer performance and pressure drop of TiO_2-water nanofluid, Experimental thermal and fluid science, Vol. 44, pp. 520-533, 2013

[66] He, Y. et al., Heat transfer and flow behaviour of aqueous suspensions of TiO_2 particles (nanofluids) flowing upward through a vertical pipe, International journal of heat and mass transfer, Vol. 50, pp. 2272-2281, 2007

[67] Goodarzi, M et al., Investigation of heat transfer and pressure drop of a counter flow corrugated plate heat exchanger using MWCNT based nanofluids, International communications in heat and mass transfer, Vol. 66, pp. 172-179, 2015

[68] Huang, D., Wu and Z., Sunden, B., Pressure drop and convective heat transfer of Al_2O_3/water and MWCNT/water nanofluids in a chevron plate heat exchanger, International journal of heat and mass transfer, Vol. 89, pp. 620-626, 2015

[69] Stöber, W., Fink, A., Bohn, E., Controlled growth of monodisperse silica spheres in the micron range, Journal of colloid and interface science, 26, 62 (1968), DOI:10.1016/0021-9797(68)90272-5

[70] Kaiyi, L., Zhaoqun, W., A novel method for preparing monodispersed polystyrene nanoparticles, Front. Chem. China 2007 2(1) 17-20.

[71] Chandrasekar, M. et al., Experimental investigations and theoretical determination of thermal conductivity and viscosity of Al_2O_3/water nanofluid, Experimental thermal and fluid science, Vol. 34, pp. 210-216, 2010

[72] Cengel, Y. A., Heat transfer - A practical approach, 2. Edition, McGraw-Hill, pp. 444, 2003 ISBN: 0-07-115150-8

[73] White, F. M., Viscous fluid flow (third edition), McGraw-Hill, 2006. ISBN: 007-124493-X